



**NAVAL
POSTGRADUATE
SCHOOL**

MONTEREY, CALIFORNIA

THESIS

**CHARACTERIZATION OF ANODIZED TITANIUM-
BASED NOVEL PARADIGM SUPERCAPACITORS:
IMPACT OF SALT IDENTITY AND FREQUENCY ON
DIELECTRIC VALUES, POWER, AND ENERGY
DENSITIES**

by

Steven M. Lombardo

March 2017

Thesis Advisor:
Second Reader:

Jonathan Phillips
Claudia Luhrs

Approved for public release. Distribution is unlimited.

THIS PAGE INTENTIONALLY LEFT BLANK

| REPORT DOCUMENTATION PAGE | | | Form Approved OMB No. 0704-0188 | |
|--|--|---|--|--|
| Public reporting burden for this collection of information is estimated to average 1 hour per response, including the time for reviewing instruction, searching existing data sources, gathering and maintaining the data needed, and completing and reviewing the collection of information. Send comments regarding this burden estimate or any other aspect of this collection of information, including suggestions for reducing this burden, to Washington headquarters Services, Directorate for Information Operations and Reports, 1215 Jefferson Davis Highway, Suite 1204, Arlington, VA 22202-4302, and to the Office of Management and Budget, Paperwork Reduction Project (0704-0188) Washington, DC 20503. | | | | |
| 1. AGENCY USE ONLY (Leave blank) | 2. REPORT DATE March 2017 | 3. REPORT TYPE AND DATES COVERED Master's thesis | | |
| 4. TITLE AND SUBTITLE CHARACTERIZATION OF ANODIZED TITANIUM-BASED NOVEL PARADIGM SUPERCAPACITORS: IMPACT OF SALT IDENTITY AND FREQUENCY ON DIELECTRIC VALUES, POWER, AND ENERGY DENSITIES | | | 5. FUNDING NUMBERS JON: R5KFB | |
| 6. AUTHOR(S) Steven M. Lombardo | | | | |
| 7. PERFORMING ORGANIZATION NAME(S) AND ADDRESS(ES) Naval Postgraduate School Monterey, CA 93943-5000 | | | 8. PERFORMING ORGANIZATION REPORT NUMBER | |
| 9. SPONSORING /MONITORING AGENCY NAME(S) AND ADDRESS(ES) N/A | | | 10. SPONSORING / MONITORING AGENCY REPORT NUMBER | |
| 11. SUPPLEMENTARY NOTES The views expressed in this thesis are those of the author and do not reflect the official policy or position of the Department of Defense or the U.S. Government. IRB number ____N/A____. | | | | |
| 12a. DISTRIBUTION / AVAILABILITY STATEMENT Approved for public release. Distribution is unlimited. | | | 12b. DISTRIBUTION CODE | |
| 13. ABSTRACT (maximum 200 words) This research was designed to characterize the frequency response of Novel Paradigm (NP) Supercapacitors employing Nanotube Super Dielectric Materials as dielectrics. The result of tests with nine capacitors, each with a unique aqueous salt solution, provided detailed information required to design short pulse systems. This detailed information is required for engineering analysis of NP Supercapacitors in systems of interest to the U.S. Navy (USN) such as the railgun, electromagnetic aircraft launch system, and free electron laser. Key findings show salt identity and concentration impact performance, very high energy densities (>150 J/cm ³) are found for slow discharges (~100 s), and power density increases as discharge rate increases. Finally, the best power density measured at a discharge rate relevant to USN application (~0.01 s) was 90 W/cm ³ using an aqueous salt identity of 30 wt% Ammonium Chloride. This is a significant improvement (>3x) relative to available commercial supercapacitors. | | | | |
| 14. SUBJECT TERMS capacitor, super dielectric material, titanium dioxide, nanotubes, ammonium chloride, sodium nitrate, potassium hydroxide | | | 15. NUMBER OF PAGES 165 | |
| | | | 16. PRICE CODE | |
| 17. SECURITY CLASSIFICATION OF REPORT Unclassified | 18. SECURITY CLASSIFICATION OF THIS PAGE Unclassified | 19. SECURITY CLASSIFICATION OF ABSTRACT Unclassified | 20. LIMITATION OF ABSTRACT UU | |

THIS PAGE INTENTIONALLY LEFT BLANK

Approved for public release. Distribution is unlimited.

**CHARACTERIZATION OF ANODIZED TITANIUM-BASED NOVEL
PARADIGM SUPERCAPACITORS: IMPACT OF SALT IDENTITY AND
FREQUENCY ON DIELECTRIC VALUES, POWER, AND ENERGY
DENSITIES**

Steven M. Lombardo
Lieutenant, United States Navy
B.S.M.E., University of South Florida, 2009

Submitted in partial fulfillment of the
requirements for the degree of

MASTER OF SCIENCE IN MECHANICAL ENGINEERING

from the

**NAVAL POSTGRADUATE SCHOOL
March 2017**

Approved by: Jonathan Phillips, Ph.D.
Thesis Advisor

Claudia Luhrs, Ph.D.
Second Reader

Garth Hobson, Ph.D.
Chair, Department of Mechanical and Aerospace Engineering

THIS PAGE INTENTIONALLY LEFT BLANK

ABSTRACT

This research was designed to characterize the frequency response of Novel Paradigm (NP) Supercapacitors employing Nanotube Super Dielectric Materials as dielectrics. The result of tests with nine capacitors, each with a unique aqueous salt solution, provided detailed information required to design short pulse systems. This detailed information is required for engineering analysis of NP Supercapacitors in systems of interest to the U.S. Navy (USN) such as the railgun, electromagnetic aircraft launch system, and free electron laser.

Key findings show salt identity and concentration impact performance, very high energy densities ($>150 \text{ J/cm}^3$) are found for slow discharges ($\sim 100 \text{ s}$), and power density increases as discharge rate increases. Finally, the best power density measured at a discharge rate relevant to USN application ($\sim 0.01 \text{ s}$) was 90 W/cm^3 using an aqueous salt identity of 30 wt% Ammonium Chloride. This is a significant improvement ($>3x$) relative to available commercial supercapacitors.

THIS PAGE INTENTIONALLY LEFT BLANK

TABLE OF CONTENTS

| | | |
|-------------|--|-----------|
| I. | INTRODUCTION..... | 1 |
| A. | MOTIVATION | 1 |
| B. | BACKGROUND | 5 |
| II. | EXPERIMENTAL METHODS | 13 |
| A. | ANODIZATION PROCESS AND SAMPLE PREPARATION | 13 |
| 1. | Sample Preparation | 13 |
| 2. | Solution Preparation..... | 14 |
| 3. | System Set-up | 17 |
| B. | SEM OPERATIONS | 22 |
| 1. | Sample Preparation | 22 |
| 2. | Image Analysis | 24 |
| C. | TEST PROCEDURES..... | 29 |
| 1. | Test Apparatus Set-up..... | 29 |
| 2. | EC Lab Software Set-up..... | 34 |
| 3. | Post-test Analysis | 41 |
| III. | RESULTS | 43 |
| A. | OVERVIEW | 43 |
| 1. | Charge Equals Discharge | 44 |
| 2. | Charge Fixed | 45 |
| B. | DEIONIZED WATER..... | 46 |
| 1. | Charge Equals Discharge | 46 |
| 2. | Charge Fixed | 48 |
| C. | AMMONIUM CHLORIDE RESULTS..... | 50 |
| 1. | NH₄Cl 10 wt% Charge Equals Discharge | 50 |
| 2. | NH₄Cl 20 wt% Charge Equals Discharge | 52 |
| 3. | NH₄Cl 30 wt% Charge Equals Discharge | 54 |
| 4. | NH₄Cl 10 wt% Charge Fixed..... | 56 |
| 5. | NH₄Cl 20 wt% Charge Fixed..... | 58 |
| 6. | NH₄Cl 30 wt% Charge Fixed..... | 60 |
| D. | SODIUM NITRATE..... | 62 |
| 1. | NaNO₃ 10 wt% Charge Equals Discharge..... | 62 |
| 2. | NaNO₃ 20 wt% Charge Equals Discharge..... | 64 |
| 3. | NaNO₃ 30 wt% Charge Equals Discharge..... | 66 |
| 4. | NaNO₃ 10 wt% Charge Fixed..... | 68 |
| 5. | NaNO₃ 20 wt% Charge Fixed..... | 70 |

| | | |
|-----|--|-----|
| 6. | NaNO ₃ 30 wt% Charge Fixed | 72 |
| E. | POTASSIUM HYDROXIDE | 74 |
| 1. | KOH 10 wt% Charge Equals Discharge | 74 |
| 2. | KOH 20 wt% Charge Equals Discharge | 76 |
| 3. | KOH 30 wt% Charge Equals Discharge | 78 |
| 4. | KOH 10 wt% Charge Fixed..... | 80 |
| 5. | KOH 20 wt% Charge Fixed..... | 82 |
| 6. | KOH 30 wt% Charge Fixed..... | 84 |
| IV. | DISCUSSION | 87 |
| A. | AMMONIUM CHLORIDE RESULTS CHARGE EQUALS DISCHARGE | 88 |
| B. | SODIUM NITRATE RESULTS CHARGE EQUALS DISCHARGE | 92 |
| C. | POTASSIUM HYDROXIDE RESULTS CHARGE EQUALS DISCHARGE | 96 |
| D. | COMBINED RESULTS CHARGE EQUALS DISCHARGE..... | 100 |
| E. | AMMONIUM CHLORIDE RESULTS CHARGE FIXED | 104 |
| F. | SODIUM NITRATE RESULTS CHARGE FIXED..... | 108 |
| G. | POTASSIUM HYDROXIDE RESULTS CHARGE FIXED..... | 112 |
| H. | COMBINED RESULTS CHARGE FIXED..... | 116 |
| V. | CONCLUSION AND FUTURE WORK | 121 |
| | APPENDIX A. RAILGUN EQUATIONS | 127 |
| | APPENDIX B. EMALS EQUATIONS | 131 |
| | APPENDIX C. COMMERCIAL CAPACITOR FIGURES..... | 133 |
| | LIST OF REFERENCES..... | 141 |
| | INITIAL DISTRIBUTION LIST | 143 |

LIST OF FIGURES

| | | |
|------------|---|----|
| Figure 1. | Ragone Chart Graphically Compares Energy Density to Power. Source: [14]..... | 7 |
| Figure 2. | Graphical Representation of Decreasing Dipole Length | 8 |
| Figure 3. | Anodization Materials and Tools..... | 13 |
| Figure 4. | 15-Minute Anode Soak Period in Ethanol | 14 |
| Figure 5. | Stir Stick Modification Using Scissors | 15 |
| Figure 6. | Modified Stir Stick for Ammonium Fluoride | 15 |
| Figure 7. | Ammonium Fluoride Measured into the Reactor Vessel..... | 16 |
| Figure 8. | Completed Anodization Solution with Added Ethylene Glycol..... | 17 |
| Figure 9. | Voltage Source Set-up | 18 |
| Figure 10. | Verifying Power Source Output with Digital Voltmeter | 18 |
| Figure 11. | Stand Set-up to Suspend Samples above the Reactor Vessel | 19 |
| Figure 12. | Plastic Locking Forceps and Scissor Lift..... | 19 |
| Figure 13. | Anode and Cathode Submerged in the Reactor Vessel | 20 |
| Figure 14. | Close-up of the Anode (right) and Cathode (left) Alignment..... | 21 |
| Figure 15. | Pelco 2251 Vacuum Desiccator | 22 |
| Figure 16. | SEM Individual Sample Mounts with Attached Carbon Tape | 23 |
| Figure 17. | Three Samples Mounted to the Multi-mount and Clearly Labeled for Identification in the SEM Vacuum Chamber..... | 23 |
| Figure 18. | Titanium Dioxide Nanotube Surface | 26 |
| Figure 19. | Exposed Titanium Substrate with Nanotubes Removed..... | 26 |
| Figure 20. | Nanotubes at Site 2 of Sample 1 | 27 |
| Figure 21. | Nanotubes at Site 3 of Sample 3 | 28 |
| Figure 22. | Nanotubes at Site 4 of Sample 4 | 28 |

| | | |
|------------|---|----|
| Figure 23. | Materials and Tools for Sample Capacitor Testing | 29 |
| Figure 24. | Microscope Slide with Grafoil Spacers Attached to the Edges | 30 |
| Figure 25. | Center Test Electrode of Grafoil Attached and Wiped to Avoid Short-Circuits | 31 |
| Figure 26. | Modified Clothespin for Mounting the Anodized Sample | 32 |
| Figure 27. | Microscope Slide Prepared with Arranged Anodized Sample | 32 |
| Figure 28. | First Spring Clamp Installed to Secure Anodize Sample..... | 33 |
| Figure 29. | Second Spring Clamp Installed to Complete the Test Rig Set-up | 33 |
| Figure 30. | Anodized Sample Connected to the Biologic Equipment and Ready for Testing..... | 34 |
| Figure 31. | Depressing the Turn to Modify Mode Key for Experiment Set-up | 35 |
| Figure 32. | New in the Experiment Menu | 35 |
| Figure 33. | Electrochemical Techniques Drop-down Menu | 36 |
| Figure 34. | Modulo Bat - MB Option in the Electrochemical Applications Menu | 36 |
| Figure 35. | Setting the Charge Cycles of the EC-Lab Software..... | 37 |
| Figure 36. | Setting the Discharge Cycles of the EC-Lab Software | 38 |
| Figure 37. | Setting the Number of Loops Per Experiment to 10..... | 38 |
| Figure 38. | EC-Lab Integral Function Method..... | 41 |
| Figure 39. | EC-Lab Linear Fit Function Method | 42 |
| Figure 40. | EC-Lab Integral and Linear Fit Function Adjustment..... | 42 |
| Figure 41. | Raw Data Comparison of Salt Solutions at 20 mA Discharge (Charge=Discharge Rate)..... | 44 |
| Figure 42. | Raw Data Comparison of Salt Solutions at 20 mA Discharge (Charge≠Discharge Rate)..... | 45 |
| Figure 43. | Deionized Water (Charge=Discharge)..... | 46 |
| Figure 44. | DI Water Energy Density vs. Discharge Time (Charge=Discharge)..... | 47 |

| | | |
|------------|---|----|
| Figure 45. | Deionized Water (Charge≠Discharge)..... | 48 |
| Figure 46. | DI Water Energy Density vs. Discharge Time (Charge≠Discharge)..... | 49 |
| Figure 47. | NH ₄ Cl 10% Concentration (Charge=Discharge)..... | 50 |
| Figure 48. | NH ₄ Cl 10% Energy Density vs. Discharge Time (Charge=Discharge)..... | 51 |
| Figure 49. | NH ₄ Cl 20% Concentration (Charge=Discharge)..... | 52 |
| Figure 50. | NH ₄ Cl 20% Energy Density vs. Discharge Time (Charge=Discharge)..... | 53 |
| Figure 51. | NH ₄ Cl 30% Concentration (Charge=Discharge)..... | 54 |
| Figure 52. | NH ₄ Cl 30% Energy Density vs. Discharge Time (Charge=Discharge)..... | 55 |
| Figure 53. | NH ₄ Cl 10% Concentration (Charge≠Discharge)..... | 56 |
| Figure 54. | NH ₄ Cl 10% Energy Density vs. Discharge Time (Charge≠Discharge)..... | 57 |
| Figure 55. | NH ₄ Cl 20% Concentration (Charge≠Discharge)..... | 58 |
| Figure 56. | NH ₄ Cl 20% Energy Density vs. Discharge Time (Charge≠Discharge)..... | 59 |
| Figure 57. | NH ₄ Cl 30% Concentration (Charge≠Discharge)..... | 60 |
| Figure 58. | NH ₄ Cl 30% Energy Density vs. Discharge Time (Charge≠Discharge)..... | 61 |
| Figure 59. | NaNO ₃ 10% Concentration (Charge=Discharge)..... | 62 |
| Figure 60. | NaNO ₃ 10% Energy Density vs. Discharge Time (Charge=Discharge)..... | 63 |
| Figure 61. | NaNO ₃ 20% Concentration (Charge=Discharge)..... | 64 |
| Figure 62. | NaNO ₃ 20% Energy Density vs. Discharge Time (Charge=Discharge)..... | 65 |
| Figure 63. | NaNO ₃ 30% Concentration (Charge=Discharge)..... | 66 |
| Figure 64. | NaNO ₃ 30% Energy Density vs. Discharge Time (Charge=Discharge)..... | 67 |

| | | |
|------------|---|----|
| Figure 65. | NaNO ₃ 10% Concentration (Charge≠Discharge) | 68 |
| Figure 66. | NaNO ₃ 10% Energy Density vs. Discharge Time (Charge≠Discharge) | 69 |
| Figure 67. | NaNO ₃ 20% Concentration (Charge≠Discharge) | 70 |
| Figure 68. | NaNO ₃ 20% Energy Density vs. Discharge Time (Charge≠Discharge) | 71 |
| Figure 69. | NaNO ₃ 30% Concentration (Charge≠Discharge) | 72 |
| Figure 70. | NaNO ₃ 30% Energy Density vs. Discharge Time (Charge≠Discharge) | 73 |
| Figure 71. | KOH 10% Concentration (Charge=Discharge) | 74 |
| Figure 72. | KOH 10% Energy Density vs. Discharge Time (Charge=Discharge) | 75 |
| Figure 73. | KOH 20% Concentration (Charge=Discharge) | 76 |
| Figure 74. | KOH 20% Energy Density vs. Discharge Time (Charge=Discharge) | 77 |
| Figure 75. | KOH 30% Concentration (Charge=Discharge) | 78 |
| Figure 76. | KOH 30% Energy Density vs. Discharge Time (Charge=Discharge) | 79 |
| Figure 77. | KOH 10% Concentration (Charge≠Discharge) | 80 |
| Figure 78. | KOH 10% Energy Density vs. Discharge Time (Charge≠Discharge) | 81 |
| Figure 79. | KOH 20% Concentration (Charge≠Discharge) | 82 |
| Figure 80. | KOH 20% Energy Density vs. Discharge Time (Charge≠Discharge) | 83 |
| Figure 81. | KOH 30% Concentration (Charge≠Discharge) | 84 |
| Figure 82. | KOH 30% Energy Density vs. Discharge Time (Charge≠Discharge) | 85 |
| Figure 83. | Capacitance vs. Discharge Time (NH ₄ Cl) (Charge=Discharge) | 88 |
| Figure 84. | Dielectric vs. Discharge Time (NH ₄ Cl) (Charge=Discharge) | 89 |
| Figure 85. | Energy Density vs. Discharge Time (NH ₄ Cl) (Charge=Discharge) | 90 |
| Figure 86. | Power Density vs. Discharge Time (NH ₄ Cl) (Charge=Discharge) | 91 |
| Figure 87. | Capacitance vs. Discharge Time (NaNO ₃) (Charge=Discharge) | 92 |

| | | |
|-------------|---|-----|
| Figure 88. | Dielectric vs. Discharge Time (NaNO ₃) (Charge=Discharge) | 93 |
| Figure 89. | Energy Density vs. Discharge Time (NaNO ₃) (Charge=Discharge) | 94 |
| Figure 90. | Power Density vs. Discharge Time (NaNO ₃) (Charge=Discharge)..... | 95 |
| Figure 91. | Capacitance vs. Discharge Time (KOH) (Charge=Discharge)..... | 96 |
| Figure 92. | Dielectric vs. Discharge Time (KOH) (Charge=Discharge)..... | 97 |
| Figure 93. | Energy Density vs. Discharge Time (KOH) (Charge=Discharge) | 98 |
| Figure 94. | Power Density vs. Discharge Time (KOH) (Charge=Discharge)..... | 99 |
| Figure 95. | Capacitance vs. Discharge Time (All Salt Solutions) (Charge=Discharge)..... | 100 |
| Figure 96. | Dielectric vs. Discharge Time (All Salt Solutions) (Charge=Discharge)..... | 101 |
| Figure 97. | Energy Density vs. Discharge Time (All Salt Solutions) (Charge=Discharge)..... | 102 |
| Figure 98. | Power Density vs. Discharge Time (All Salt Solutions) (Charge=Discharge)..... | 103 |
| Figure 99. | Capacitance vs. Discharge Time (NH ₄ Cl) (Charge≠Discharge)..... | 104 |
| Figure 100. | Dielectric vs. Discharge Time (NH ₄ Cl) (Charge≠Discharge) | 105 |
| Figure 101. | Energy Density vs. Discharge Time (NH ₄ Cl) (Charge≠Discharge) | 106 |
| Figure 102. | Power Density vs. Discharge Time (NH ₄ Cl) (Charge≠Discharge) | 107 |
| Figure 103. | Capacitance vs. Discharge Time (NaNO ₃) (Charge≠Discharge)..... | 108 |
| Figure 104. | Dielectric vs. Discharge Time (NaNO ₃) (Charge≠Discharge) | 109 |
| Figure 105. | Energy Density vs. Discharge Time (NaNO ₃) (Charge≠Discharge) | 110 |
| Figure 106. | Power Density vs. Discharge Time (NaNO ₃) (Charge≠Discharge)..... | 111 |
| Figure 107. | Capacitance vs. Discharge Time (KOH) (Charge≠Discharge)..... | 112 |
| Figure 108. | Dielectric vs. Discharge Time (KOH) (Charge≠Discharge)..... | 113 |
| Figure 109. | Energy Density vs. Discharge Time (KOH) (Charge≠Discharge) | 114 |

| | | |
|-------------|---|-----|
| Figure 110. | Power Density vs. Discharge Time (KOH) (Charge≠Discharge)..... | 115 |
| Figure 111. | Capacitance vs. Discharge Time (All Salt Solutions) (Charge≠Discharge)..... | 116 |
| Figure 112. | Dielectric vs. Discharge Time (All Salt Solutions) (Charge≠Discharge)..... | 117 |
| Figure 113. | Energy Density vs. Discharge Time (All Salt Solutions) (Charge≠Discharge)..... | 118 |
| Figure 114. | Power vs. Discharge Time (All Salt Solutions) (Charge≠Discharge) | 119 |
| Figure 115. | Ragone Plot of Supercapacitors vs. Batteries with NH ₄ Cl 30 wt% and KOH 30 wt%. Adapted from [18]...... | 121 |
| Figure 116. | Basic Circuit Diagram of a Capacitor (Left) and the Associated Voltage vs. Time Charge Cycle (Right). Source: [19]...... | 128 |
| Figure 117. | Current vs. Time Discharge Cycle of a Generic Capacitor. Adapted from [20]. | 128 |
| Figure 118. | Capacitance vs. Discharge Time (220 mF) (Charge=Discharge) | 133 |
| Figure 119. | Capacitance vs. Discharge Time (220 mF) (Charge≠Discharge) | 134 |
| Figure 120. | Capacitance vs. Discharge Time (470 mF) (Charge=Discharge) | 135 |
| Figure 121. | Capacitance vs. Discharge Time (470 mF) (Charge≠Discharge) | 136 |
| Figure 122. | Capacitance vs. Discharge Time (1 F) (Charge=Discharge) | 137 |
| Figure 123. | Capacitance vs. Discharge Time (1 F) (Charge≠Discharge) | 138 |
| Figure 124. | Capacitance vs. Discharge Time (2.2 F) (Charge=Discharge) | 139 |
| Figure 125. | Capacitance vs. Discharge Time (2.2 F) (Charge≠Discharge) | 140 |

LIST OF TABLES

| | | |
|----------|--|-----|
| Table 1. | Sample Site Nanotube Lengths..... | 24 |
| Table 2. | Sample Site Nanotube Lengths with Outliers Removed..... | 25 |
| Table 3. | Charge and Discharge Schedule | 40 |
| Table 4. | Data Extrapolated to 10 and 100 Seconds for Charge Equals Discharge Rate Tests..... | 123 |
| Table 5. | Data Extrapolated to 10 and 100 Seconds for Fixed Charge Rate Tests | 124 |

THIS PAGE INTENTIONALLY LEFT BLANK

LIST OF ACRONYMS AND ABBREVIATIONS

| | |
|--------------------|--|
| a | Acceleration |
| C | Capacitance |
| d | Distance |
| DI | Deionized Water |
| DMSO | Dimethyl Sulfoxide |
| EDLC | Electric Double Layer Capacitors |
| EMALS | Electromagnetic Aircraft Launch System |
| F | Farad |
| FEL | Free Electron Laser |
| F-SDM | Fabric Super Dielectric Material |
| Hz | Hertz |
| J | Joules |
| J/cm ³ | Joules per Cubic Centimeter |
| kg | Kilograms |
| KOH | Potassium Hydroxide |
| m | Meters |
| m ³ | Cubic Meters |
| M | Mass |
| mA | Milliamperere |
| MJ | Megajoule |
| m/s | Meters per Second |
| m/s ² | Meters per Second per Second |
| MW | Megawatt |
| N | Newton |
| NaCl | Sodium Chloride |
| NaNO ₃ | Sodium Nitrate |
| NH ₄ Cl | Ammonium Chloride |
| NMP | N-Methyl-2-Pyrrolidone |
| NP | Novel Paradigm |
| NPS | Naval Postgraduate School |

| | |
|--------|------------------------------------|
| NTSDM | Nanotube Super Dielectric Material |
| PPC | Polypropylene Carbonate |
| RC | Resistor-Capacitor |
| ρ | Density (Rho) |
| SDM | Super Dielectric Material |
| t | Time |
| TiO | Titanium (II) Oxide |
| USN | United States Navy |
| v | Velocity |
| V | Volts |
| W | Watts |
| wt | Weight |

ACKNOWLEDGMENTS

I would like to thank Professor Jonathan Phillips for his creative ideas, limitless knowledge, and endless enthusiasm throughout my research. Your patience, while teaching me capacitor theory for the umpteenth time at the eleventh hour, was always gratefully appreciated. If research is a layer cake, we baked a nine-tier wedding cake for the ages.

I would like to thank Professor Hugo Zea for walking me through the anodization process multiple times on late Friday afternoons, Professor William Wu for guaranteeing the SEM's safety from my more "graceful" moments, and Professor Claudia Luhrs for explaining complex topics at the basement level that I could understand. I could not have survived Naval Postgraduate School without your guidance and I am forever in your debt.

Lastly, I would like to thank my family; my parents, Mary and Fred, for their untold optimism when my confidence wavered, and my siblings, Vincent and Sandra, for their covert encouragement when deflating my bloated ego. Words cannot describe how grateful I am for your unconditional love and steadfast support.

THIS PAGE INTENTIONALLY LEFT BLANK

I. INTRODUCTION

This research builds on previous projects conducted at the Naval Postgraduate School (NPS) designed to increase the performance of capacitors, specifically Novel Paradigm (NP) Supercapacitors. The NPS supercapacitor research group first demonstrated that aqueous salt solutions contained in inert matrices could be exceptional dielectrics using porous granulated material, such as aluminum oxide powder saturated with Deionized (DI) water and Sodium Chloride (NaCl) solutions [1]. The research group then demonstrated other oxide matrices saturated with salt-water solutions could be exceptional dielectrics [2]. Specifically, transition metal oxide nanotube arrays could be saturated with an aqueous solution to enhance the dielectric material values and form nanotube super dielectric materials (NSTDM) [2]. This type of structure was found to have remarkable energy density as high as 400 J/cm^3 at low discharge rates [2]. This research extends earlier efforts and provides details regarding the impact of controllable parameters including salt identity and concentration on NSTDM performance. Additionally, this thesis provides the first detailed data set for changes in capacitance, dielectric constant, power, and energy density for NSTDM as a function of discharge time. This temporal performance data is required by designers of pulse power systems.

A. MOTIVATION

The United States Navy (USN) continues to work toward an all-electric warship with exponentially increasing power requirements [3]. Power requirements are directly tied to the technological advancement in weapons for self-defense and offensive mission objectives. The inclusion of advanced weapon systems, in addition to an increase in ship's service requirements, would require power from prime mover generators to divert throughout the ship's electrical grid for weapon deployment [3]. This diversion of propulsion power would result in an exposed ship with greatly diminished propulsion capability during weapon engagement.

Utilization of high-power storage decouples power required to operate ship's propulsion from high-power systems, such as the railgun, Free Electron Laser (FEL), and

Electromagnetic Aircraft Launch System (EMALS). To operate these systems, energy storage devices require high energy density and high charge/discharge frequency. Batteries, capacitors, and fly-wheels are all under consideration at this time; each device has its advantages and disadvantages [3].

The Pentagon is committed to development of the railgun. After more than a decade of research and \$500 million invested, power requirements continue to be an issue of concern; each railgun shot requires 32 MJ of energy [4]. This exceeds the output of most ships currently in the USN fleet. Currently, the only ship capable of the required output is the Zumwalt-class destroyer [4] but only if the vessel is stationary at the launch location without any power diverted to its main propulsion. As mentioned by Bennett [4], “New capacitors, more resistant materials and better pulse power storage systems could all contribute to making the railgun more efficient.” Due to a Nunn-McCurdy Amendment Breach, the Zumwalt-class destroyer will be reduced to a fleet of three [5]. Unless energy storage methods can be reduced in size, additional ships in the USN fleet will be unable to accommodate the railgun. Utilizing values from Stewart [6], shown in Appendix A, calculations are conducted to estimate the capacitor volume to fire the weapon is 31 m^3 .

Ultimately, the ideal capacitors would match the energy density of the best batteries. At this time, Lithium Ion batteries are approximately measured at 2880 J/cm^3 [7]. If current capacitors could, at a minimum, meet the 1000 J/cm^3 [8] threshold, the volume of the capacitors required to launch railgun projectiles would be reduced to $9.38\text{E-}1 \text{ m}^3$. This reduces the size of the required capacitor bank by a factor of 30.

Another weapon requiring tremendous power is the FEL. The FEL is a ship mounted self-defense apparatus that uses a laser beam to transfer significant energy to an approaching target in order to raise the temperature of the target beyond its design limit [9]. The material of the approaching target will either fail by deterioration of the metal superstructure or by overheating explosive components to the point of detonation. The remaining fragments fall to the ocean surface as the projection path has been altered by target’s collapse. Current estimates by the Office of Naval Research expect the laser to require approximately 100 kW [10] power output for a maximum of 10 seconds [9].

Based on the power storage data from [7], these requirements correspond to capacitor bank volume of $1.5\text{E-}1 \text{ m}^3$.

A third device requiring high power is the EMALS. It is expected to replace steam technology on the new Gerald R. Ford-class aircraft carriers. The main goal of replacing antiquated steam catapults is to reduce the overall footprint of the machine's space and limit the use of chemicals used during maintenance and operation of the launch system. Energy storage devices play a key role in the footprint of the system's design. The smallest aircraft is required to launch at 100 m/s and contact time with the ship deck is approximately 2 seconds [11]. This requires an acceleration of 50 m/s^2 [6]. Using this acceleration and the largest expected aircraft weight of 45,000 kg [12], the required force to attain the desired launch velocity is $2.25\text{E}6 \text{ N}$. Using current supercapacitor technology, the launch force corresponds to a capacitor bank volume of 750 m^3 . This value is corrected to adjust for capacitor inefficiencies as done with the calculated railgun values in Appendix A. Utilizing the ideal value of 1000 J/cm^3 , the corresponding capacitor bank volume would be reduced to 22.5 m^3 . As with all previous calculations, this volume includes the correction factor for inefficiencies during discharge. Calculations are covered in their entirety in Appendix B.

Given the clear need for a smaller capacitor footprint for the systems powering new electric systems shipboard, such as the railgun, the USN is considering many options. This thesis regards improving and understanding one of those options, an option conceived and developed at the Naval Postgraduate School: NP Supercapacitors. In particular, this thesis is concerned with an accurate evaluation of the ability of novel electrical energy storage devices to deliver power over very short time periods.

At this time, only low frequencies, on the order of 10^{-3} Hz , have been analyzed using the Resistor-Capacitor (RC) time constant method [2]. Porous powder based materials saturated with liquid into a paste and anodized metal foils with a regular array of hollow nanotubes filled with liquid have demonstrated energy densities greater than 500 J/cm^3 at low frequencies of approximately 10^{-2} Hz [2]. This is significantly higher than traditional dielectric materials, but does not answer the questions regarding power

delivery from the NP supercapacitor over time periods more relevant to the USN on the order of 100 Hz.

The objective of this thesis explored a particular class of NP supercapacitors, specifically NP supercapacitors employing NTSDMs with different salt mixtures. Research was designed to characterize these systems thoroughly, such that engineering calculations regarding the size of an NP supercapacitor bank required for USN applications could accurately be predicted. In particular, this required measurements of performance as a function of frequency. There is no basis for predicting this performance from existing data and therefore required SDM evaluations as a solution to the USN's energy storage requirements.

Conducting a set of experiments, with a promising class of SDM lends itself to building a library of potential candidates for future work. Specifically in this thesis, NP supercapacitors made using SDM consisting of anodized titania metal foils saturated separately in three concentrations of NH_4Cl , NaNO_3 , and KOH solutions. After a 15 minute saturation period, the NP supercapacitors were tested for the key parameters of capacitance, dielectric constant, energy density and power density as a function of frequency with a modern galvanostat. Utilizing the standard definition equation for capacitance as seen in Equation 1, the prediction model of SDM performance utilizing the three selected salts was refined. A final comparison to a distilled water and select supercapacitors was conducted.

$$C = \frac{q}{V} \tag{1}$$

q = Number of charges on the electrodes

V = Net voltage between electrodes

C = Capacitance

B. BACKGROUND

Capacitors first discovered in the 1700s utilized water as the dielectric material between conductive plates [13]. Starting in the late 19th century, commercially manufactured capacitors relied on solid dielectric materials to meet specifications for newly invented radios with increasing frequency ranges [13].

Solid dielectric materials, although excellent as electronic circuit elements in tuners, rectifiers, and computer memory have been found to be poor devices for energy storage [13]. In contrast to the SDM seen in Figure 2, solid dielectrics have a finite ability to polarize limited energy density and fail to meet USN requirements for the projected energy storage and power delivery requirements of future USN all-electric ships. In response to the needs of the USN and other technologies for increases in the energy density/power delivery characteristics of capacitors, there has been a wave of research and development of new capacitor technologies.

To understand the various research and development efforts undertaken, it is necessary to understand the fundamentals of energy storage in a capacitor. The basic design of a capacitor is two parallel plates store energy with an abundance of electrons on a single plate. The application of a voltage source, such as a battery, leads to electrons collecting at the negative plate, and an equal number of electrons leaving the positive plate. The capacitor as a whole is net neutral. This is equivalent to a flow of electrons through the circuit from positive plate to the negative plate. By removing the charging power source and failing to provide a conductive path between plates, electrons are in theory stored on the negative plate. The plates are separated by a dielectric material that not only insulates the plates from short-circuiting but increases, relative to air, the amount of charge stored at a given voltage. These ideas are expressed mathematically for a parallel plate capacitor in Equation 2.

$$C = \frac{\epsilon\epsilon_0 A}{t} \quad (2)$$

A = Electrode area

t = Thickness of the dielectric

ϵ = Dielectric constant of the material

ϵ_0 = Permittivity of air, 8.85E-12 [Farad/m]

Further review of Equation 2 showed the capacitance of a parallel plate capacitor can be increased by three controllable factors; cross sectional area, dielectric thickness, and dielectric constant. To date, nearly all modern research in capacitors has been designed to increase the surface area, (A); this is the basic technology associated with Electric Double Layer Capacitors (EDLC) more commonly known as supercapacitors [8]. Supercapacitors employ high surface areas of conductive material in place of metal plates. In practice, this reduces to inexpensive carbon materials.

As displayed in Figure 1, the Ragone chart lists supercapacitors as having high power and energy densities [14]. Batteries have excellent energy density but lack power. This translates into the inability to discharge at the required speeds for USN applications. Traditional electrolytic capacitors have excellent power but lack energy density. This translates into the quick discharge times but with an inability to store the energy required for USN applications. Although Figure 1 appears to place supercapacitors as the perfect device for USN applications, this research has shown supercapacitors cannot discharge power at the required rates or equal to the best electrolytic capacitors.

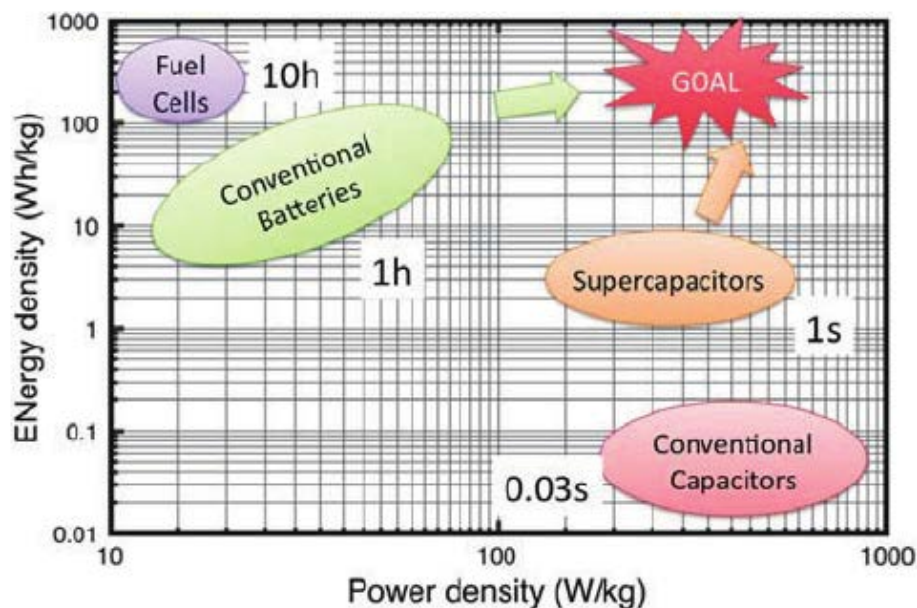


Figure 1. Ragone Chart Graphically Compares Energy Density to Power.
Source: [14].

This work completed at NPS by Gandy [2], Fromille [8], and Cortes [15] demonstrated an entirely new means to increase energy density, as per Equation 2. As an alternative to simply increasing the surface area of the electrodes, the NPS NP supercapacitor group demonstrated that unprecedented dielectric constants could be attained using solutions containing dissolved salts held in insulating matrices formed by nanotube anodization. The first example of such a material was NaCl dissolved in water with porous alumina added to the solution to increase conductivity. In the earliest work, Fromille and Phillips [8] demonstrated porous alumina, sufficiently filled with NaCl dissolved in water to create 'paste'-like material, consistently had dielectric constants on the order of 10^9 . Previous to this work it was believed barium titanate, with dielectric constants no greater than 10^4 had the highest dielectric constant of any material.

A simple model was postulated to explain the result: Dissolved ions in solution within the dielectric of a parallel plate capacitor move under the influence of an applied field to create dipoles equal to the length of the pore containing the ionized liquid. As seen in Figure 2, these dipoles create fields that oppose the field created by electrons on the electrodes. That is, due to an opposite polarization of the dipoles in the dielectric to

the charges on the plate, at every point in space the dielectric dipole fields are opposite in direction to the 'two plate' dipole created fields.

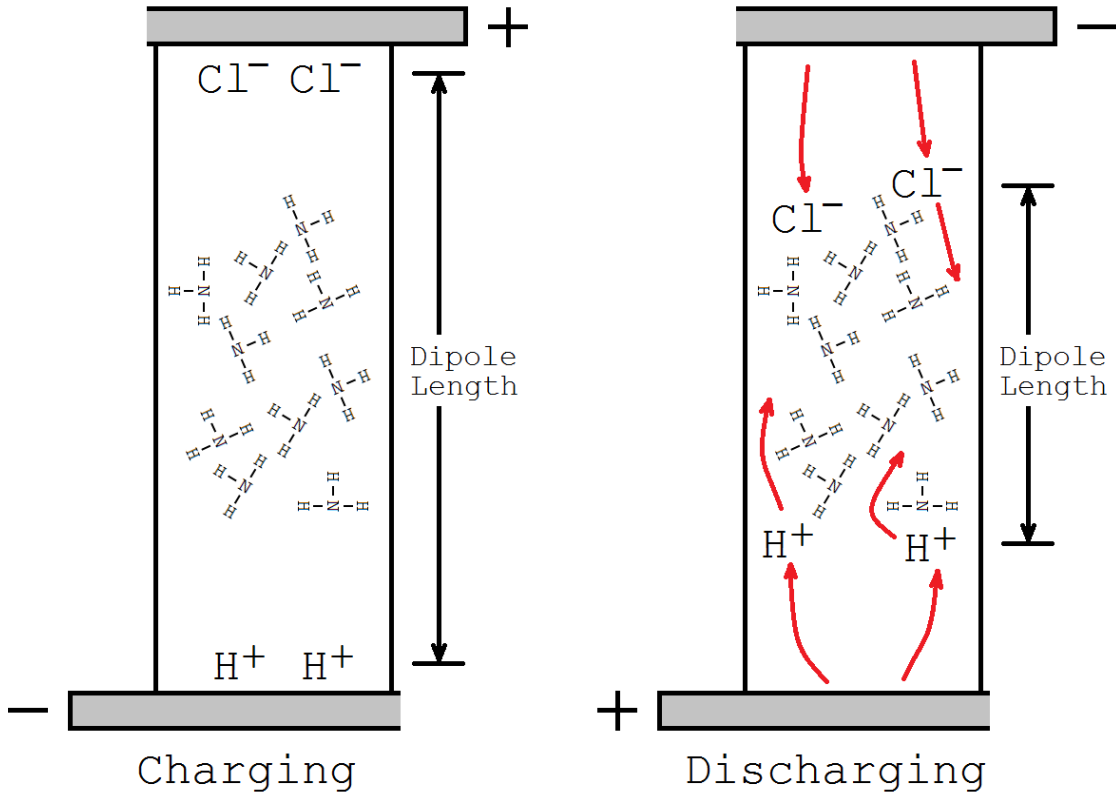


Figure 2. Graphical Representation of Decreasing Dipole Length

As the net value of a field at any point in space is the sum of the field created by every charge, where \mathbf{r} is a vector directed along a line connecting the charge and the point in space, and \mathbf{E} is also a vector:

$$\vec{\mathbf{E}} = \sum_{i=1}^{\infty} \frac{q_i}{\mathbf{r}_i} . \quad (3)$$

The dipole fields from the dielectric reduce the net magnitude of the field created by the capacitor at every point in space. Since voltage, a measure of electron energy is integral of the field over path:

$$V = \int \vec{E} \cdot d\vec{l}, \quad (4)$$

where the path is measured from infinity to the plate and the field is lowered by the dipoles at every point along the path. The voltage associated with each new electron attached to the plate is concomitantly lowered by the presence of the dipoles. Thus, capacitance, $C=q/V$ is raised because voltage (V) is lowered. The same analysis applies to solid-state dielectrics, but in solid-state dielectrics the dipoles are tiny, no more than 0.1 Å [16]. Calculations suggested the field lowering effects, and similarly capacitance increases, of large dipoles formed from ions in a liquid drop should be thousands of times larger than that created by small dipoles in a solid state dielectric. The actual observed increase in capacitance, even in the first study, was closer to a million.

As noted previously, capacitance increases linearly with increases in dielectric constant. Moreover, energy of a capacitor follows this simple equation:

$$Energy = \frac{1}{2} CV^2 \quad (5)$$

Thus, energy will increase with increasing capacitance. Given the finding that capacitance could be increased by many orders of magnitude indicated the super dielectric materials invented at the Naval Postgraduate School could lead to significant increases in energy density [8].

Simply inventing a better dielectric proved to be only the first step in making the energy density of SDM based capacitors equal that of highly evolved supercapacitors. In fact, it can easily be shown that the energy density of an electrostatic capacitor is given by this equation:

$$EnergyDensity = \left(\frac{1}{2} \right) \left(\frac{\epsilon\epsilon_0 V^2}{t^2} \right) \quad (6)$$

Higher energy density requires an increasing dielectric constant and minimizing distance between plates. The powder based dielectrics developed in the early SDM studies proved to be difficult to use in very thin dielectric layers [1]. That is, the actual

value of the distance (t) between electrodes was too high, even with the very large dielectric values, for high energy density to be realized.

The next step carried out at the NPS, was creating high energy density SDM based capacitors, so called NP Supercapacitors, employing anodized titanium films [2]. The anodization process creates an apparently perfect geometry, for high capacitance according to the SDM theory. That is, the anodized film consists of an insulating material, titanium dioxide, arranged in columns perpendicular to the original metal surface [2]. In general, these columns are only a few microns high. The spaces between these columns are voids, shaped like perfect cylinders. Filling these void spaces with salt-water, and placing this material between the electrodes of a parallel plate capacitor, should result in the generation of perfectly oriented large dipoles with high dielectric values, and simultaneously a small value of ' t ' as required to maximize energy density.

More recently, the NPS team provided an additional demonstration of the SDM hypothesis where any electrically non-conductive matrix containing liquid with a sufficient concentration of dissolved ions will have a very high dielectric constant on the order of 10^9 . This new type of SDM was based on nylon fabric saturated with salt water otherwise known as Fabric Super Dielectric Materials (F-SDM); as seen with F-SDM, as the frequency of the charge-discharge cycle increases, the capacitance and energy density decrease [17]. This is of specific concern to the USN, as the desired applications are expected to occur in less than two seconds and not the currently tested 50 seconds. Unlike commercial capacitors, nanotube and fabric SDMs will demonstrate symmetric discharge patterns at with respect to the applied voltage [17].

Building on the previous research, the NPS team took advantage of SDM theory to lengthen dipoles to their maximum potential within the nanotube cavity. Utilizing additional salt identities and fluctuating concentration, this research continued to build an understanding of which ionic molecules are best suited for dissolution in an aqueous solution. This provided the highest dielectric values resulting in exceptional energy densities. In addition to salt identity and concentration, this research was the first to observe the correlation of NTSDM performance as a function of frequency. Data collected supports SDM theory demonstrating as frequency increases, the effective dipole

length is reduced and dielectric values decrease on a power log scale. Figure 2 demonstrates the reduction of the effective dipole that occurred when the electric field was removed. As long as the electric field existed, the ions created a sufficient dipole that was equal and opposite of the electric field created by a power source. When the power source was removed, the ions moved to reach a relaxed state at a shorter dipole length. When frequency was increased to very high levels, the ions were physically unable to move at the required rate to cancel the field and a phase shift was created between the direction of the electric field vector and the dipole vector. In terms of ability to store energy, as frequency increased the effective dipole length decreased confirming capacitance and energy density decrease.

THIS PAGE INTENTIONALLY LEFT BLANK

II. EXPERIMENTAL METHODS

A. ANODIZATION PROCESS AND SAMPLE PREPARATION

Preparing the anodized titania nanotube sample was a three-step process: sample preparation, solution preparation, and system set-up.

1. Sample Preparation

Tools used to accomplish sample preparation are shown in Figure 3. A Sharpie permanent ink marker and SI ruler were used to mark the sheet of titanium where the material will be cut. Sharp scissors were used to cut the 99.65% pure titanium of 0.05 thickness into 1 cm by 3 cm anodes and one cathode measuring 1.5 cm by 3.5 cm. The remaining tools in Figure 3 were used during the anodization process.



Figure 3. Anodization Materials and Tools

While wearing latex gloves, forceps were sterilized with ethanol. Holding each anode sample with the sterilized forceps and the samples were rinsed with ethanol. Finally, the anode sample was placed in a clean test tube with approximately 10 ml of fresh ethanol. The sample was placed aside to soak for 15 minutes. The entire sample was submerged in ethanol during the soak period. Repeat the same steps as the anodes for the cathode. As shown in Figure 4, all anode samples and one cathode are now prepared in individual sample test tubes.

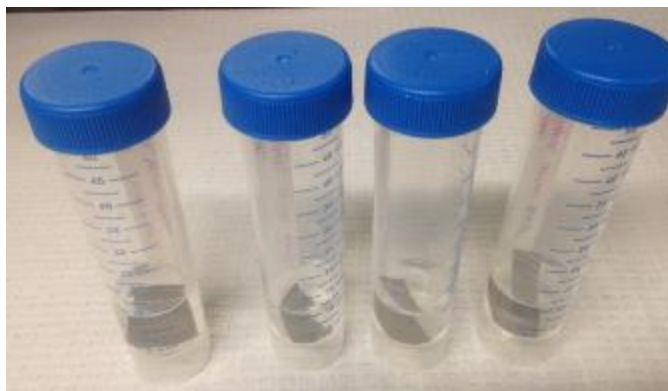


Figure 4. 15-Minute Anode Soak Period in Ethanol

2. Solution Preparation

To prepare the solution, utilize a clean sample cup to mix the solution in. Place the cup on the digital scale and zero the scale. As shown in Figure 5, make an axial cut on the stir stick to create a miniature scoop. As shown in Figure 6, cut off the excess stir stick so that it does not interfere when scooping Ammonium Fluoride (NH_4F) from the container. Utilizing a plastic spoon or modified plastic stir stick, add $13.58\text{E}-2$ grams of NH_4F to the sample cup, working quickly to return the NH_4F to its desiccant storage container to avoid moisture contamination. Figure 7 shows the correct amount of NH_4F has been added to the reactor vessel on the scale.



Figure 5. Stir Stick Modification Using Scissors



Figure 6. Modified Stir Stick for Ammonium Fluoride

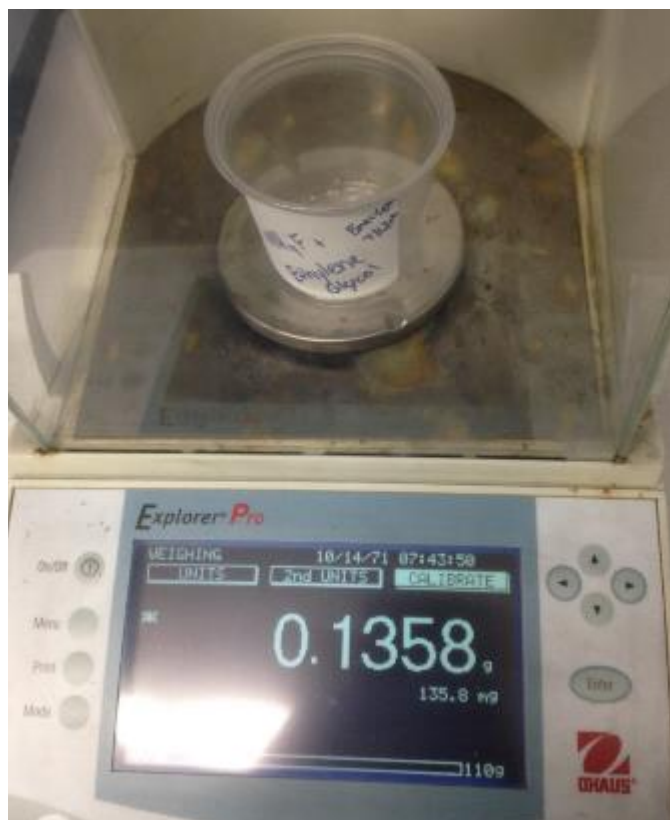


Figure 7. Ammonium Fluoride Measured into the Reactor Vessel

Zero the scale. Utilizing a pipet, add 1.6 ml of distilled water to the sample cup to dissolve the NH_4F shown in Figure 7. Shake the sample instead of stirring to avoid fiber contamination of the solution. Use a graduate cylinder that has been washed with distilled water and allowed to air dry to add 80 ml of Ethylene Glycol to the solution. If the solution must be stirred, utilize a clean plastic spoon or plastic stir stick. Figure 8 shows the solution is now prepared and ready to anodize samples.

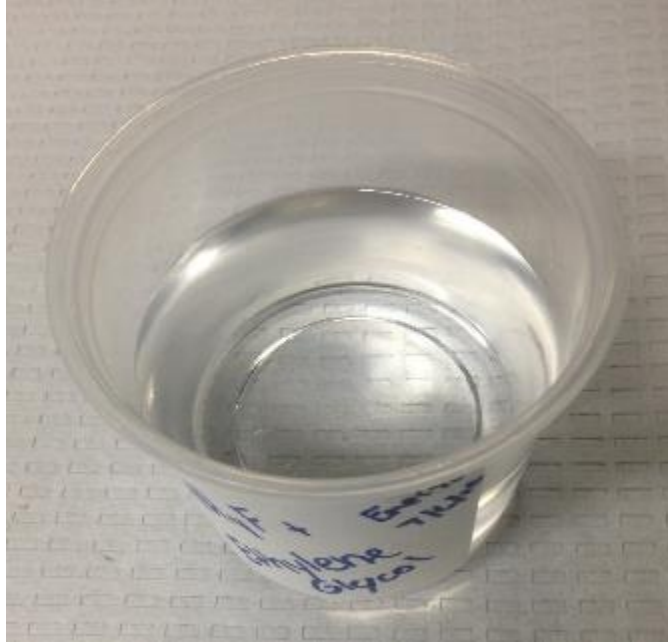


Figure 8. Completed Anodization Solution with Added Ethylene Glycol

3. System Set-up

The last step for anodization preparation is system set-up. Three Power Design INC. Transistor Power Supply Model 4005 voltage generators, shown in Figure 9, are set in series and utilized to adjust the voltage to approximately 20 Volts each. A multimeter, shown in Figure 10, is used in parallel to verify the cumulative voltage is set to 60 Volts.

Figure 11 shows the use of chemistry support stands to bridge a spring across a sample lift plate. This spring will serve to mount the alligator clips that hold the anode and cathode at the proper orientation in the solution.



Figure 11. Stand Set-up to Suspend Samples above the Reactor Vessel

Utilizing sterile locking forceps, shown in Figure 12, remove the cathode from the test tube and rinse with distilled water. Air-dry the cathode in front a blow dryer. The cathode should have a mirror finish at this time. If a mirror image is not observed, repeat the rinsing and drying steps until a mirror finish is present. Carefully mount the cathode to the alligator clip connected to the negative terminal of the last voltage generator.



Figure 12. Plastic Locking Forceps and Scissor Lift

Remove the anode sample from the test tube and repeat the same rinsing steps as was completed with the cathode. More so than the cathode, it is imperative the anode sample has a mirror surface. Mount the anode to the alligator clip connected to the positive terminal of the first voltage generator. Verify the voltage is set to 60 Volts. Ensure the anode is mounted directly in front of the cathode. This is verified by viewing the cathode at a perpendicular distance of approximately 20 cm. The anode should be completely concealed behind the cathode. If any edges are visible, adjust the anode using forceps. The samples should be positioned parallel to one another and separated by approximately 2 cm. As shown in Figure 13, raise the lift tray so that approximately 2 cm of the anode are submerged in the anodization solution. Start a countdown timer for 46 minutes.

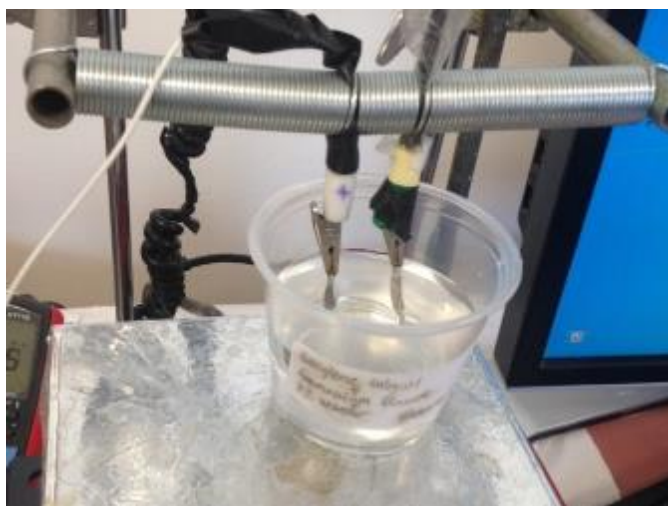


Figure 13. Anode and Cathode Submerged in the Reactor Vessel

If the system is working correctly, bubbles should form immediately on the cathode and the anode should begin to turn gold in color. Figure 14 displays the discoloration of the anode that is expected to occur as the oxidation layer begins to grow. When 46 minutes has elapsed, turn the power supply off to the voltage generators. This will stop the anodization process with anodized nanotubes measuring 8 μm in nominal length. The length must be verified with SEM images.

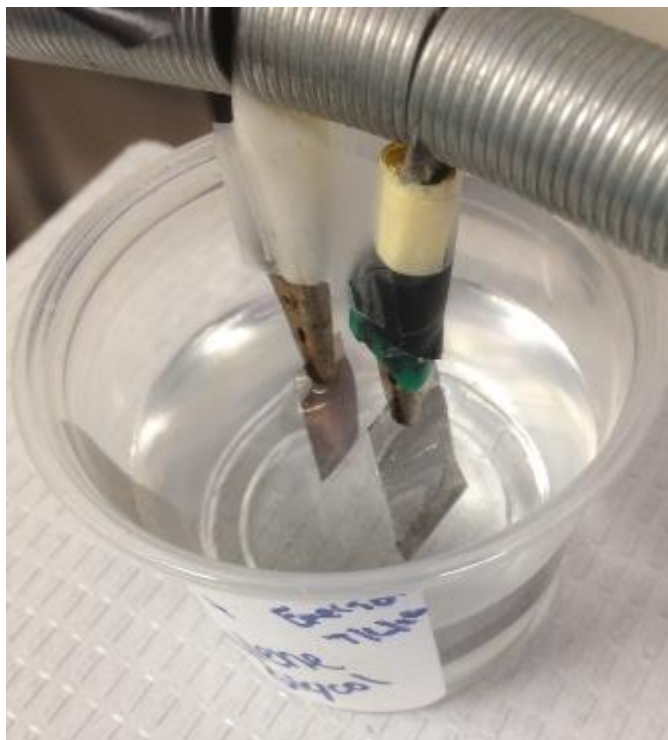


Figure 14. Close-up of the Anode (right) and Cathode (left) Alignment

Using forceps, remove the anode from the alligator clip and rinse with ethanol. After the ethanol rinse, use distilled water to rinse the anode samples. Use a heat gun (Master Model HG-301A) on low to air dry the samples. Place the completed sample in a clean, dry test tube. Repeat these steps for the cathode. Label each anode sample with date, sample number, and test tube contents. Properly dispose of the solution mixture in accordance with institute policy.

B. SEM OPERATIONS

1. Sample Preparation

Samples are prepared for the SEM by placing in a vacuum chamber for 24 hours. Seen in Figure 15, the vacuum chamber used at NPS is a Pelco 2251 Vacuum Desiccator with W. M. Welch Vacuum Pump powered by a General Electric 0.5 horsepower 1725 rpm AC electric motor and Balston Filter. The vacuum chamber is set to 30 inHg.

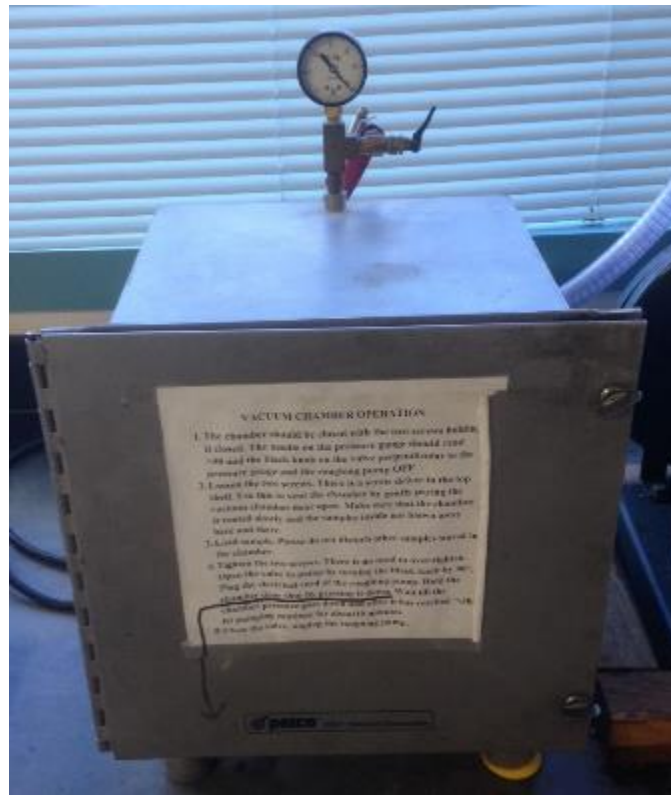


Figure 15. Pelco 2251 Vacuum Desiccator

Figure 16 demonstrates how the three TED PELLA, INC. aluminum specimen mounts with TED PELLA, INC. 9 mm OD Pelcon carbon tape are prepared for sample mounting. Figure 17 displays how the samples are mounted to the carbon tape at the very ends where the titanium substrate is exposed and no risk to the anodization layer occurs upon removal.



Figure 16. SEM Individual Sample Mounts with Attached Carbon Tape

Additionally, Figure 17 shows the individual samples with specimen mounts installed on the multi-specimen mount in the radial pattern. The multi-specimen mount is labeled to assist with identifying samples after sealing in the SEM chamber. Before sealing the SEM chamber, sharp forceps are used to create 2–3 small dimples in the samples to expose nanotubes on edge. The dimples are located below the transition zone and above the 2 cm test area of the sample.

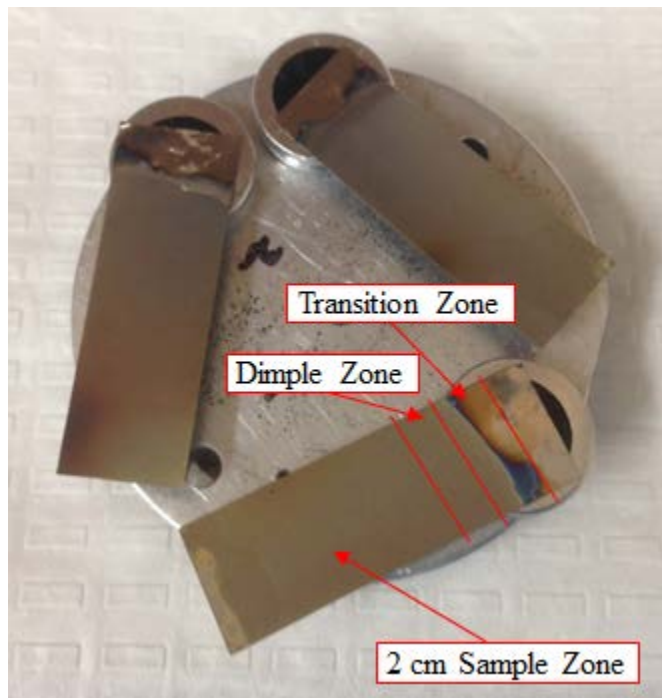


Figure 17. Three Samples Mounted to the Multi-mount and Clearly Labeled for Identification in the SEM Vacuum Chamber

A Zeiss Neon 40 Scanning Electron Microscope is utilized to view the samples. After the vacuum pumps have sufficiently reduced the chamber atmosphere, the Electron High Tension is set to 20 kV. The working distance is adjusted for each sample and approximately set to 6.5 mm. Magnification is nominally set to 10 times magnification. Each sample dimple location is viewed for nanotubes that are intact and on edge in order to accurately measure the nanotube length. A minimum of four nanotube sites are measured on each sample to determine a nominal length to be used for calculations.

2. Image Analysis

Five samples were analyzed in the SEM. Due to the carbon tape, a great deal of care was taken to remove the samples from the individual mounts. This often damaged the anodization substrate and therefore a limited numbers of samples were viewed under the microscope to ensure a maximum number of samples could be tested with salt solutions. As seen in Table 1, a minimum of four sites were viewed on each sample.

Table 1. Sample Site Nanotube Lengths

| Sample | 1 | 2 | 3 | 4 | 5 |
|---------|-----------------------------|-----------------------------|-----------------------------|-----------------------------|-----------------------------|
| Site | Length [μm] |
| 1 | 10.26 | 9.301 | 6.105 | 7.543 | 2.907 |
| 2 | 4.903 | 9.591 | 5.498 | 7.821 | 3.052 |
| 3 | 11.17 | 7.328 | 6.098 | 7.899 | 2.718 |
| 4 | 10.03 | 10.87 | 5.128 | 7.840 | 4.004 |
| 5 | 5.882 | | 6.260 | | 4.371 |
| 6 | 6.854 | | | | 3.3118 |
| 7 | | | | | 6.674 |
| 8 | | | | | 4.289 |
| 9 | | | | | 4.354 |
| 10 | | | | | 4.852 |
| 11 | | | | | 4.178 |
| 12 | | | | | 4.173 |
| 13 | | | | | 4.074 |
| Average | 8.183 | 9.273 | 5.818 | 7.776 | 4.074 |
| | | | Overall Average | | 7.025 |

As previously stated, the nanotubes were viewed axially on the substrate. In order to measure the length, dimples were pressed into the sample below the transition zone as a method to dislodge full-length nanotubes to an orientation that could be accurately measured. Table 2 removes the outliers where the tube ends were intact but the overall measured length was below the average signifying the nanotube was not full length or not perpendicular to the field of view. The nominal length is 7.66 μm and rounded up to 8 μm for a conservative thickness for calculations. Using a conservative thickness value ensures the reported dielectric values, energy densities, and power are minimums.

Table 2. Sample Site Nanotube Lengths with Outliers Removed

| Sample | 1 | 2 | 3 | 4 | 5 |
|---------|-----------------------------|-----------------------------|-----------------------------|-----------------------------|-----------------------------|
| Site | Length [μm] |
| 1 | 10.26 | 9.301 | 6.105 | 7.543 | |
| 2 | | 9.591 | 5.498 | 7.821 | |
| 3 | 11.17 | | 6.098 | 7.899 | |
| 4 | 10.03 | 10.87 | 5.128 | 7.840 | 4.004 |
| 5 | | | 6.260 | | 4.371 |
| 6 | | | | | |
| 7 | | | | | |
| 8 | | | | | 4.289 |
| 9 | | | | | 4.354 |
| 10 | | | | | 4.852 |
| 11 | | | | | 4.178 |
| 12 | | | | | 4.173 |
| 13 | | | | | 4.317 |
| Average | 10.487 | 9.921 | 5.818 | 7.776 | 4.317 |
| | | | Overall Average | | 7.664 |

As seen in Figure 18, the anodized surface of the titanium substrate provides an evenly distributed matrix of nanotubes that can be saturated with salt solution. In contrast to experiments conducted by [2], the anodization process was optimized to ensure nanotubes retain the structure at each opening.

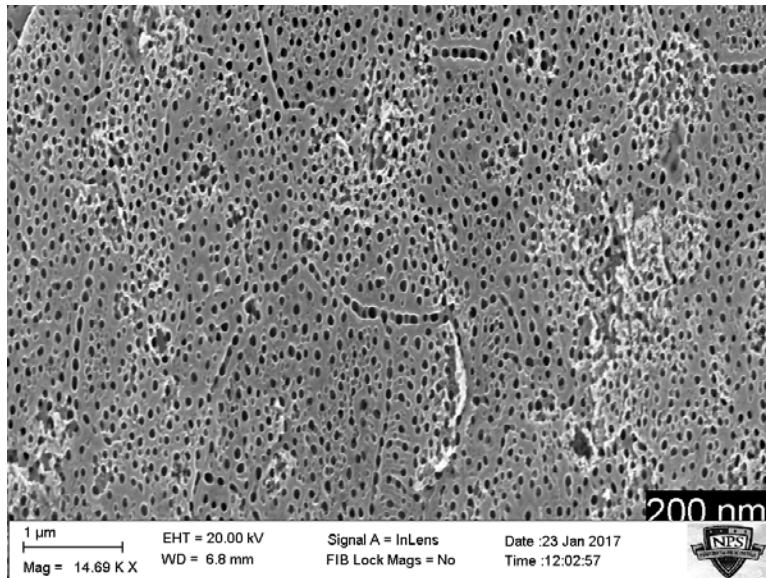


Figure 18. Titanium Dioxide Nanotube Surface

In Figure 19 the nanotubes have been removed to view the condition of the substrate. The remaining substrate displays the remnants of the nanotube end locations and the even distribution of the anodized lattice.

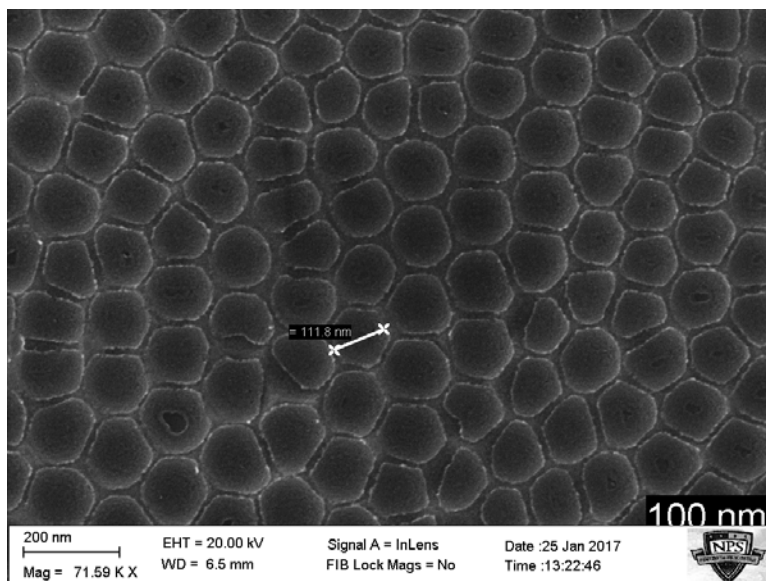


Figure 19. Exposed Titanium Substrate with Nanotubes Removed

Figure 20 displays the length of nanotubes on Sample 1 at Site 2. This is an example of an outlier that was disregarded due to nanotube orientation being skewed in relation to the viewing plane. Additionally, the existence of nanotube ends could not be confirmed and indicated the full length measured was inaccurate.

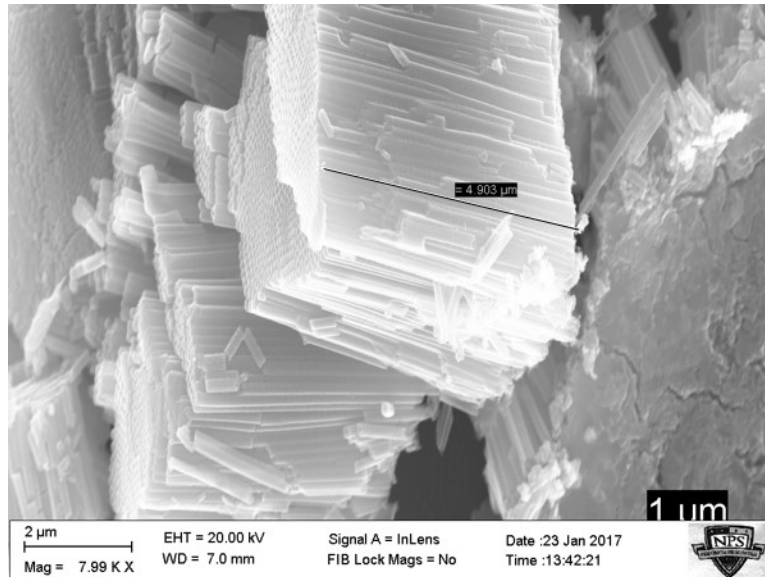


Figure 20. Nanotubes at Site 2 of Sample 1

Figure 21 displays the length of nanotubes on Sample 3 at Site 3. This is an example of an acceptable nanotube orientation being perpendicular to the viewing plane. The left side of the sample shows the rounded ends of the nanotubes are intact. The right side of the sample shows a nearly level landscape confirming the full length is measurable.

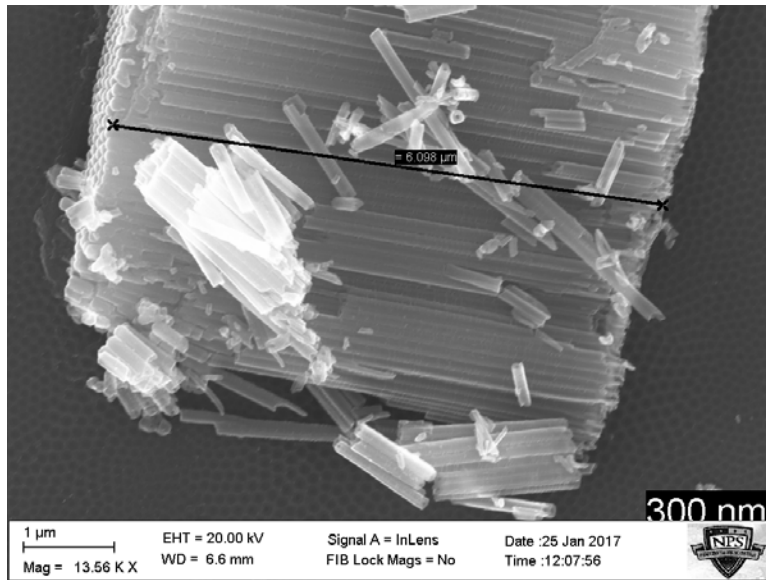


Figure 21. Nanotubes at Site 3 of Sample 3

Figure 22 displays the length of nanotubes on Sample 4 at Site 4. This is an example of an acceptable nanotube orientation being perpendicular to the viewing plane. The top of the sample shows the rounded ends of the nanotubes are intact. The bottom of the sample shows a nearly level landscape confirming the full length is measurable.

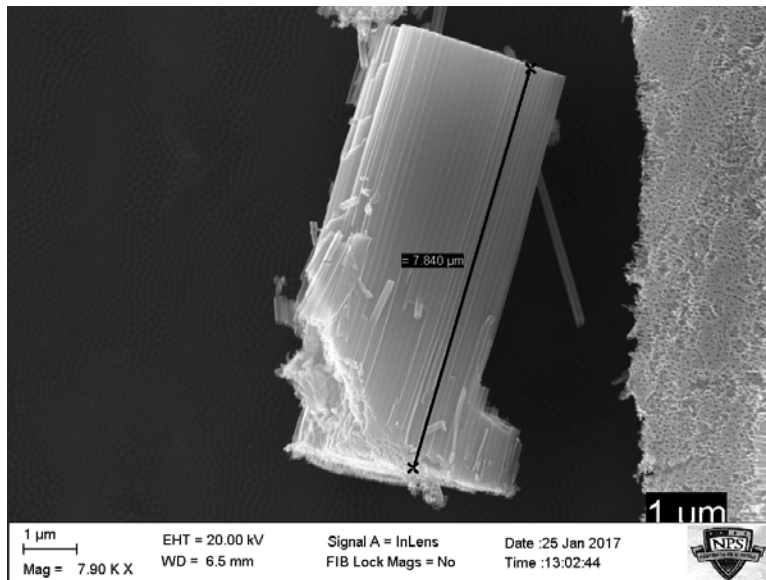


Figure 22. Nanotubes at Site 4 of Sample 4

C. TEST PROCEDURES

1. Test Apparatus Set-up

Figure 23 displays the materials used for sample testing includes multiple strips of Grafoil, transparent tape, two spring clamps (not shown), one modified clothespin, and two 7.6 cm long by 5 cm wide glass microscope slides.



Figure 23. Materials and Tools for Sample Capacitor Testing

Start by cutting the Grafoil into three strips that are 5 cm long by 0.8 cm wide. As oriented in Figure 24, use transparent tape to attach the Grafoil to one microscope slide adjacent and parallel to the shortest edge. One side will have two Grafoil strips stacked on top of one another. These strips of Grafoil will provide standoff distance between the top microscope slide and the Titanium Oxide sample. Without these spacers, the nanotubes are crushed when the spring clamps are applied and the capacitor will fail.



Figure 24. Microscope Slide with Grafoil Spacers Attached to the Edges

Next, cut a strip of Grafoil measuring 8 cm long by 0.8 cm wide. This strip of Grafoil will act as one half of the sample capacitor. Perpendicular to the strip, apply one 3 cm piece of transparent tape. Align the transparent tape to one long edge and Grafoil end to the opposite long edge of the microscope slide. As shown in Figure 25, use a clean lint free rag to gently wipe away any burrs or imperfections remaining from the scissors. This should be accomplished anytime the sample is changed to remove excess solution and decrease the likelihood of Grafoil creating a short to the Titanium substrate.

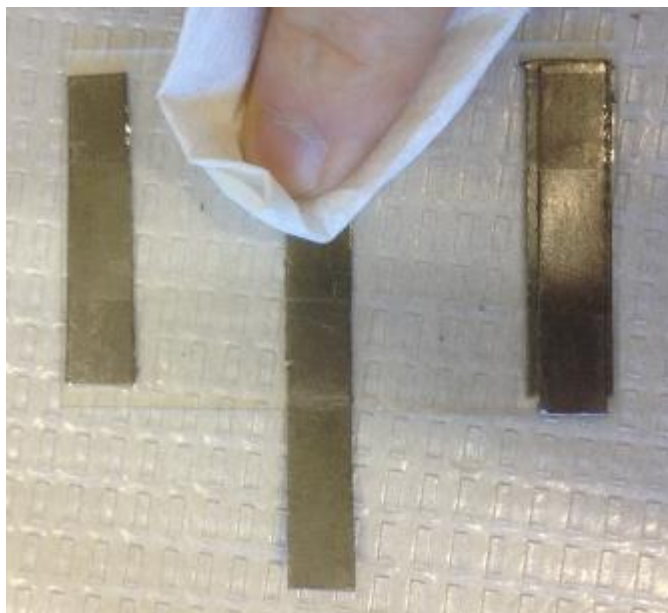


Figure 25. Center Test Electrode of Grafoil Attached and Wiped to Avoid Short-Circuits

Using a miter box saw, cut the tips off of the clothespin to form a blunt tips. Use of the modified clothespin reduces the crimp effect caused by the metal jaws of the alligator clip on the galvanostat input cable. Removing the tips allows for better adjustment of the sample on the Grafoil electrode. Cut a fourth strip of Grafoil measuring 10 cm by 0.8 cm long. Parallel to the strip, apply a small piece of transparent tape to the end. As shown in Figure 26, press the tape between the jaws of the modified clothespin and gentle wrap the Grafoil 1–2 rotations around one jaw.



Figure 26. Modified Clothespin for Mounting the Anodized Sample

Soak the sample in the test solution for 15 minutes. As oriented in Figure 27, with the Grafoil strips parallel to the work surface edge, lay the Titanium Oxide sample on the center Grafoil test strip. The non-anodized end should face opposite the Grafoil strip overhanging the microscope slide.

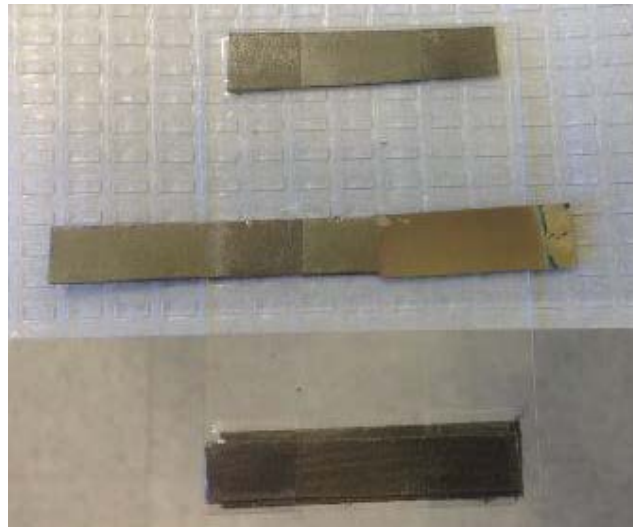


Figure 27. Microscope Slide Prepared with Arranged Anodized Sample

Place the second microscope slide on top to create a “sample sandwich” as shown in Figure 28. Using one spring clamp, brace down on one side of the test configuration.

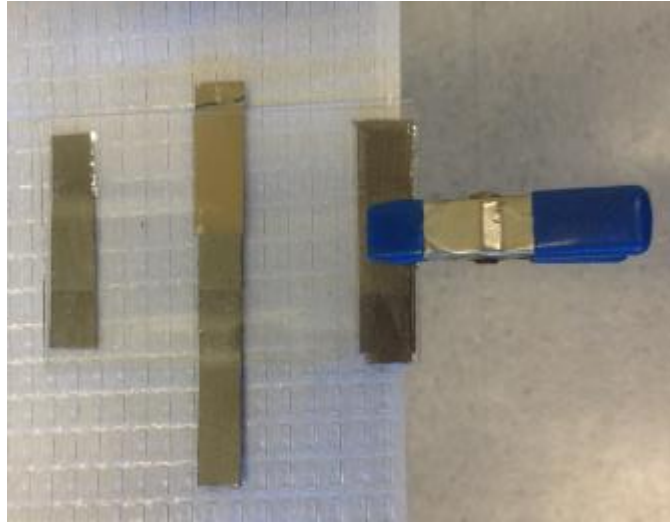


Figure 28. First Spring Clamp Installed to Secure Anodize Sample

Gently lift the test configuration and apply the second spring clamp to the opposite side as shown in Figure 29. The Titanium Oxide sample should be loosely secured between the two slides with minor movement for adjustments available. If the sample does not move, the user should add another Grafoil spacer to either side of the microscope slide or use weaker spring clamps.



Figure 29. Second Spring Clamp Installed to Complete the Test Rig Set-up

Move the test configuration to the galvanostat workstation. The Bio-Logic VSP 300 system was used in conjunction with the EC-Lab V11.02 software as shown in Figure 30.

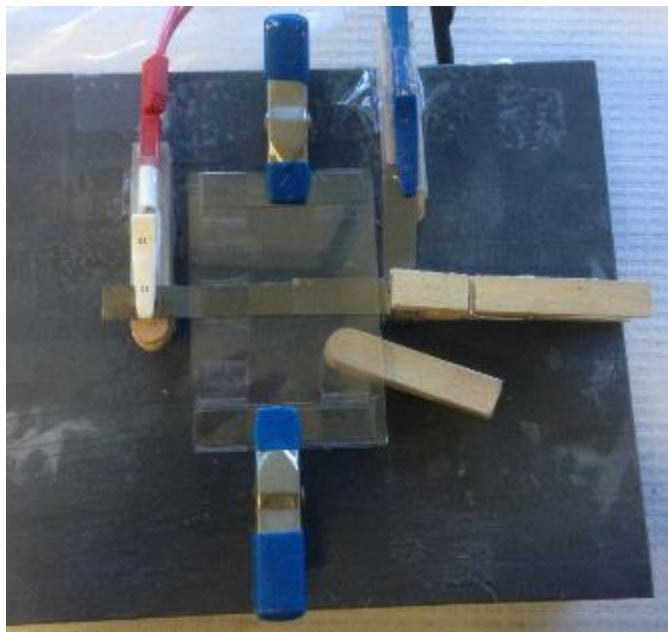


Figure 30. Anodized Sample Connected to the Biologic Equipment and Ready for Testing

2. EC Lab Software Set-up

Open the EC Lab software. In the left column under Parameter Settings, select the Turn to Modify Mode/Accept Modifications key as shown in Figure 31.

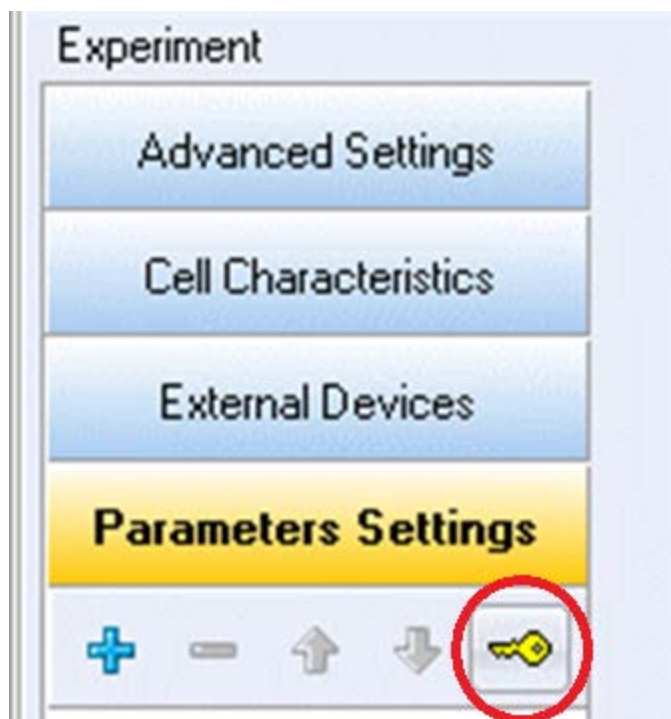


Figure 31. Depressing the Turn to Modify Mode Key for Experiment Set-up

Select New in the Experiment menu shown in Figure 32.

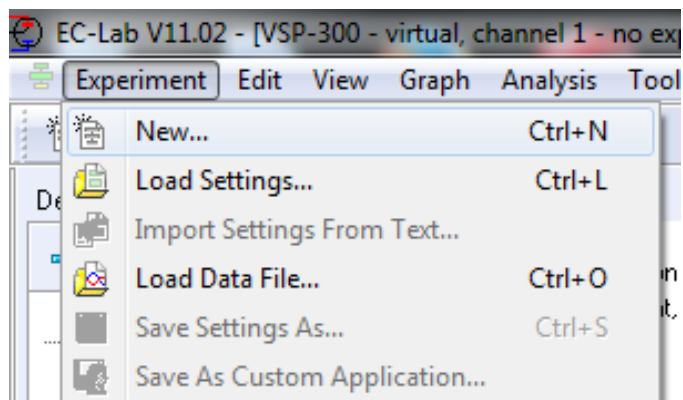


Figure 32. New in the Experiment Menu

Expand the Electrochemical Applications menu shown in Figure 33.

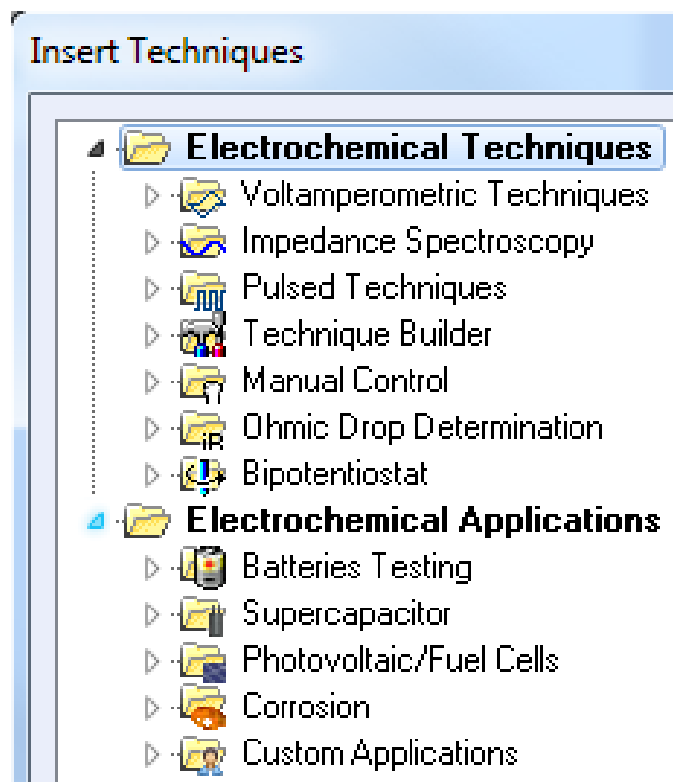


Figure 33. Electrochemical Techniques Drop-down Menu

Expand the Batteries Testing drop-down menu. As shown in Figure 34, select Modulo Bat - MB option.

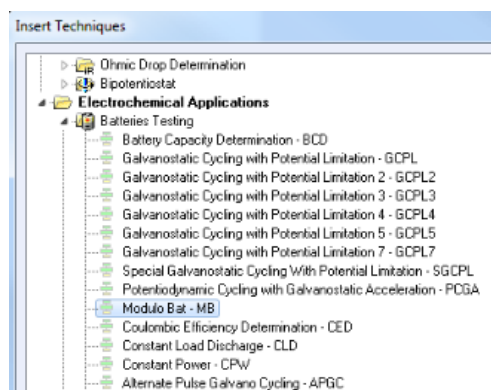


Figure 34. Modulo Bat - MB Option in the Electrochemical Applications Menu

As shown in Figure 35, in the Control box, set Type to CC for Constant Current. Set the unlabeled dropdown menu below the Control Type to Charge. Set the Apply box to I for Current. The current value was adjusted based on the testing procedures for each salt solution. Each solution was tested using 39 parameters as displayed in Table 3. The units were set to mA for milliamps per Table 3. In the Limits box, the parameter is set to Ewe for Voltage. The cycle proceeds to the Next Sequence whenever the measured voltage became greater than 2.3 Volts. In the Records box, press the blue plus sign to add a second parameter to record Voltage in Volts in addition to Time in seconds. The minimum step value was set to 0.1 for both Records parameters. In the Ranges box, the E range parameter is set to -10 V; 10 V, the I Range parameter is set to 1 amp; the Bandwidth is set to 7.

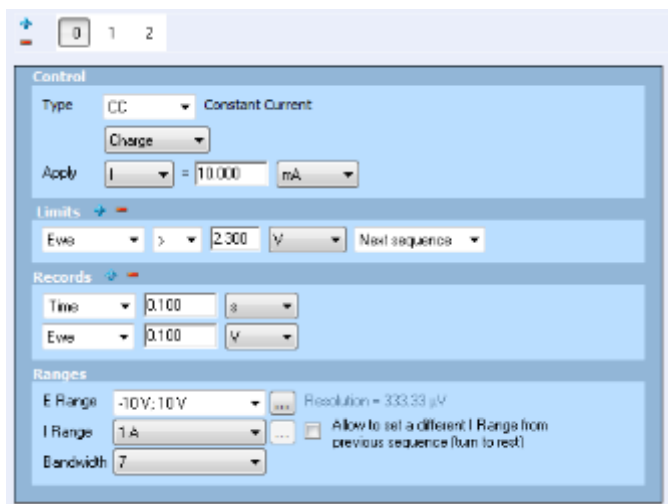


Figure 35. Setting the Charge Cycles of the EC-Lab Software

Depress the blue plus sign above the Control box to add a second sequence. In the Control box, set Type to CC for Constant Current. As shown in Figure 36, set the unlabeled dropdown menu below the Control Type to Discharge. Set the Apply box to I for Current. The current value was adjusted based on the testing procedures for each salt solution. The units were set to mA for milliamps per Table 3. In the Limits box, the parameter is set to Ewe for Voltage. The cycle proceeds to the Next Sequence whenever the measured voltage became less than 0.1 Volts. In the Records box, press the blue plus

sign to add a second parameter to record Voltage in Volts in addition to Time in seconds. The minimum step value was set to 0.1 for both Records parameters. In the Ranges box, the E range parameter is set to -10 V; 10 V, the I Range parameter is set to 1 amp, the Bandwidth is set to 7.

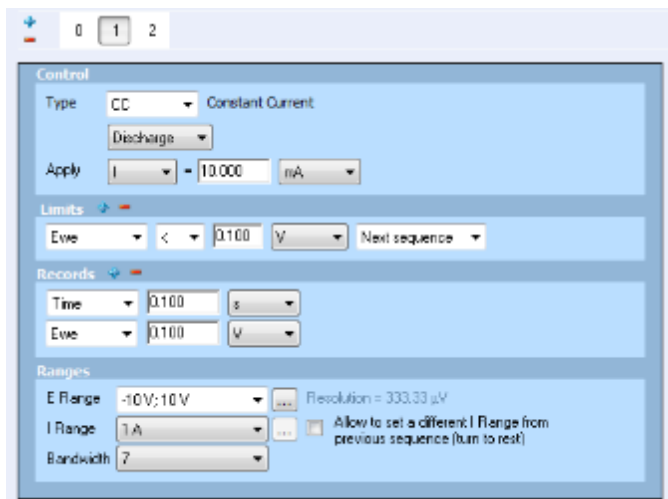


Figure 36. Setting the Discharge Cycles of the EC-Lab Software

Depress the blue plus sign above the Control box to add a third sequence. As shown in Figure 37, in the Control box, set Type to Loop. Set the Go Back to Sequence to 0 and for cycles to 10.

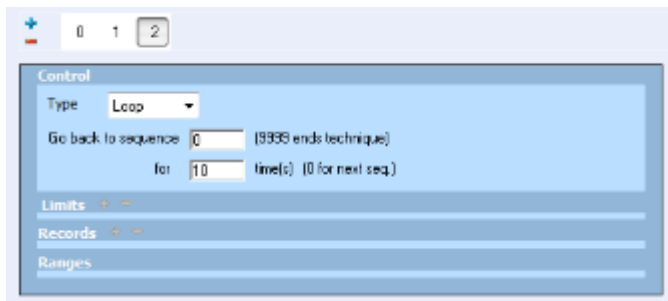


Figure 37. Setting the Number of Loops Per Experiment to 10

In the Parameter Settings menu in the left column, the blue plus sign was clicked to add additional techniques. Up to ten techniques, as listed in Table 3 are utilized at one time. Depress the Turn to Modify Mode/Accept Modifications key and click the green triangle to begin the test sequencing.

In order to test frequency of each solution, a predetermined test matrix was developed. The test parameters can be divided into two halves. One half matches the charge current to the discharge current for an even periodic frequency. The second half sets the charge current to 10 mA for all cycles but utilizes the same discharge current schedule for comparison to the first half of the experiment. Each test was completed for the three salt solutions at three different concentrations.

It should be noted that very low charge and matching discharge currents were not tested. The initial results of the first samples tested destroyed the samples with intense heat that would char the sample and ultimately render it useless for further testing. Table 3 lists the charging and discharging schedule conducted for the salt solutions, commercial capacitors, and 100% DI water.

Table 3. Charge and Discharge Schedule

| | Charge=Discharge | | Charge≠Discharge | |
|-------------|-----------------------------|---------------------|-----------------------------|---------------------|
| Test Number | Charge Rate [mA] | Discharge Rate [mA] | Charge Rate [mA] | Discharge Rate [mA] |
| 1 | 10 | 10 | 10 | 10 |
| 2 | 20 | 20 | 10 | 20 |
| 3 | 30 | 30 | 10 | 30 |
| 4 | 40 | 40 | 10 | 40 |
| 5 | 50 | 50 | 10 | 50 |
| 6 | 80 | 80 | 10 | 80 |
| 7 | 100 | 100 | 10 | 100 |
| 8 | 150 | 150 | 10 | 150 |
| 9 | 200 | 200 | 10 | 200 |
| 10 | 250 | 250 | 10 | 250 |
| | Charge=Discharge (Low) | | Charge≠Discharge (Low) | |
| 1 | 5 | 5 | 10 | 5 |
| 2 | 8 | 8 | 10 | 8 |
| 3 | 10 | 10 | 10 | 10 |
| 4 | 12 | 12 | 10 | 12 |
| 5 | 15 | 15 | 10 | 15 |
| 6 | 18 | 18 | 10 | 18 |
| 7 | 20 | 20 | 10 | 20 |
| | Charge=Discharge (Very Low) | | Charge≠Discharge (Very Low) | |
| 1 | Not Tested | | 10 | 1 |
| 2 | | | 10 | 2 |
| 3 | | | 10 | 3 |
| 4 | | | 10 | 4 |
| 5 | | | 10 | 5 |

3. Post-test Analysis

After the completion of all tests, the data was analyzed using the EC-Lab software. The integral function, utilizing a trapezoid approximation was utilized to measure the area under curves two through ten. The upper limit cursor would be placed at the peak of the curve and the lower limit cursor would be placed at lowest point of the valley as seen in Figure 38.

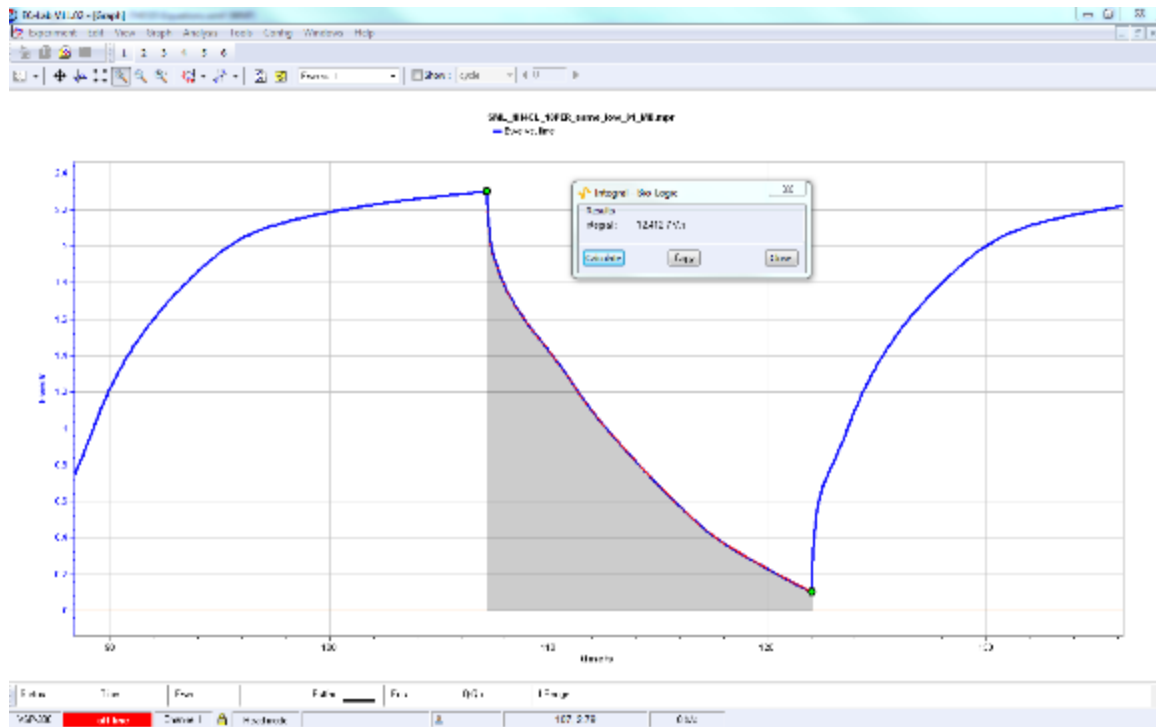


Figure 38. EC-Lab Integral Function Method

The linear fit function, a least squares approximation, was utilized to measure the slope of curves two through ten. The upper limit cursor would be placed at approximately 0.8 Volts and the lower limit cursor would be placed at lowest point of the valley as seen in Figure 39. The upper limit was limited to approximately 0.8 Volts to provide a more conservative estimate of energy density at the end of the capacitor discharge cycle.

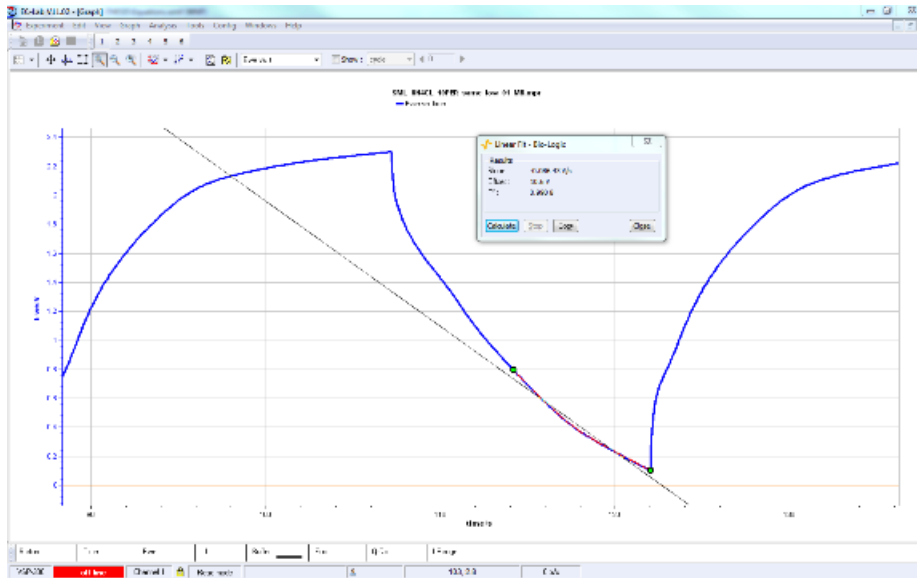


Figure 39. EC-Lab Linear Fit Function Method

When curves aliased past the x axis, the lower limit cursor would be set to the positive data point nearest the 0.1 Volts limit. An example of this method can be observed in Figure 40.

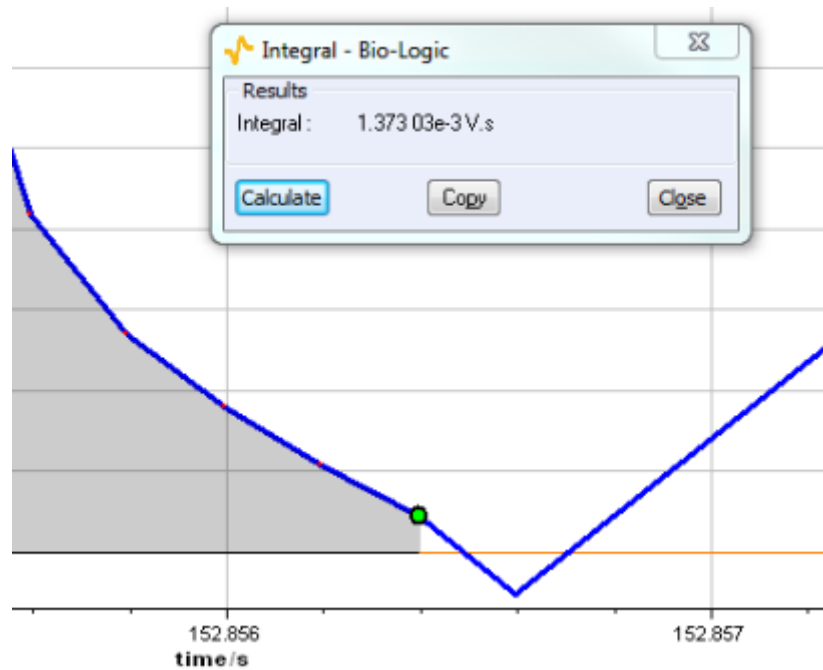


Figure 40. EC-Lab Integral and Linear Fit Function Adjustment

III. RESULTS

A. OVERVIEW

Experiments were designed to demonstrate specific characterization by discharge time for three salts identities, each at three salt concentrations, by saturating each combination into 8 μm length nanotube matrices. In order to complete this experiment, a constant current is applied during the charge and discharge phases per Table 3. Frequency tests utilize a constant current charge rate that is equal to the discharge current for an even periodic frequency. Each frequency test is repeated for 10 cycles at a constant charge and discharge current. These frequency tests are referred to as Charge equals Discharge (Charge=Discharge) for the remainder of this thesis.

A second schedule of tests utilize a constant current charge rate of 10 mA for all cycles but utilize a constant current discharge schedule per Table 3. This constant current discharge schedule is similar to the currents employed in the Charge Current equals Discharge Current tests. However, due to a fixed constant current charge rate of 10 mA for all frequency tests the cycles are asymmetric. For example, if the discharge current is 1 mA, the discharge time will be far less than the charge time. Depending on the discharge schedule, seven constant current charge rates are less than the discharge rate, two are equal to the discharge rate, and 13 are greater than the constant current discharge rate. These frequency tests are referred to as Charge Fixed (Charge \neq Discharge) for the remainder of this thesis.

When plotting fixed charge data, significant error was observed for the highly basic and acidic solutions. Neutral concentrations of NaNO_3 did not demonstrate the same error. Fixed data tests followed the equal rate tests in execution. The error can therefore be attributed to degradation of the samples by delamination of the NTSDM, corrosion by the salts, and dehydration of deionized water as testing progressed. For this reason, these data points are disregarded from the graphs and will require future research to understand the conditions and root of the error.

1. Charge Equals Discharge

As seen in Figure 41, the individual raw data is similar to an ocean wave pattern for all salt solutions. However, the salt solutions differ from the DI water that has a symmetric charge and discharge curve more similar to a wave-like pattern.

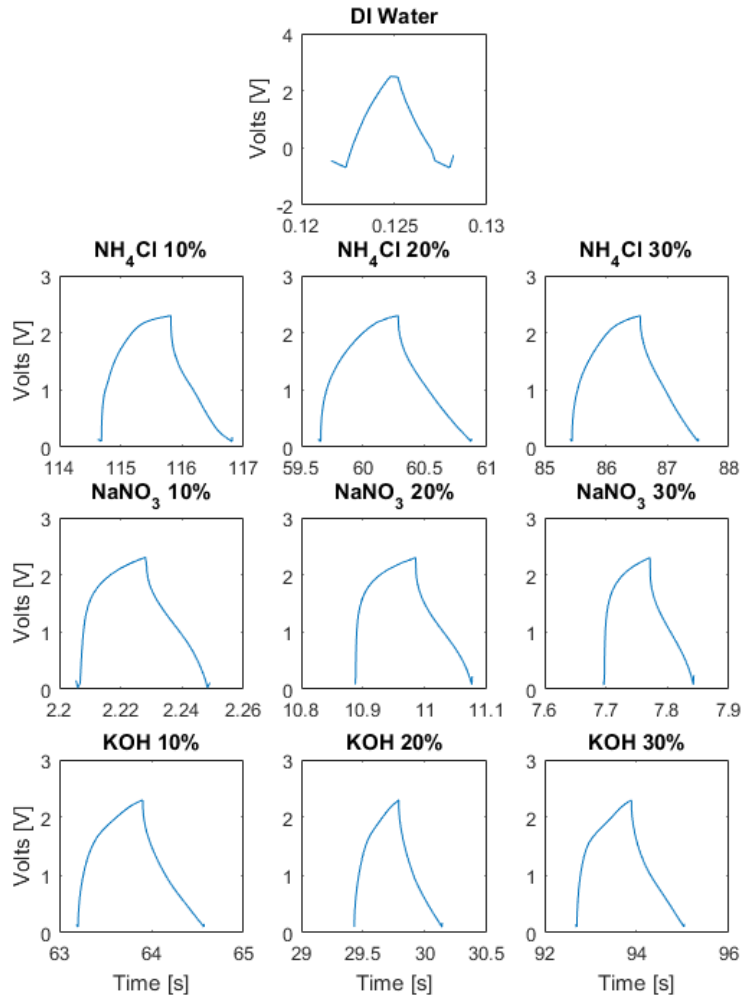


Figure 41. Raw Data Comparison of Salt Solutions at 20 mA Discharge (Charge=Discharge Rate)

2. Charge Fixed

As seen in Figure 42, the individual raw data with charging rates differing from discharge rate is a similar wave-like pattern for all salt solutions. However, the salt solutions differ from the DI water that has a symmetric charge and discharge curve with a peak that does not resemble the NTSDM sample profiles.

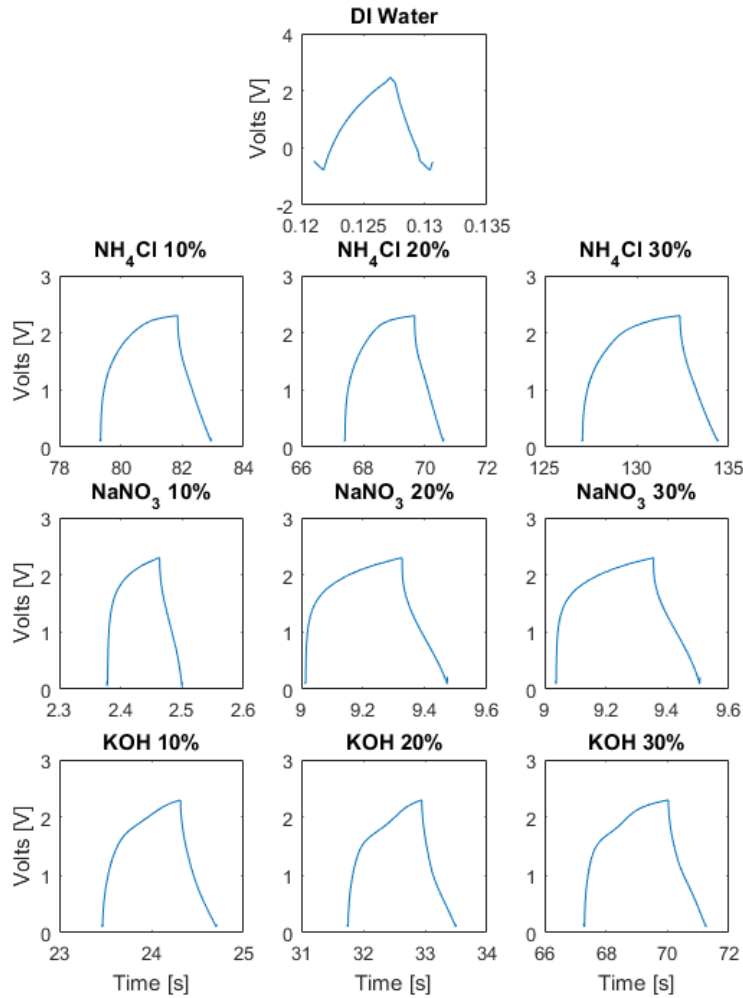


Figure 42. Raw Data Comparison of Salt Solutions at 20 mA Discharge (Charge \neq Discharge Rate)

B. DEIONIZED WATER

1. Charge Equals Discharge

As seen in Figure 43, the DI water displays the signature wave-like pattern for lower frequency testing. In contrast to the salt solutions, DI water begins to alias at a much lower discharge of only 20 mA. This is displayed in the graph as overshoot below the x-axis. As the discharge current increases, the EC-Lab software cannot adjust the charge/discharge direction at a rate fast enough to respond to the DI water characteristics. At high charge and discharge rates, the voltage often shoots above and below the limits of 2.3 and 0.1 Volts.

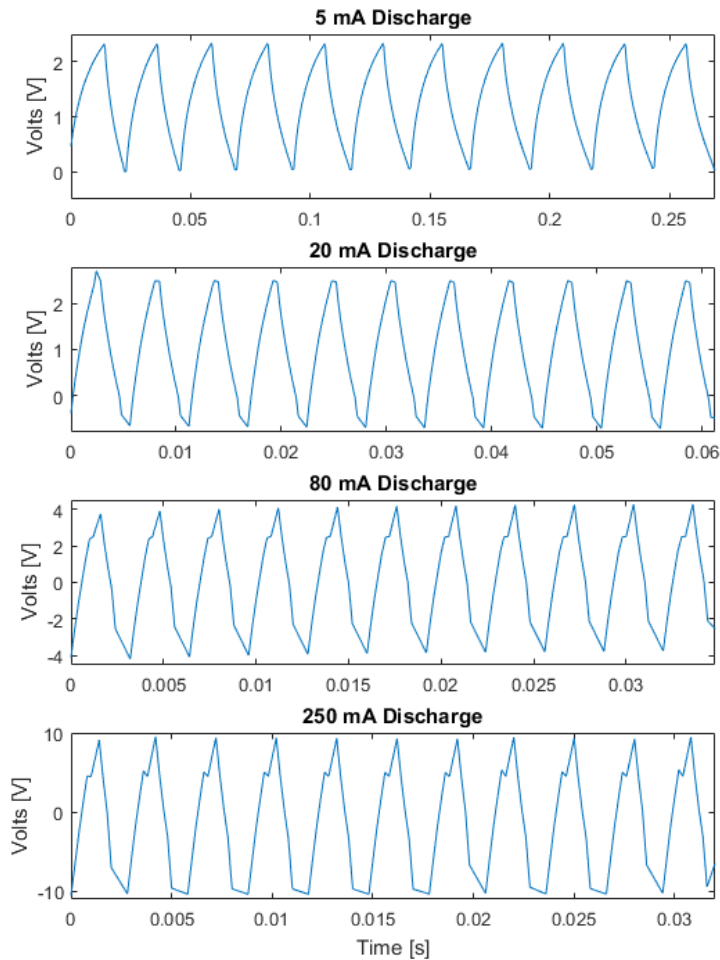


Figure 43. Deionized Water (Charge=Discharge)

Figure 44 shows the energy density characteristics for DI water when charge rate equals discharge rate. The longest discharge time was measured at $1.07\text{E-}2$ seconds, which corresponds to an energy density of $3.12\text{E-}2 \text{ J/cm}^3$. The longest discharge time corresponds to the highest dielectric constant of $1.59\text{E}5$. The shortest discharge time was measured at $3.0\text{E-}4$ seconds, which corresponds to an energy density of $16.08\text{E-}2 \text{ J/cm}^3$. The shortest discharge time corresponds to a dielectric constant of $5.36\text{E}4$. Per the power trendline, a discharge of 100 seconds would predict an energy density of $2.0\text{E-}4 \text{ J/cm}^3$.

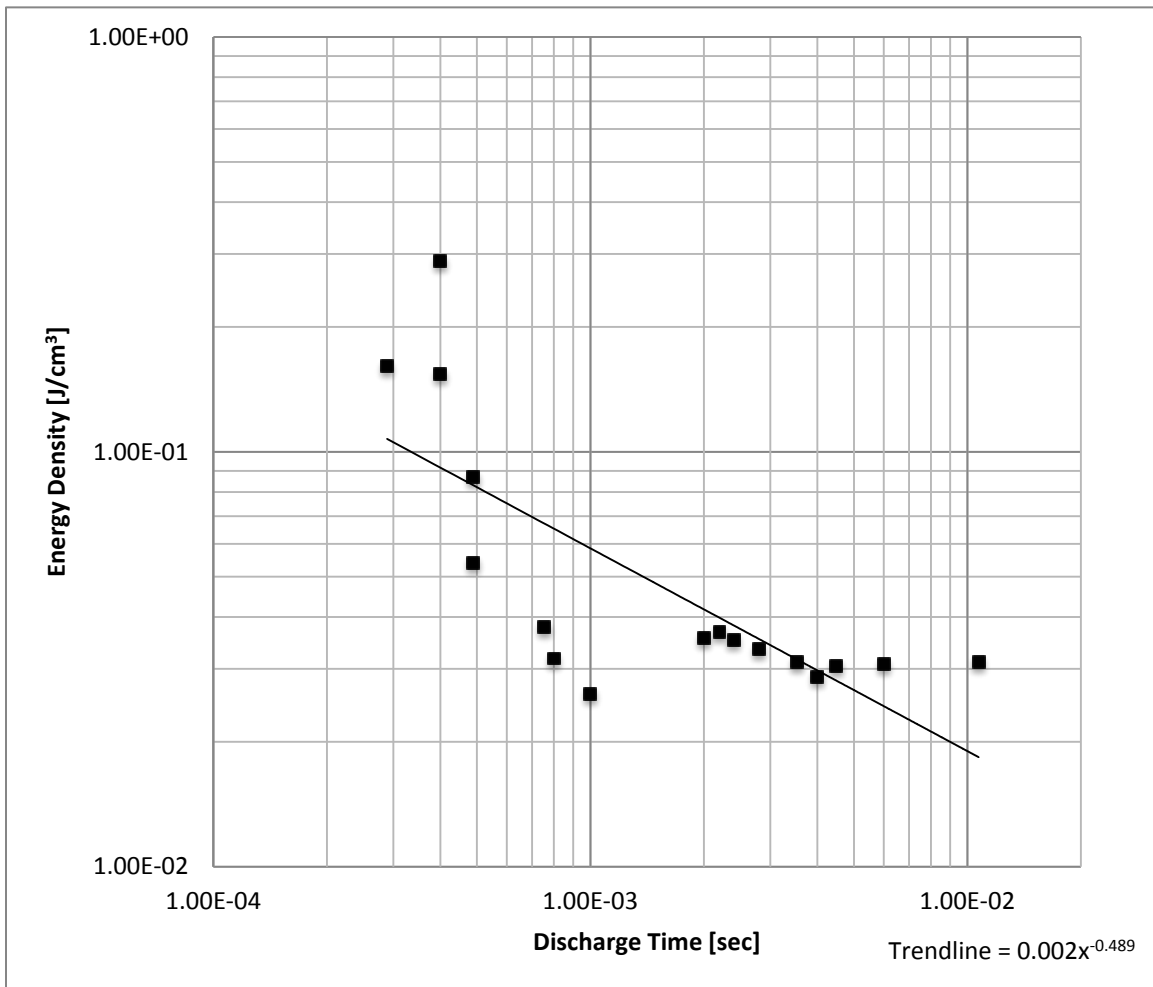


Figure 44. DI Water Energy Density vs. Discharge Time (Charge=Discharge)

2. Charge Fixed

As seen in Figure 45, the DI water displays the signature wave-like pattern for lower frequency testing. Despite the frequency weighted to accommodate a fixed constant current charge rate of 10 mA, the DI water begins to alias at a much lower discharge of only 20 mA. This is displayed in the graph as overshoot below the x-axis. As the discharge current increases, the EC-Lab software cannot adjust the charge/discharge direction at a rate fast enough to respond to the DI water characteristics. Due to a low charge rate held steady at 10 mA, the voltage does not overshoot the 2.3 V upper limit. As the discharge rate increases, the voltage overshoots farther below the 0.1 V lower limit.

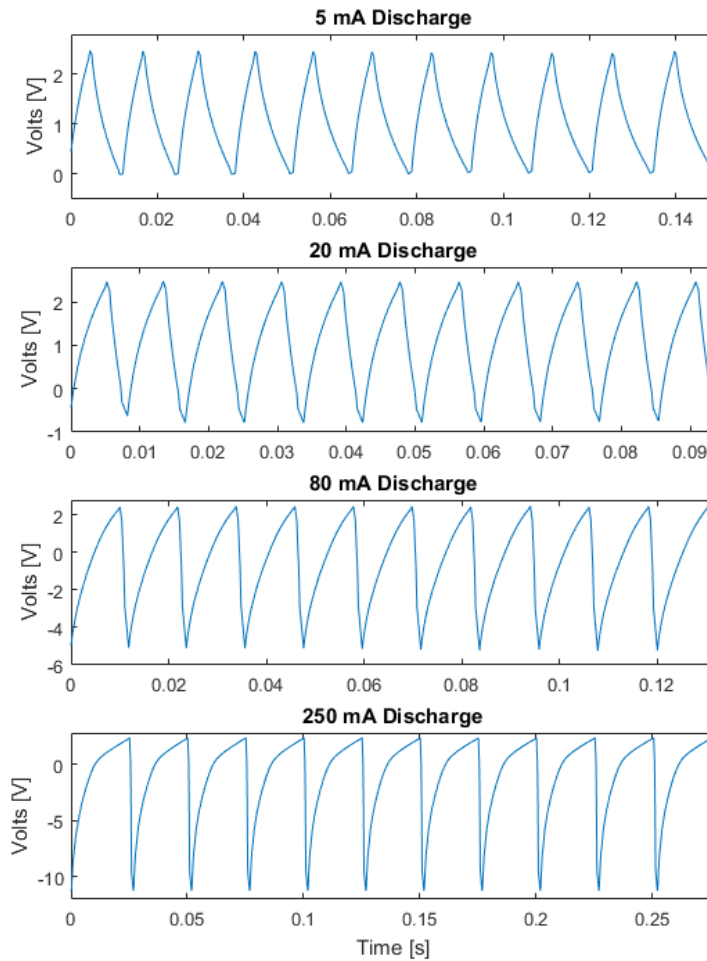


Figure 45. Deionized Water (Charge≠Discharge)

Figure 46 shows the energy density characteristics for DI water when charge rate is constant at 10 mA. The longest discharge time was measured at 5.90E-2 seconds, which corresponds to an energy density of 2.37E-2 J/cm³. The longest discharge time corresponds to the highest dielectric constant of 2.79E5. The shortest discharge time was measured at 4.0E-4 seconds, which corresponds to an energy density of 7.82E-2 J/cm³. The shortest discharge time corresponds to a dielectric constant of 2.03E5. Per the power trendline, a discharge of 100 seconds would predict an energy density of 3.6E-3 J/cm³.

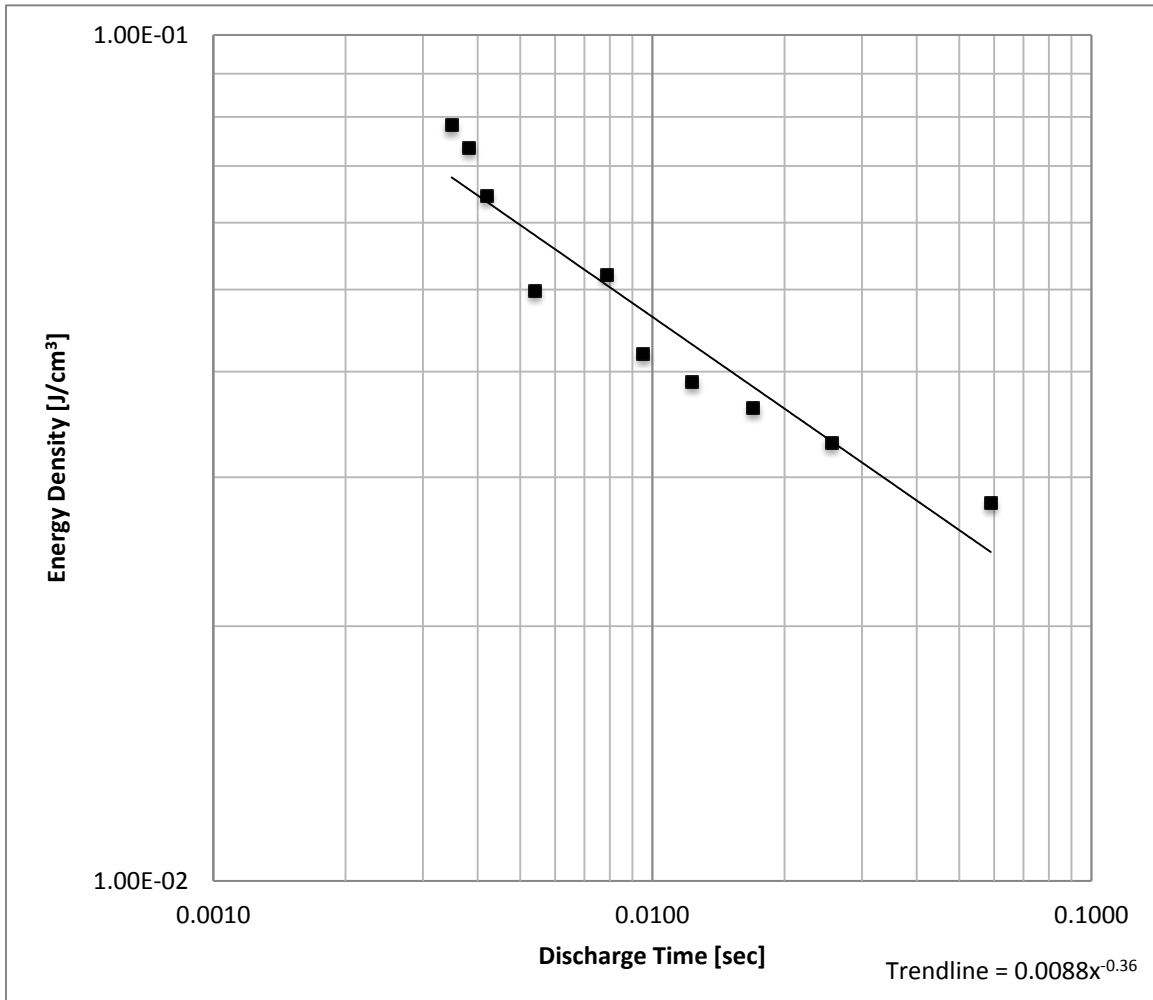


Figure 46. DI Water Energy Density vs. Discharge Time (Charge≠Discharge)

C. AMMONIUM CHLORIDE RESULTS

1. NH_4Cl 10 wt% Charge Equals Discharge

Unlike DI water, NH_4Cl at 10% concentration, shown in Figure 47, holds the signature wave-like pattern through higher frequency testing. Aliasing does occur at the highest current tested of 250 mA.

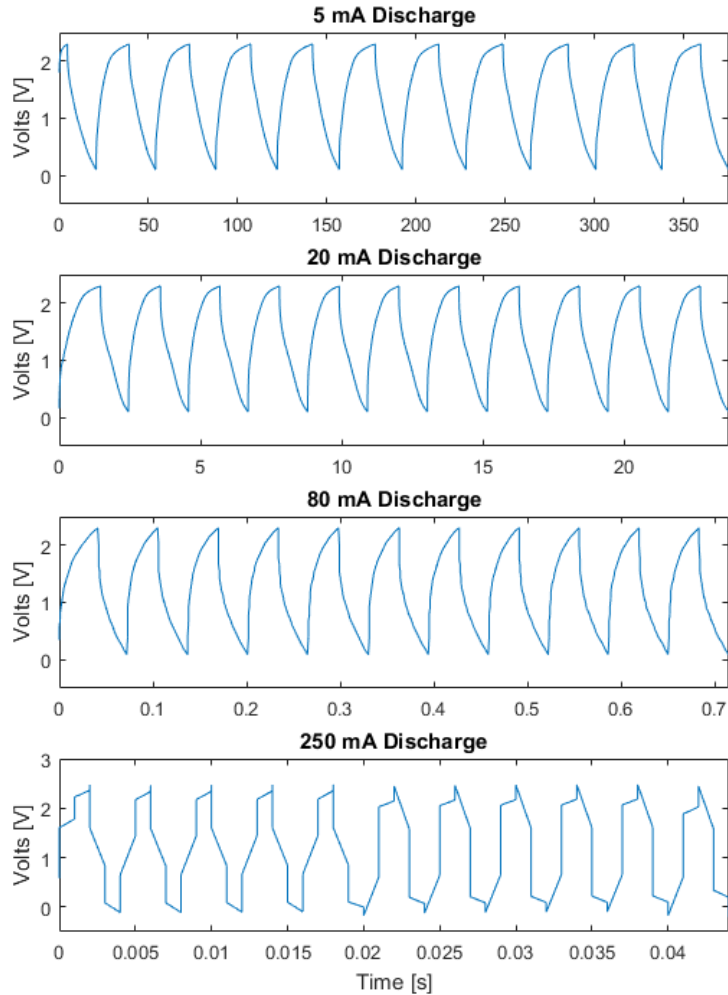


Figure 47. NH_4Cl 10% Concentration (Charge=Discharge)

Figure 48 shows the energy density characteristics for NH₄Cl at 10% concentration by weight when charge rate equals discharge rate. The longest discharge time was measured at 15 seconds, which corresponds to an energy density of 41 J/cm³. The longest discharge time corresponds to the highest dielectric constant of 2.7E8. The shortest discharge time was measured at 1.4E-3 seconds, which corresponds to an energy density of 21.44E-2 J/cm³. The shortest discharge time corresponds to the lowest dielectric constant of 1.25E6. Per the power trendline, a discharge of 100 seconds would predict an energy density of 139 J/cm³.

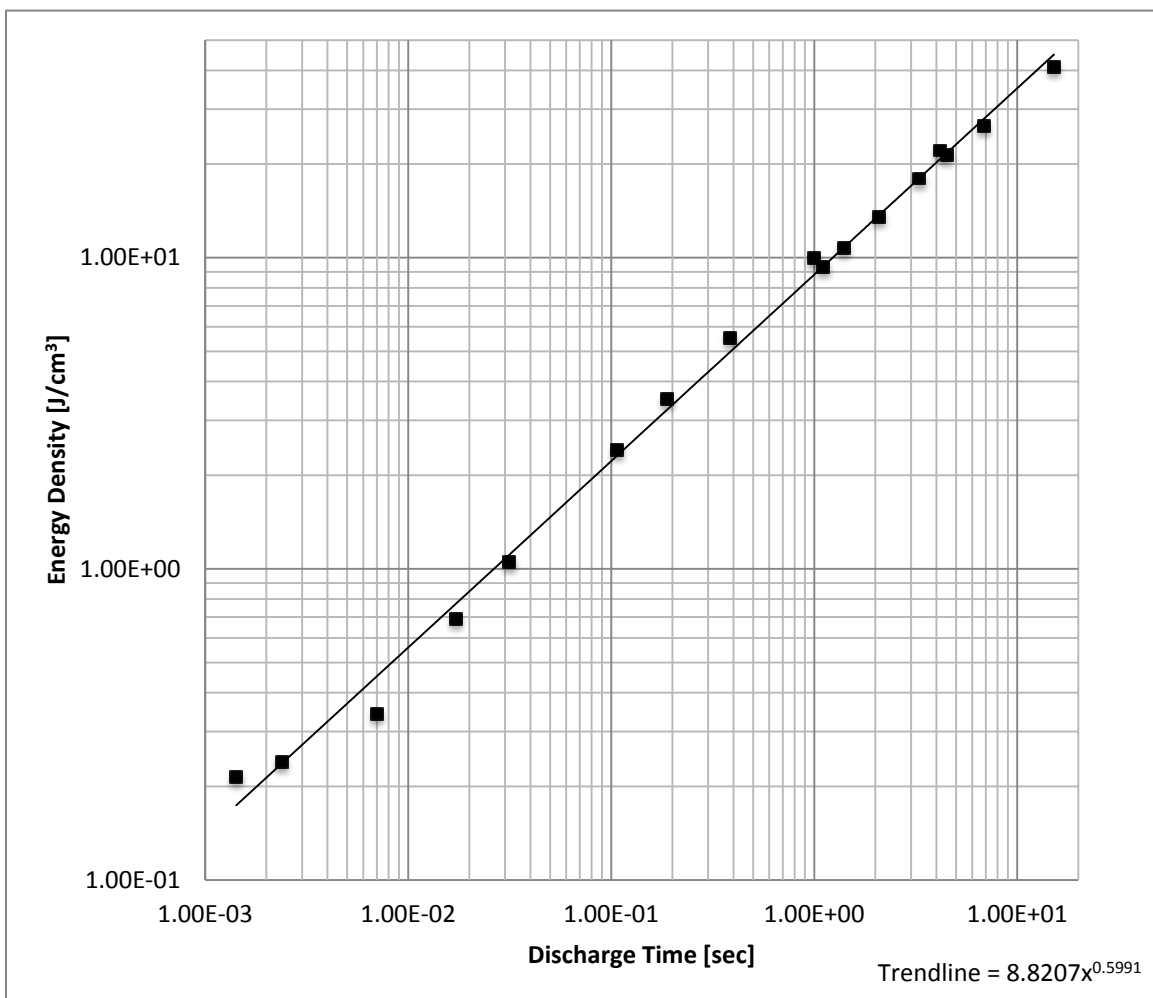


Figure 48. NH₄Cl 10% Energy Density vs. Discharge Time (Charge=Discharge)

2. NH₄Cl 20 wt% Charge Equals Discharge

Unlike DI Water, NH₄Cl at 20% concentration, shown in Figure 49, holds the signature wave-like pattern through higher frequency testing. Aliasing does occur at the highest frequency tested of 250 mA but not to the same extent at the 10% concentration.

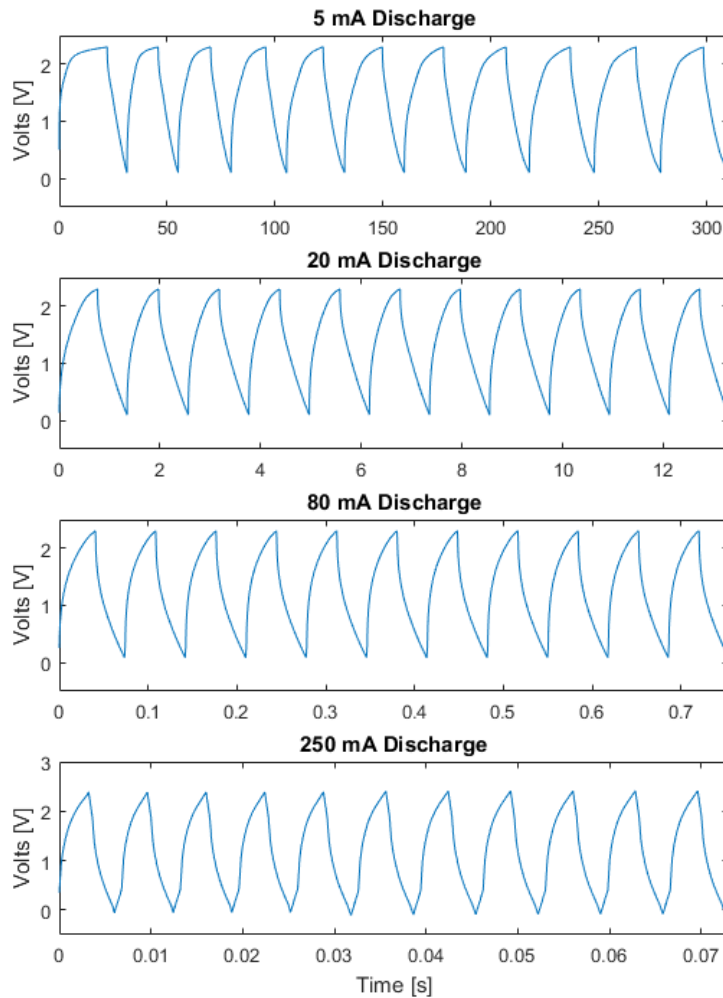


Figure 49. NH₄Cl 20% Concentration (Charge=Discharge)

Figure 50 shows the energy density characteristics for NH₄Cl at 20% concentration by weight when charge rate equals discharge rate. The longest discharge time was measured at 10 seconds, which corresponds to an energy density of 27 J/cm³. The longest discharge time corresponds to the second highest dielectric constant of 1.67E8. The shortest discharge time was measured at 2.6E-3 seconds, which corresponds to an energy density of 3.81E-1 J/cm³. The shortest discharge time corresponds to the lowest dielectric constant of 2.28E6. Per the power trendline, a discharge of 100 seconds would predict an energy density of 103 J/cm³.

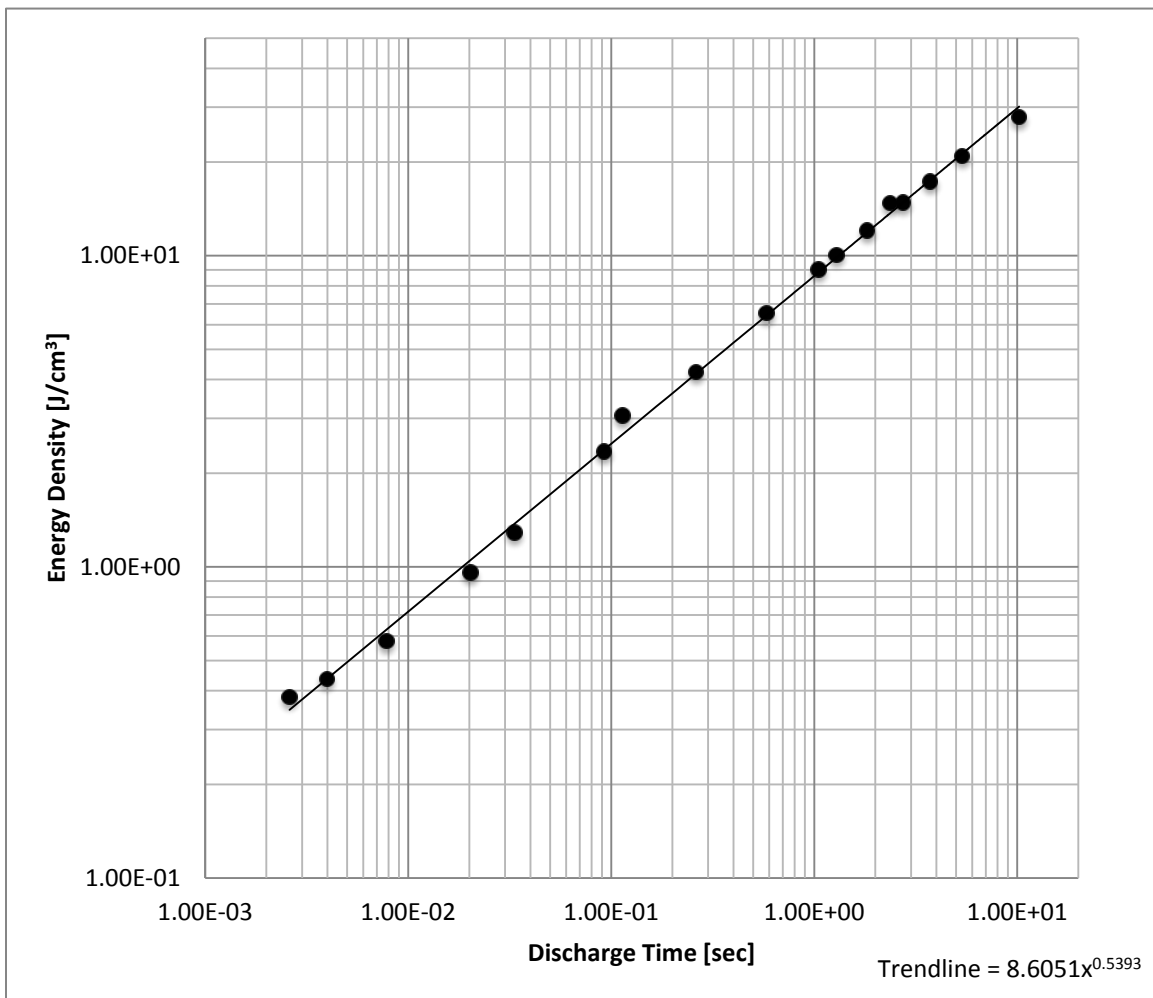


Figure 50. NH₄Cl 20% Energy Density vs. Discharge Time (Charge=Discharge)

3. NH_4Cl 30 wt% Charge Equals Discharge

Unlike DI water, NH_4Cl at 30% concentration, shown in Figure 51, holds the signature wave-like pattern through higher frequency testing. Aliasing does occur at the highest frequency tested of 250 mA but not to the same extent at the 10% concentration. A frequency vibration is observed at higher discharge currents in the raw data.

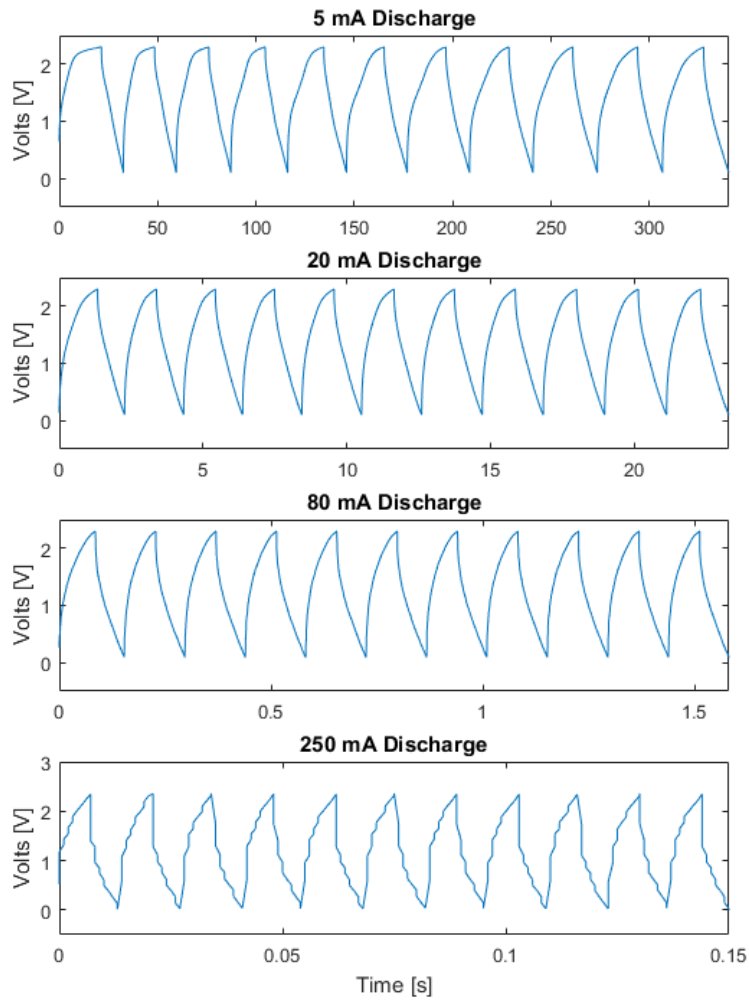


Figure 51. NH_4Cl 30% Concentration (Charge=Discharge)

Figure 52 shows the energy density characteristics for NH₄Cl at 30% concentration by weight when charge rate equals discharge rate. The longest discharge time was measured at 11 seconds, which corresponds to an energy density of 34 J/cm³. The longest discharge time corresponds to the highest dielectric constant of 1.77E8. The shortest discharge time was measured at 6.4E-3 seconds, which corresponds to an energy density of 7.05E-1 J/cm³. The shortest discharge time corresponds to the lowest dielectric constant of 6.39E6. Per the power trendline, a discharge of 100 seconds would predict an energy density of 110 J/cm³.

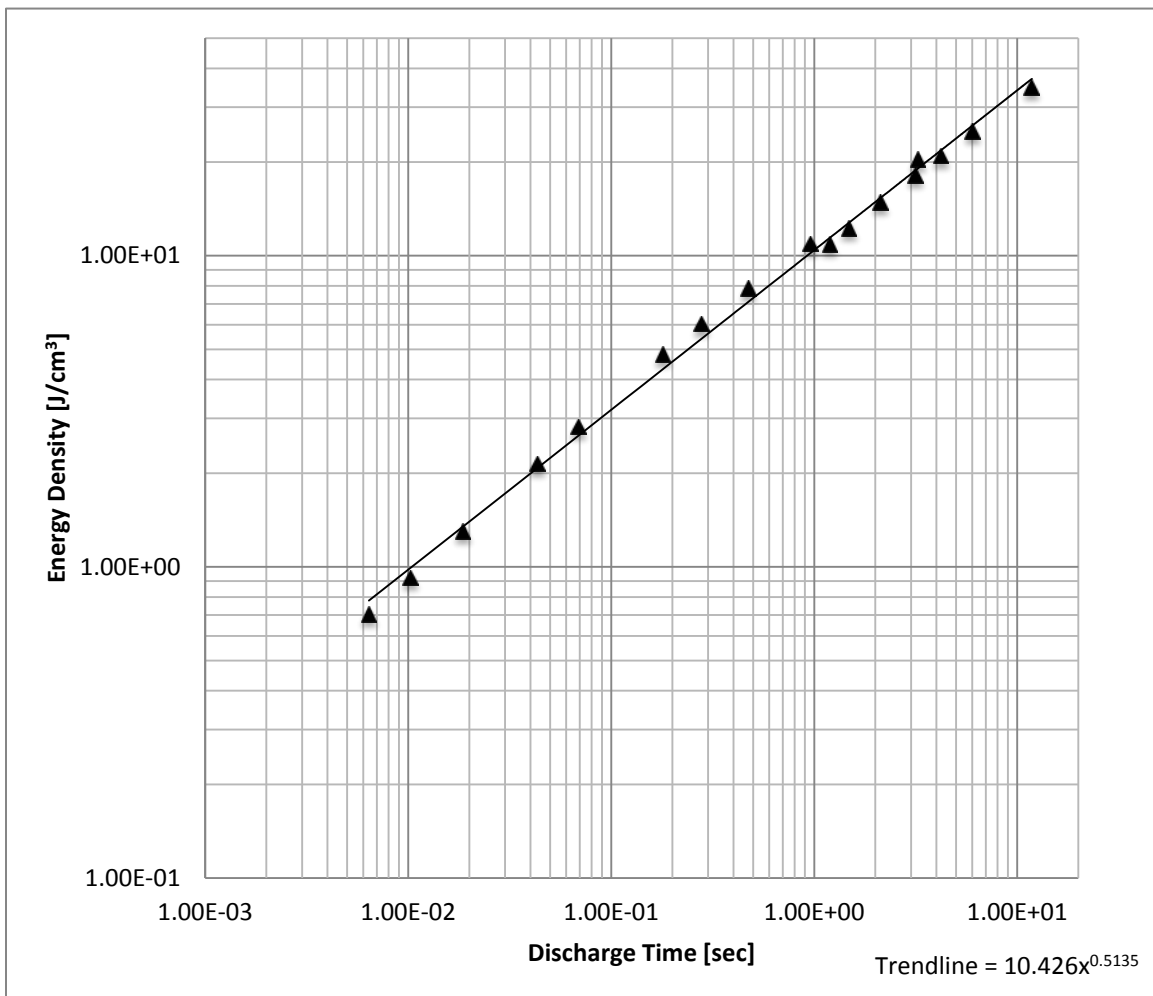


Figure 52. NH₄Cl 30% Energy Density vs. Discharge Time (Charge=Discharge)

4. NH_4Cl 10 wt% Charge Fixed

NH_4Cl at 10% concentration, shown in Figure 53, holds the signature wave-like pattern through lower frequency testing. A significant change in the wave-like pattern is observed when the discharge rate is set to 80 mA. Frequency range was consistent and 2.3 volts was attainable for all discharge rates. Aliasing was observed at the 150 mA discharge rate.

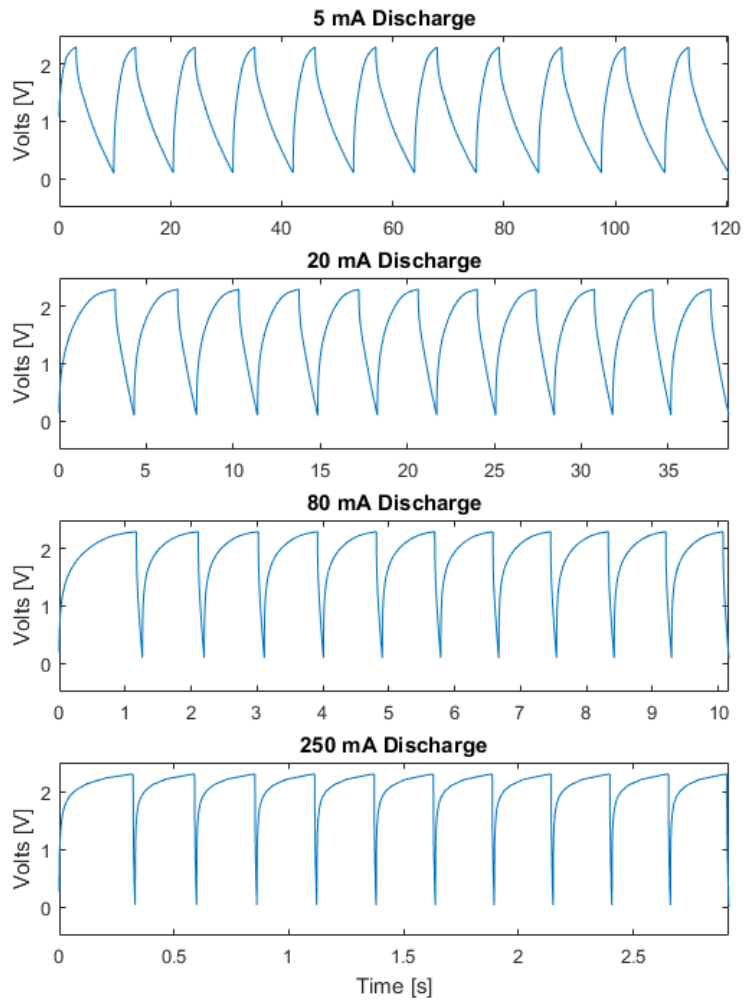


Figure 53. NH_4Cl 10% Concentration (Charge \neq Discharge)

Figure 54 shows the energy density characteristics for NH₄Cl at 10% concentration by weight when charge rate is constant at 10 mA. The longest discharge time was measured at 3 seconds, which corresponds to an energy density of 18 J/cm³. The longest discharge time corresponds to the highest dielectric constant of 8.1E7. The shortest discharge time was measured at 8.2E-3 seconds, which corresponds to an energy density of 1.0 J/cm³. The shortest discharge time corresponds to the lowest dielectric constant of 7.26E6. Per the power trendline, a discharge of 100 seconds would predict an energy density of 122 J/cm³.

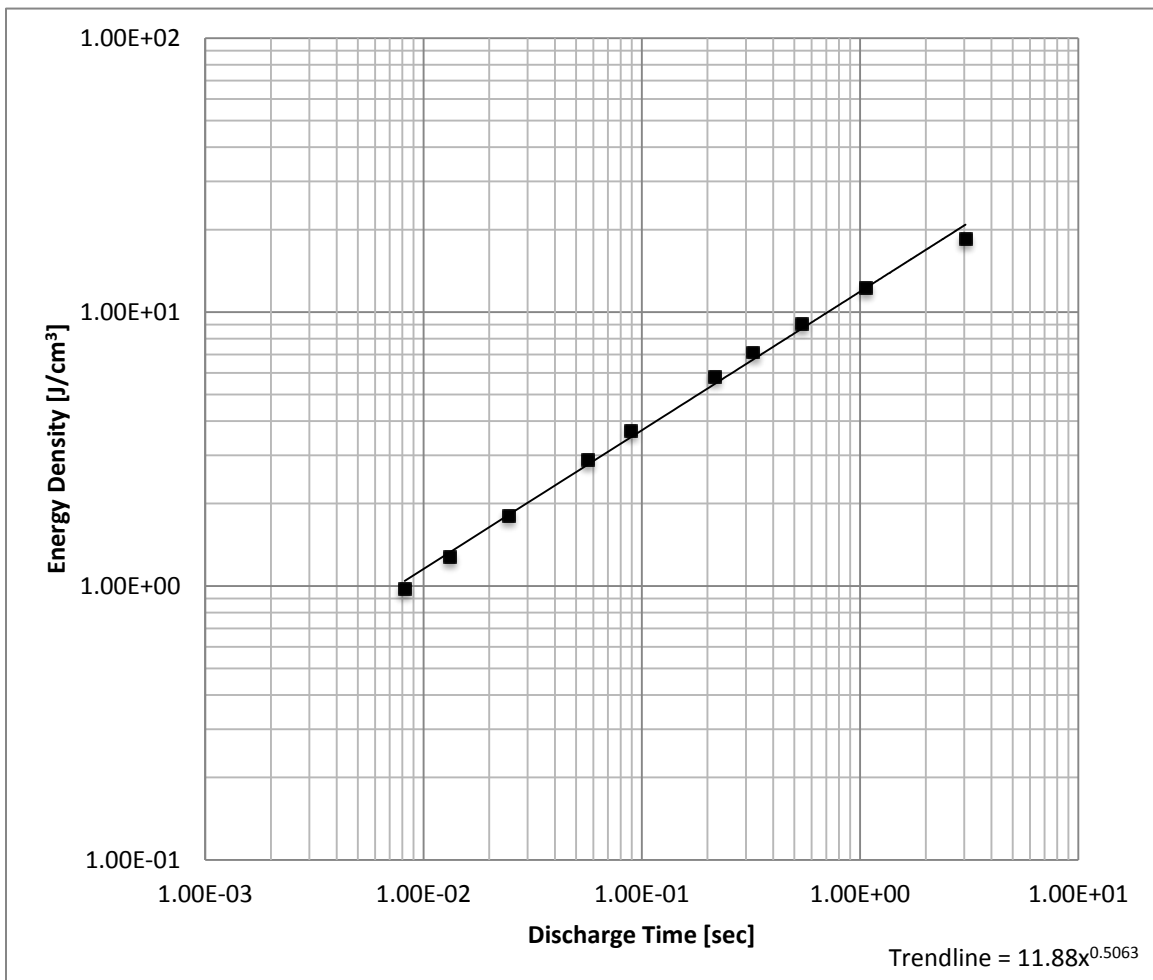


Figure 54. NH₄Cl 10% Energy Density vs. Discharge Time (Charge≠Discharge)

5. NH_4Cl 20 wt% Charge Fixed

NH_4Cl at 20% concentration, shown in Figure 55, holds the signature wave-like pattern through lower frequency testing. A significant change in the wave-like pattern is observed when the discharge rate is set to 80 mA. Frequency range was consistent and 2.3 volts was attainable for all discharge rates. Aliasing was observed at the 100 mA discharge rate.

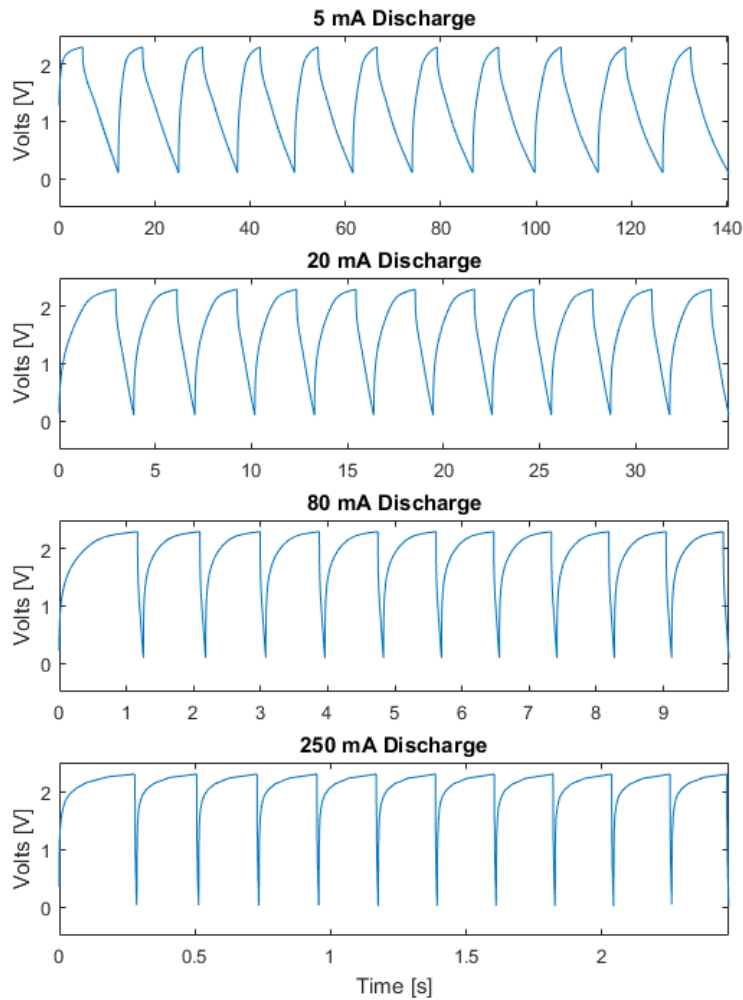


Figure 55. NH_4Cl 20% Concentration (Charge \neq Discharge)

Figure 56 shows the energy density characteristics for NH₄Cl at 20% concentration by weight when charge rate is constant at 10 mA. The longest discharge time was measured at 2.5 seconds, which corresponds to an energy density of 15.2 J/cm³. The longest discharge time corresponds to the highest dielectric constant of 6.73E7. The shortest discharge time was measured at 6.8E-3 seconds, which corresponds to an energy density of 0.74 J/cm³. The shortest discharge time corresponds to the lowest dielectric constant of 6.35E6. Per the power trendline, a discharge of 100 seconds would predict an energy density of 131.5 J/cm³.

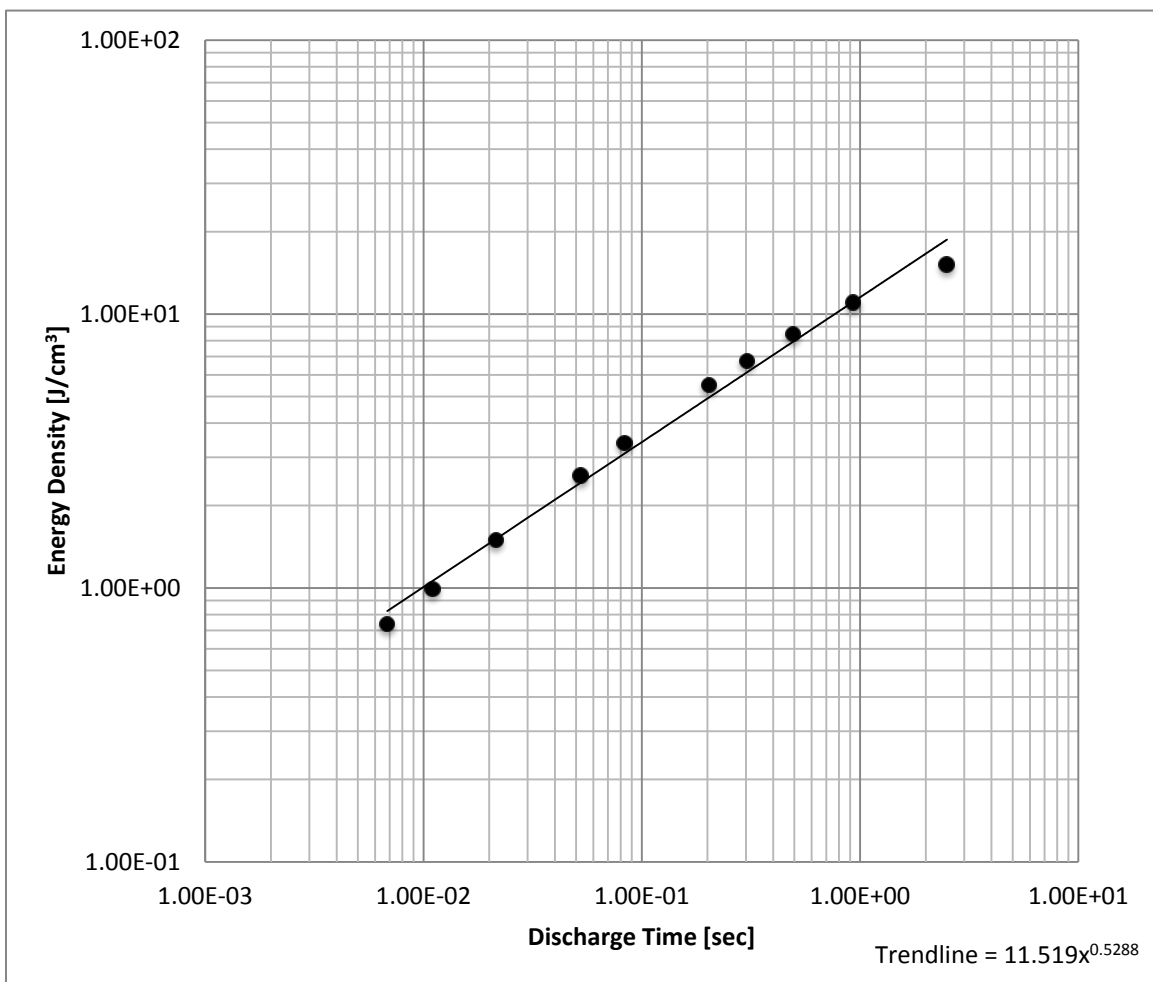


Figure 56. NH₄Cl 20% Energy Density vs. Discharge Time (Charge≠Discharge)

6. NH_4Cl 30 wt% Charge Fixed

NH_4Cl at 30% concentration, shown in Figure 57, holds the signature wave-like pattern through lower frequency testing. A significant change in the wave-like pattern is observed when the discharge rate is set to 80 mA. Frequency range was consistent and 2.3 volts was attainable for all discharge rates. Aliasing was observed at the 80 mA discharge rate.

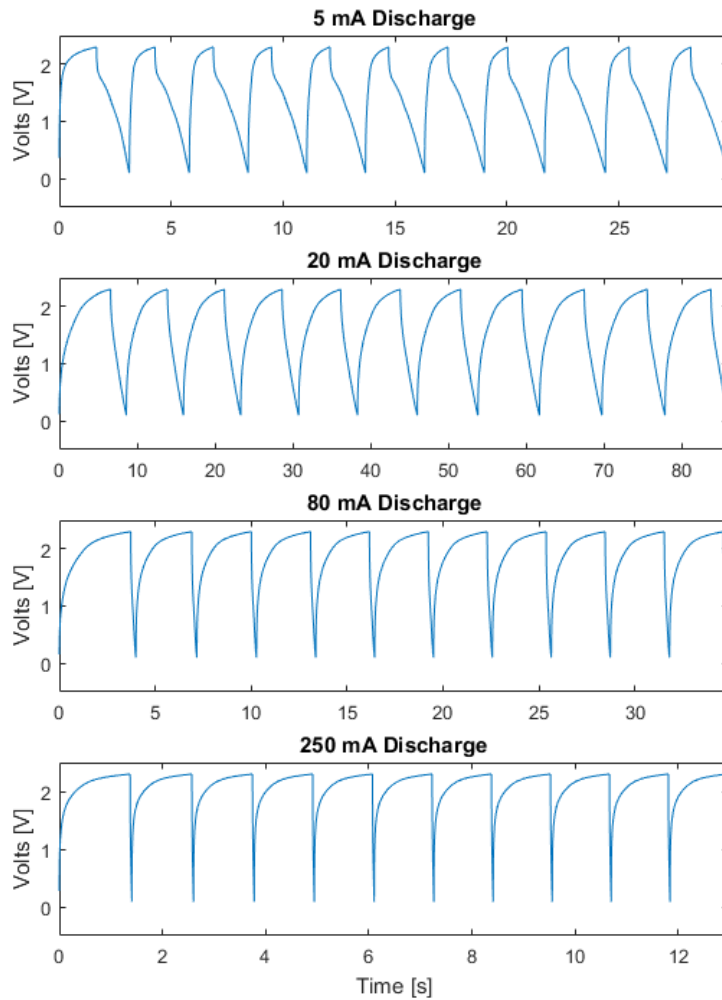


Figure 57. NH_4Cl 30% Concentration (Charge \neq Discharge)

Figure 58 shows the energy density characteristics for NH₄Cl at 30% concentration by weight when charge rate is constant at 10 mA. The longest discharge time was measured at 4.6 seconds, which corresponds to an energy density of 28 J/cm³. The longest discharge time corresponds to a dielectric constant of 1.29E8. The shortest discharge time was measured at 3.24E-2 seconds, which corresponds to an energy density of 4 J/cm³. The shortest discharge time corresponds to a dielectric constant of 2.85E7. Per the power trendline, a discharge of 100 seconds would predict an energy density of 118 J/cm³.

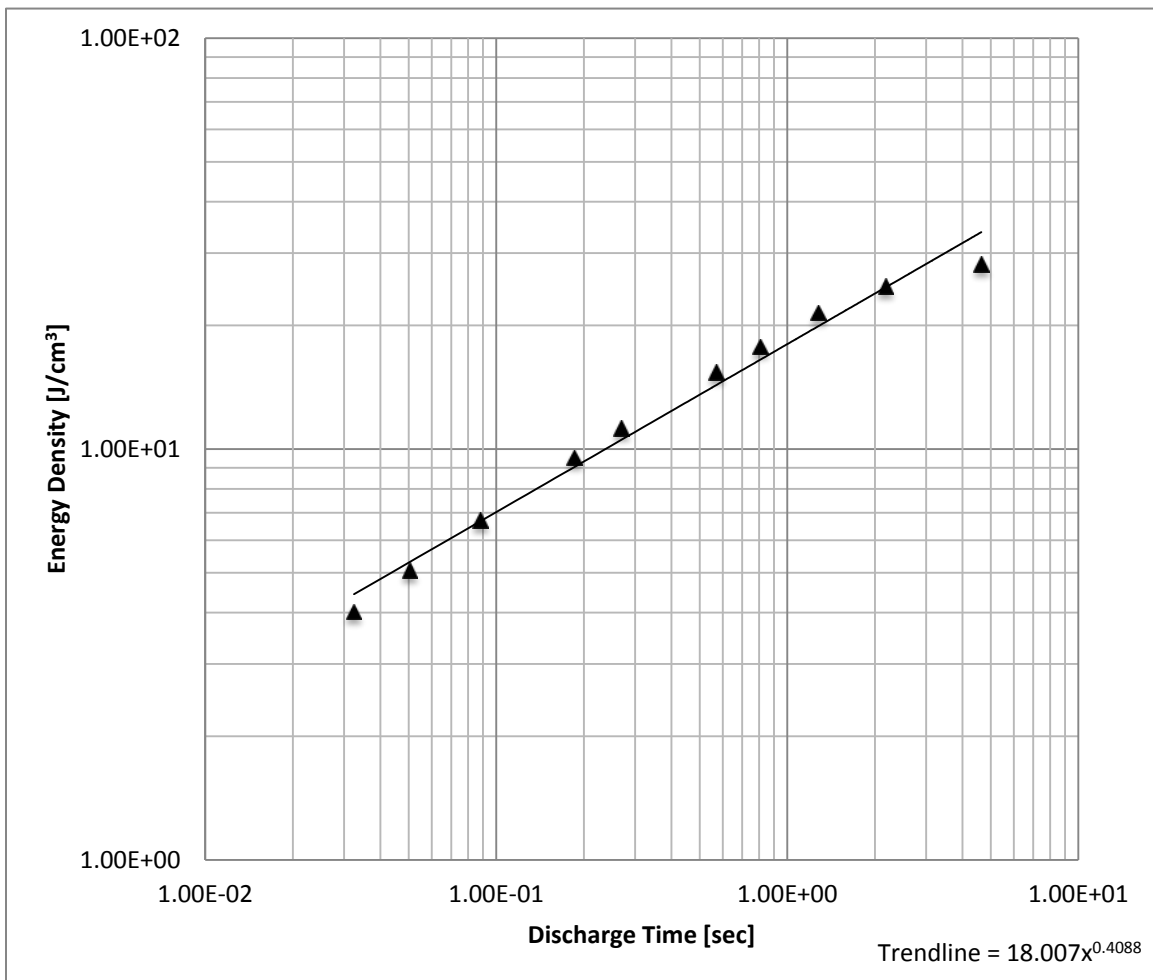


Figure 58. NH₄Cl 30% Energy Density vs. Discharge Time (Charge≠Discharge)

D. SODIUM NITRATE

1. NaNO_3 10 wt% Charge Equals Discharge

NaNO_3 at 10% concentration, shown in Figure 59, holds the signature wave-like pattern through lower frequency testing. A significant change in the wave-like pattern is observed when the discharge rate is set to 80 mA. Frequency range was consistent and 2.3 volts was attainable for all discharge rates. Aliasing was observed at the 20 mA discharge rate.

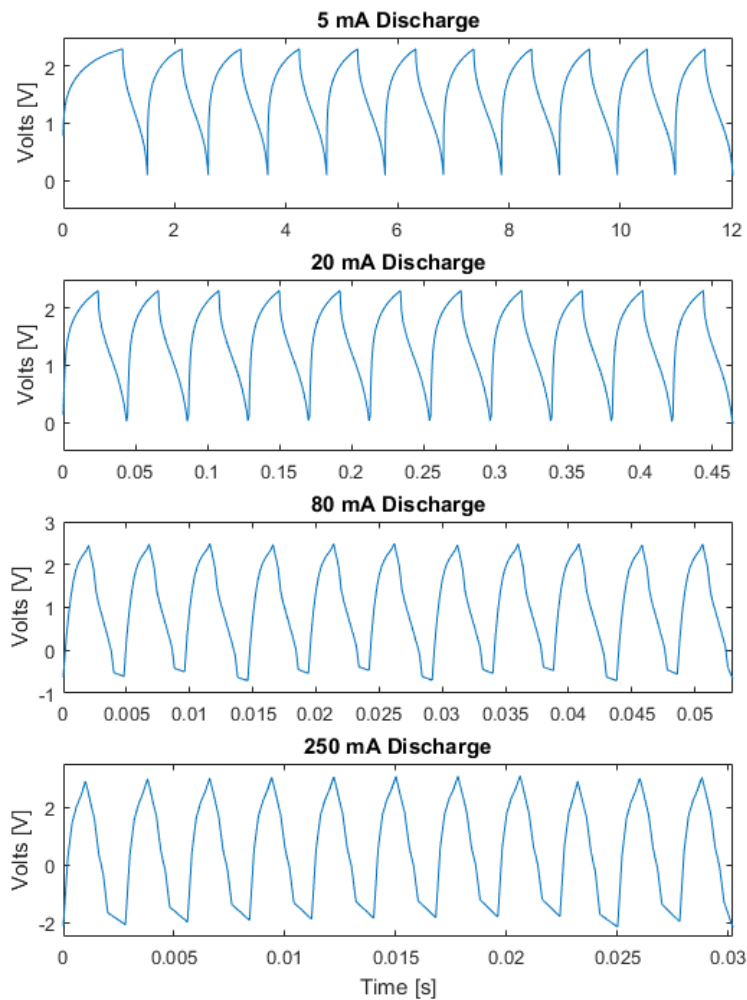


Figure 59. NaNO_3 10% Concentration (Charge=Discharge)

Figure 60 shows the energy density characteristics for NaNO₃ at 10% concentration by weight when charge rate equals discharge rate. The longest discharge time was measured at 0.5 seconds, which corresponds to an energy density of 1.8 J/cm³. The longest discharge time corresponds to the highest dielectric constant of 3.92E6. The shortest discharge time was measured at 6.0E-4 seconds, which corresponds to an energy density of 1.8E-1 J/cm³. The shortest discharge time corresponds to the lowest dielectric constant of 1.91E5. Per the power trendline, a discharge of 100 seconds would predict an energy density of 9 J/cm³.

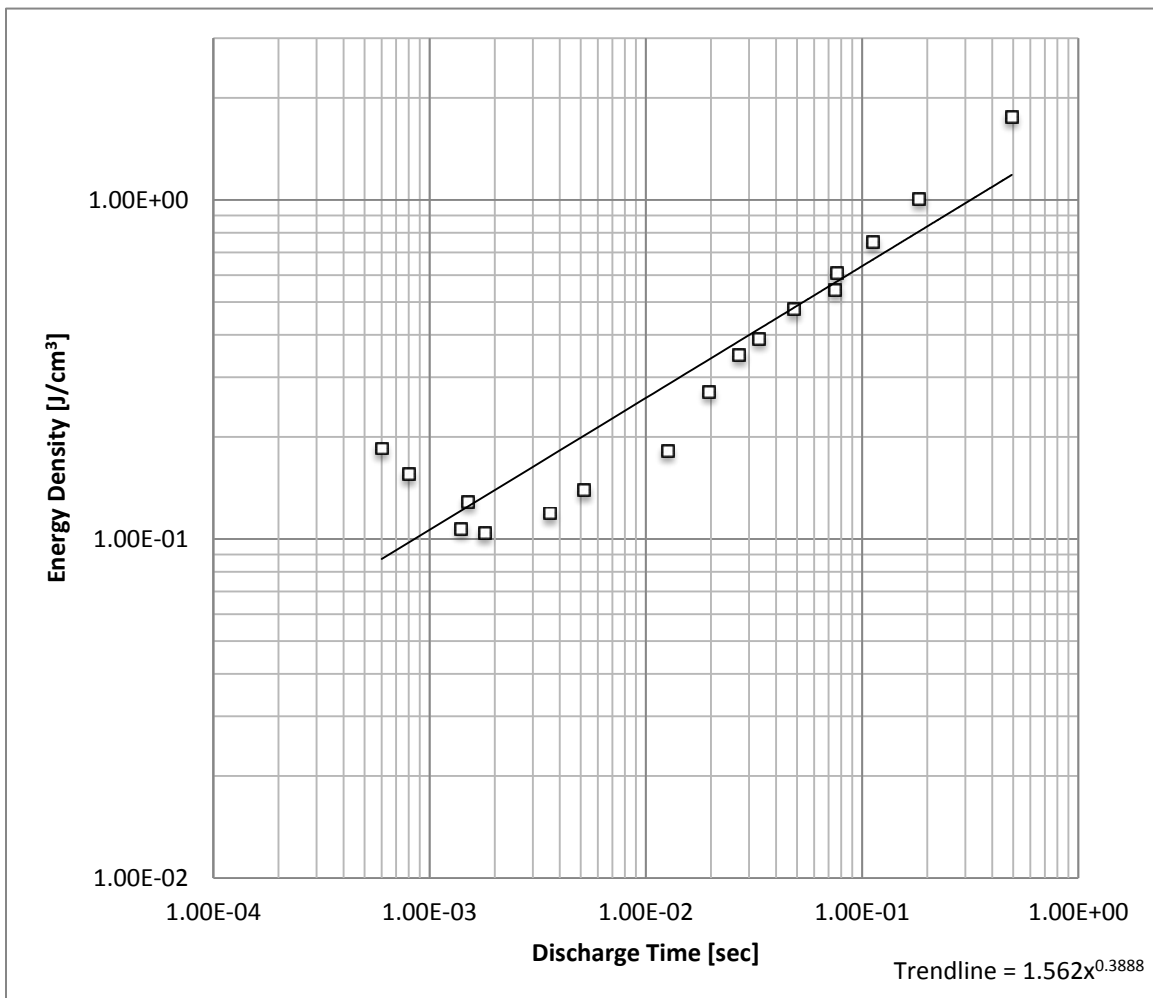


Figure 60. NaNO₃ 10% Energy Density vs. Discharge Time (Charge=Discharge)

2. NaNO_3 20 wt% Charge Equals Discharge

NaNO_3 at 20% concentration, shown in Figure 61, holds the signature wave-like pattern through lower frequency testing. A significant change in the wave-like pattern is observed when the discharge rate is set to 30 mA. Frequency range was consistent and 2.3 volts was attainable for all discharge rates. Aliasing was observed at the 30 mA discharge rate.

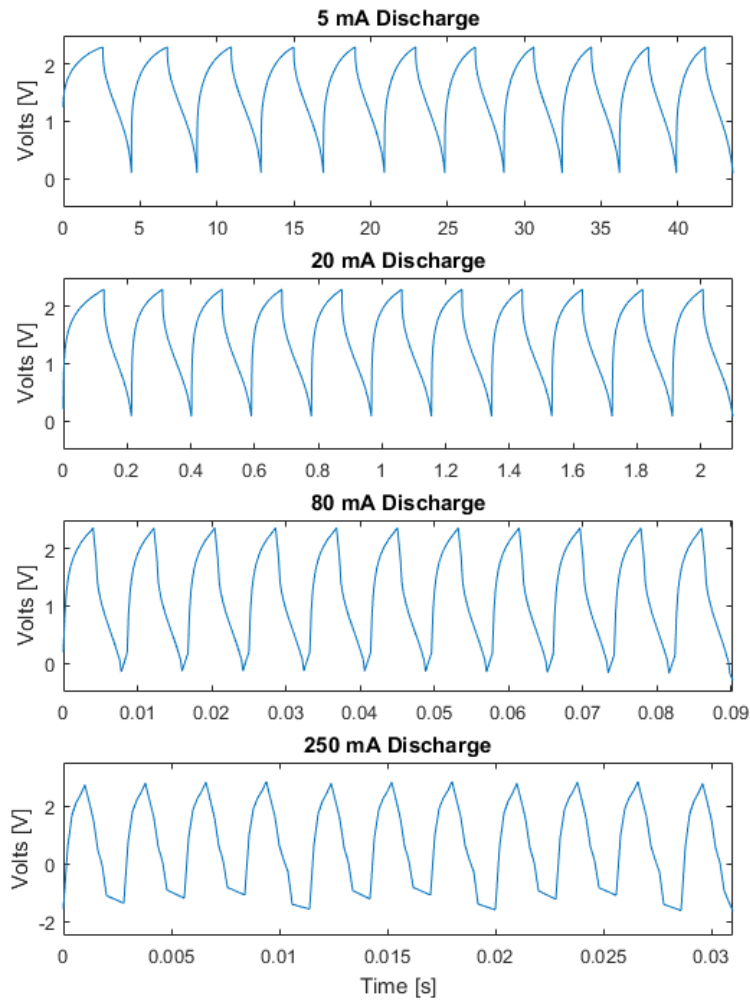


Figure 61. NaNO_3 20% Concentration (Charge=Discharge)

Figure 62 shows the energy density characteristics for NaNO₃ at 20% concentration by weight when charge rate equals discharge rate. The longest discharge time was measured at 1.9 seconds, which corresponds to an energy density of 6.7 J/cm³. The longest discharge time corresponds to the highest dielectric constant of 1.65E7. The shortest discharge time was measured at 8.0E-4 seconds, which corresponds to an energy density of 1.8E-1 J/cm³. The shortest discharge time corresponds to the second lowest dielectric constant of 4.53E5. Per the power trendline, a discharge of 100 seconds would predict an energy density of 39 J/cm³.

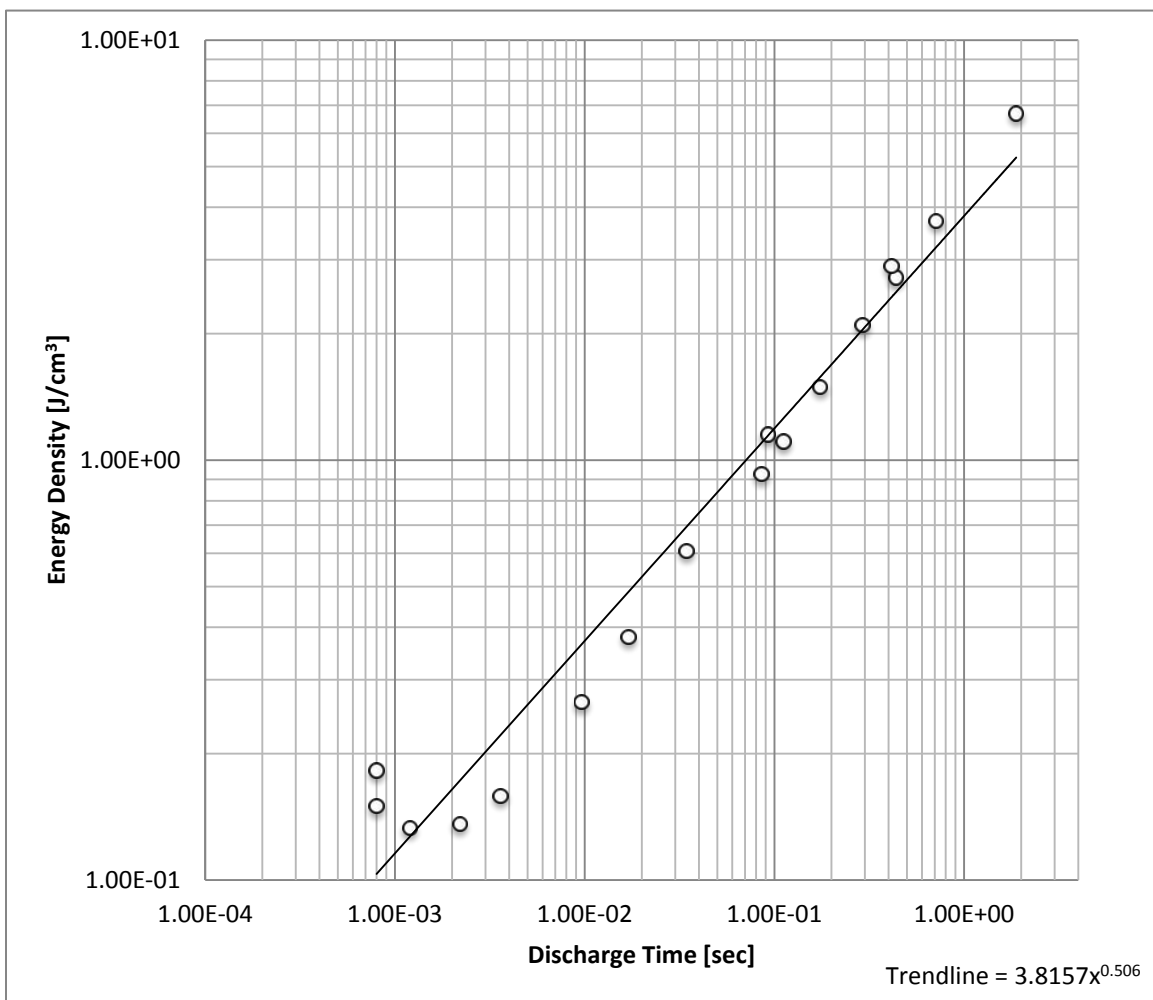


Figure 62. NaNO₃ 20% Energy Density vs. Discharge Time (Charge=Discharge)

3. NaNO_3 30 wt% Charge Equals Discharge

NaNO_3 at 30% concentration, shown in Figure 63, holds the signature wave-like pattern through lower frequency testing. A significant change in the wave-like pattern is observed when the discharge rate is set to 80 mA. Frequency range was consistent and 2.3 volts was attainable for all discharge rates. Aliasing was observed at the 30 mA discharge rate.

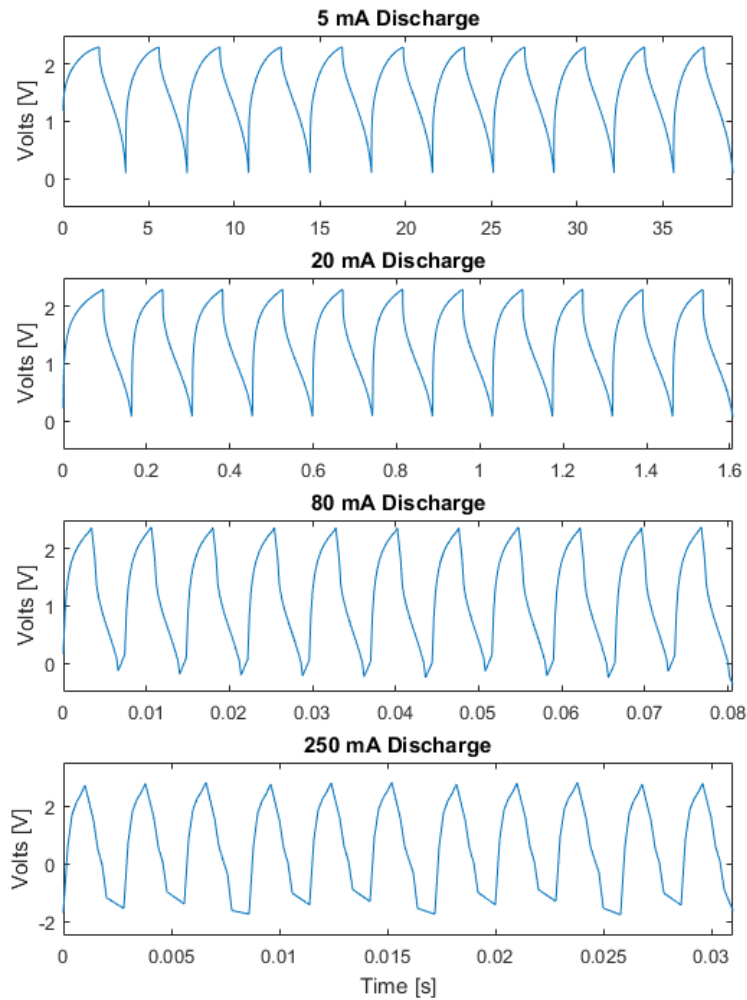


Figure 63. NaNO_3 30% Concentration (Charge=Discharge)

Figure 64 shows the energy density characteristics for NaNO₃ at 30% concentration by weight when charge rate equals discharge rate. The longest discharge time was measured at 1.7 seconds, which corresponds to an energy density of 6 J/cm³. The longest discharge time corresponds to the highest dielectric constant of 1.33E7. The shortest discharge time was measured at 8.0E-4 seconds, which corresponds to an energy density of 1.7E-1 J/cm³. The shortest discharge time corresponds to the third lowest dielectric constant of 4.51E5. Per the power trendline, a discharge of 100 seconds would predict an energy density of 43 J/cm³.

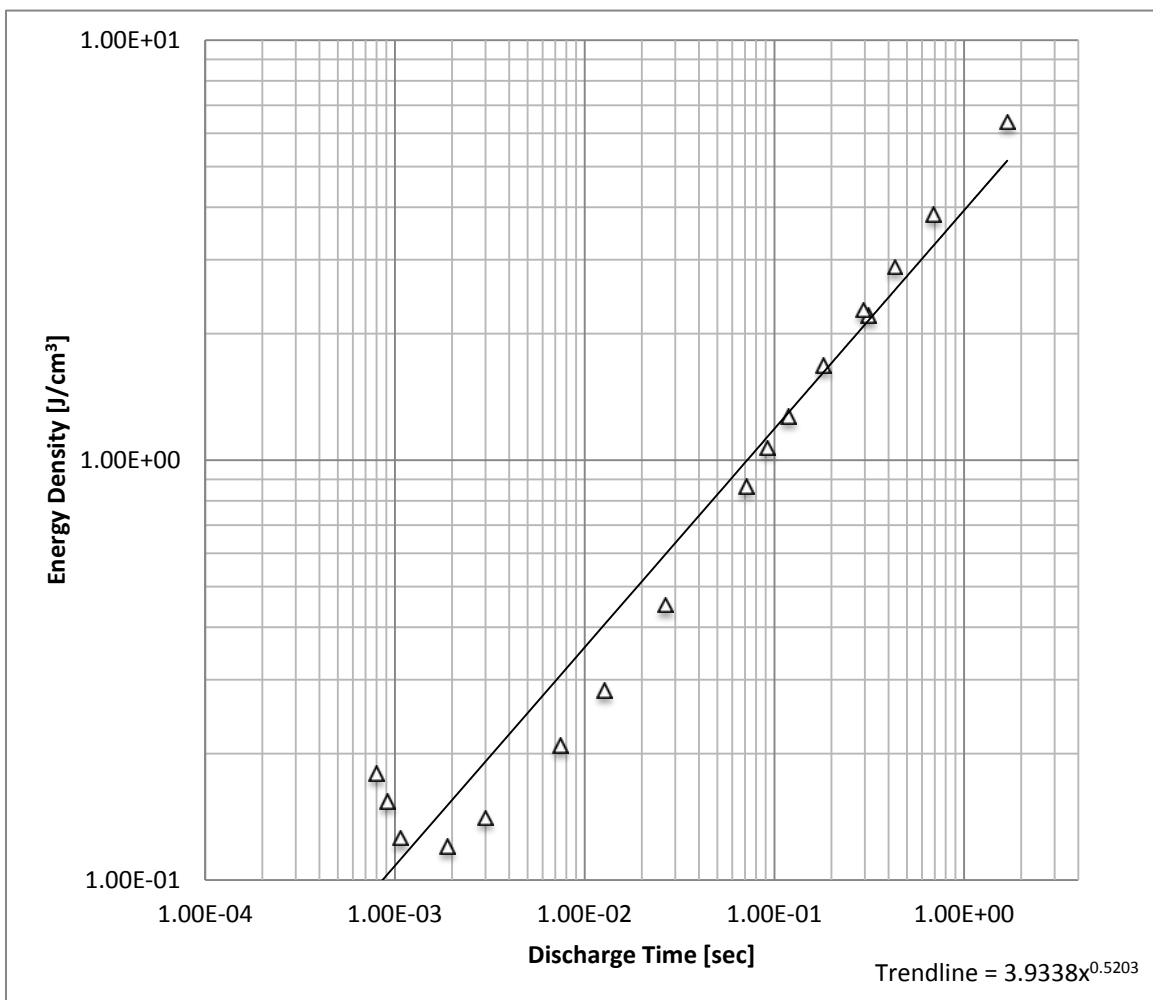


Figure 64. NaNO₃ 30% Energy Density vs. Discharge Time (Charge=Discharge)

4. NaNO_3 10 wt% Charge Fixed

NaNO_3 at 10% concentration, shown in Figure 65, holds the signature wave-like pattern through lower frequency testing. No significant change in the wave-like pattern was observed over all discharge rates. Frequency range was consistent and 2.3 volts was attainable for all discharge rates. Aliasing was observed at the 30 mA discharge rate.

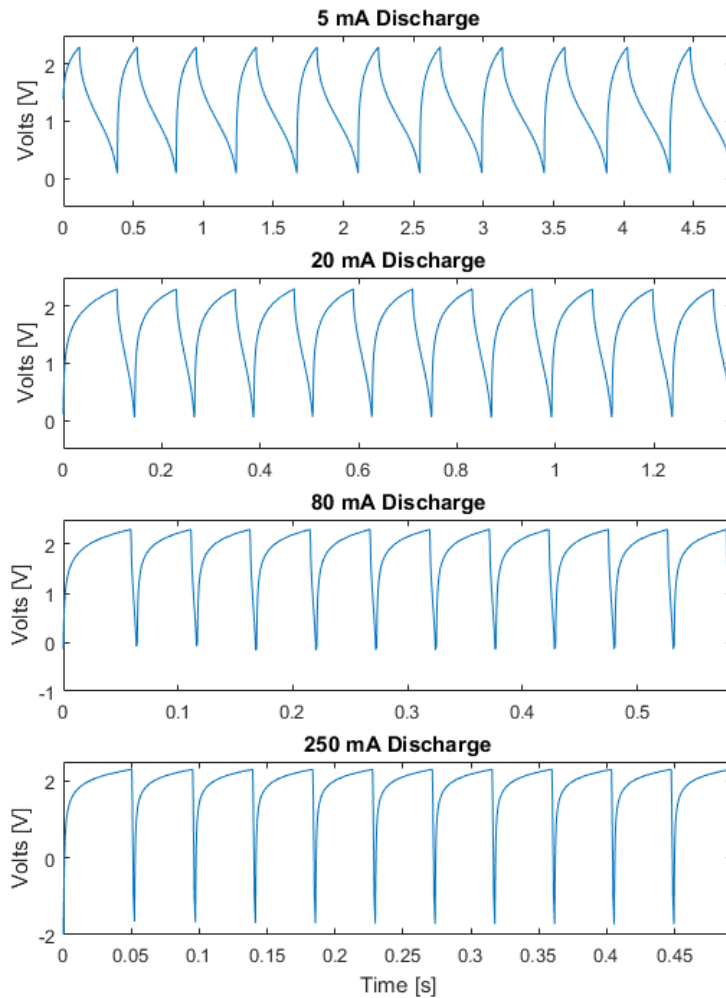


Figure 65. NaNO_3 10% Concentration (Charge \neq Discharge)

Figure 66 shows the energy density characteristics for NaNO₃ at 10% concentration by weight when charge rate is constant at 10 mA. The longest discharge time was measured at 0.1 seconds, which corresponds to an energy density of 0.6 J/cm³. The longest discharge time corresponds to a dielectric constant of 1.75E6. The shortest discharge time was measured at 8.0E-4 seconds, which corresponds to an energy density of 1.7E-1 J/cm³. The shortest discharge time corresponds to a dielectric constant of 4.76E5. Per the power trendline, a discharge of 100 seconds would predict an energy density of 5 J/cm³.

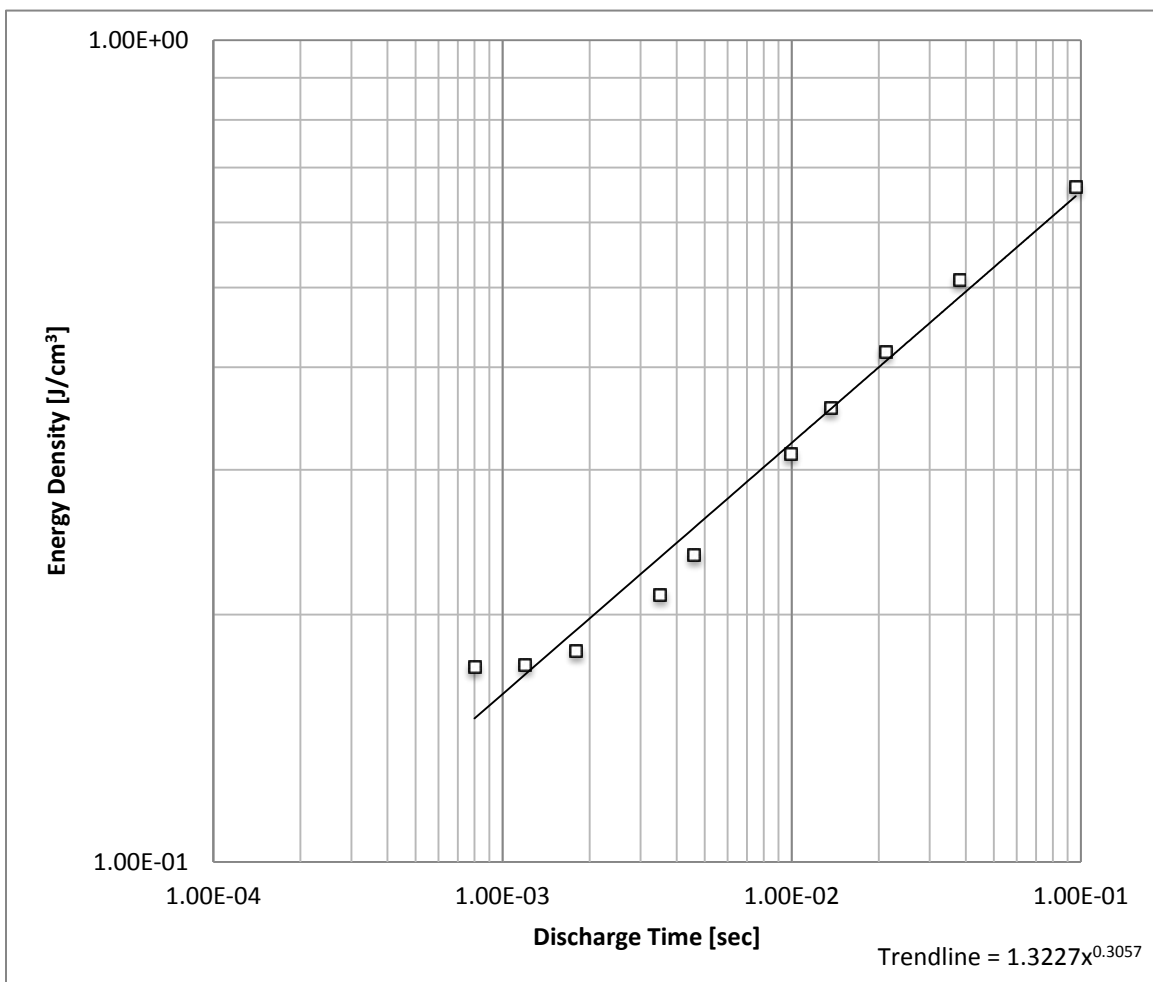


Figure 66. NaNO₃ 10% Energy Density vs. Discharge Time (Charge≠Discharge)

5. NaNO₃ 20 wt% Charge Fixed

NaNO₃ at 20% concentration, shown in Figure 67, holds the signature wave-like pattern through lower frequency testing. No significant change in the wave-like pattern was observed over all discharge rates. Frequency range was consistent and 2.3 volts was attainable for all discharge rates. Aliasing was observed at the 80 mA discharge rate.

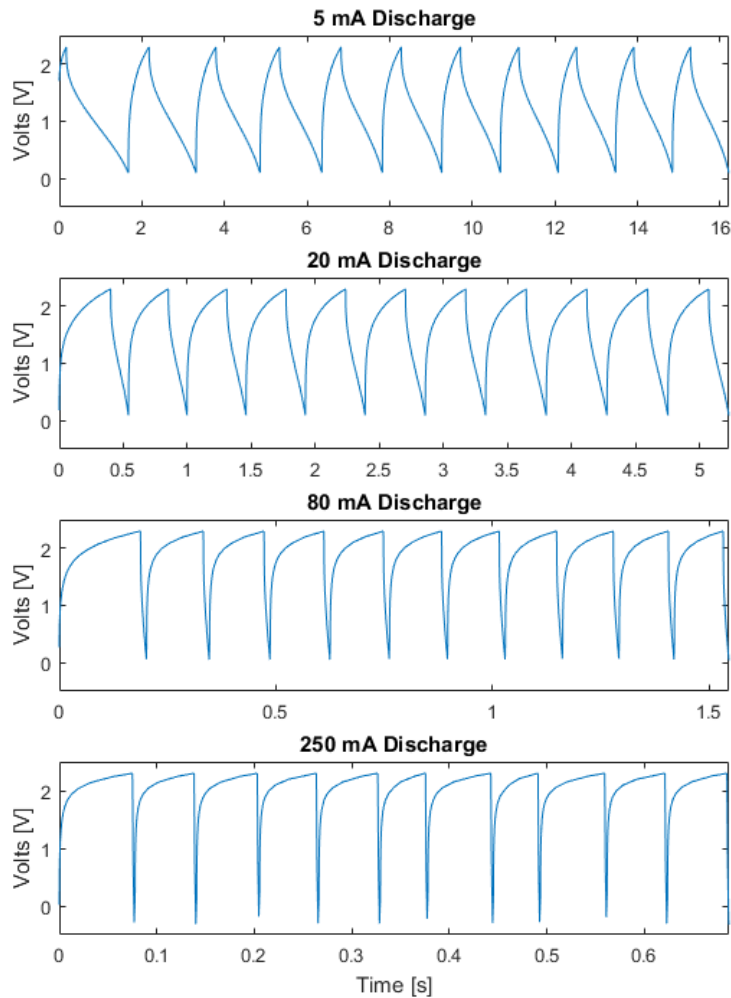


Figure 67. NaNO₃ 20% Concentration (Charge≠Discharge)

Figure 68 shows the energy density characteristics for NaNO₃ at 20% concentration by weight when charge rate is constant at 10 mA. The longest discharge time was measured at 0.4 seconds, which corresponds to an energy density of 2.4 J/cm³. The longest discharge time corresponds to a dielectric constant of 9.25E6. The shortest discharge time was measured at 1.4E-3 seconds, which corresponds to an energy density of 2.1E-1 J/cm³. The shortest discharge time corresponds to a dielectric constant of 1.13E6. Per the power trendline, a discharge of 100 seconds would predict an energy density of 29 J/cm³.

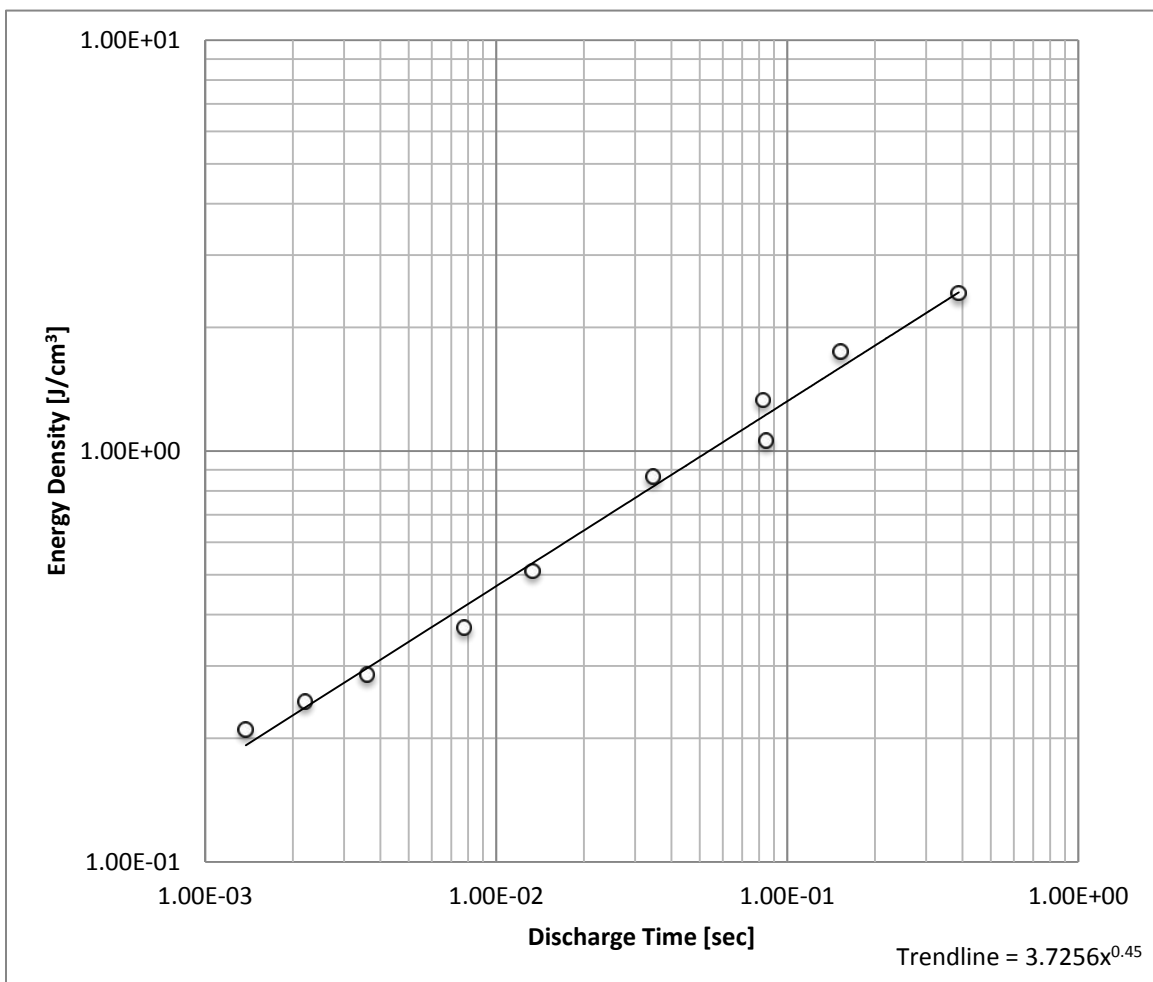


Figure 68. NaNO₃ 20% Energy Density vs. Discharge Time (Charge≠Discharge)

6. NaNO_3 30 wt% Charge Fixed

NaNO_3 at 30% concentration, shown in Figure 69, holds the signature wave-like pattern through lower frequency testing. No significant change in the wave-like pattern was observed over all discharge rates. Frequency range was consistent and 2.3 volts was attainable for all discharge rates. Aliasing was observed at the 50 mA discharge rate.

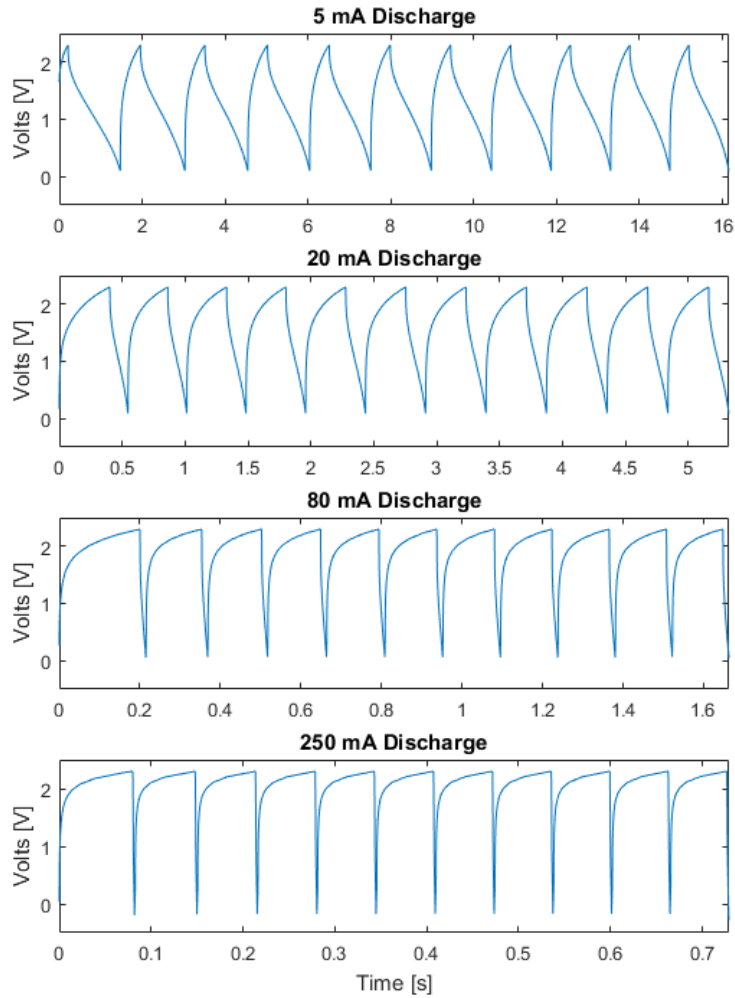


Figure 69. NaNO_3 30% Concentration (Charge \neq Discharge)

Figure 70 shows the energy density characteristics for NaNO₃ at 30% concentration by weight when charge rate is constant at 10 mA. The longest discharge time was measured at 0.4 seconds, which corresponds to an energy density of 2.6 J/cm³. The longest discharge time corresponds to a dielectric constant of 7.76E6. The shortest discharge time was measured at 1.7E-3 seconds, which corresponds to an energy density of 2.4E-1 J/cm³. The shortest discharge time corresponds to a dielectric constant of 1.35E6. Per the power trendline, a discharge of 100 seconds would predict an energy density of 39 J/cm³.

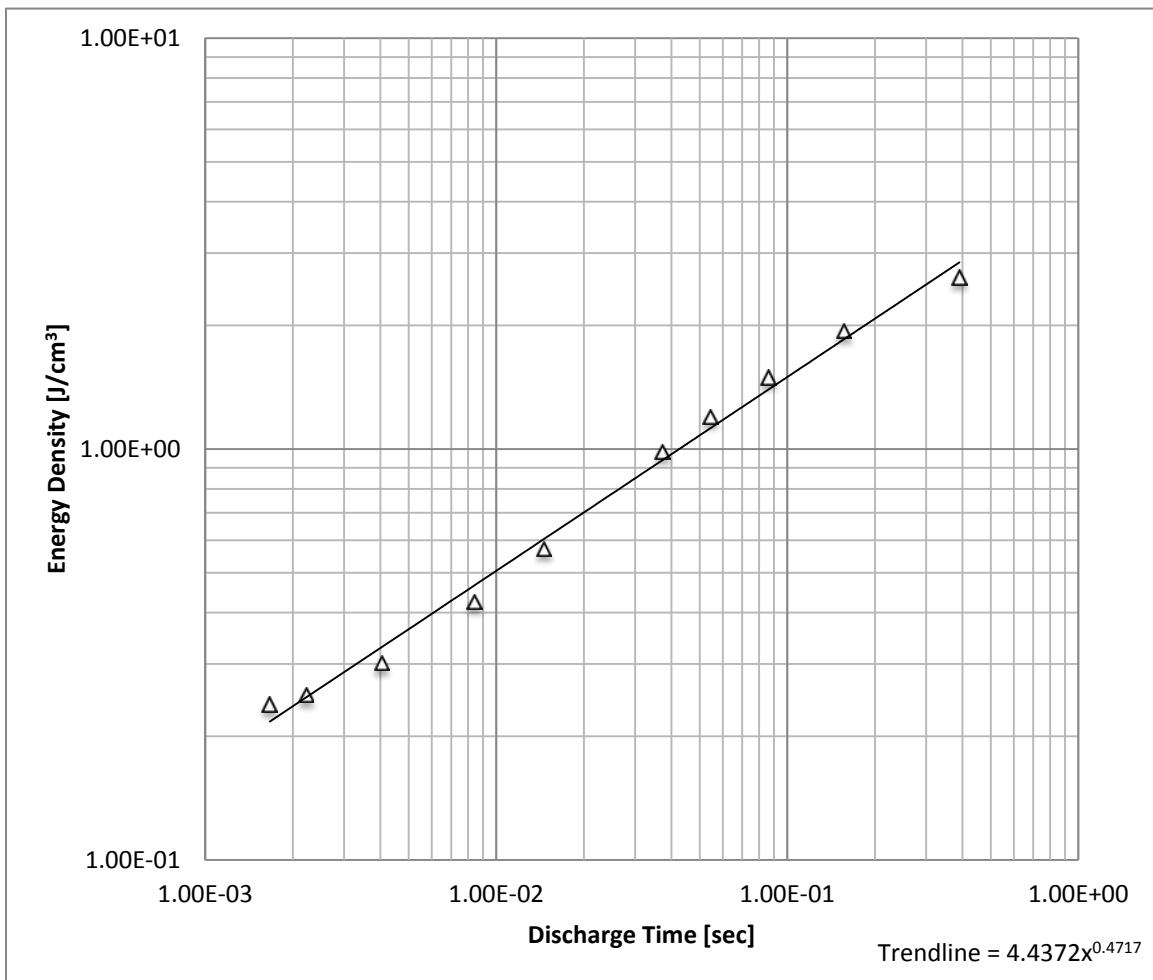


Figure 70. NaNO₃ 30% Energy Density vs. Discharge Time (Charge≠Discharge)

E. POTASSIUM HYDROXIDE

1. KOH 10 wt% Charge Equals Discharge

KOH at 10% concentration, shown in Figure 71, holds the signature wave-like pattern through lower frequency testing. No significant change in the wave-like pattern is observed for all discharge rates. Frequency range was consistent and 2.3 volts was attainable for all discharge rates. Aliasing was observed at the 80 mA discharge rate.

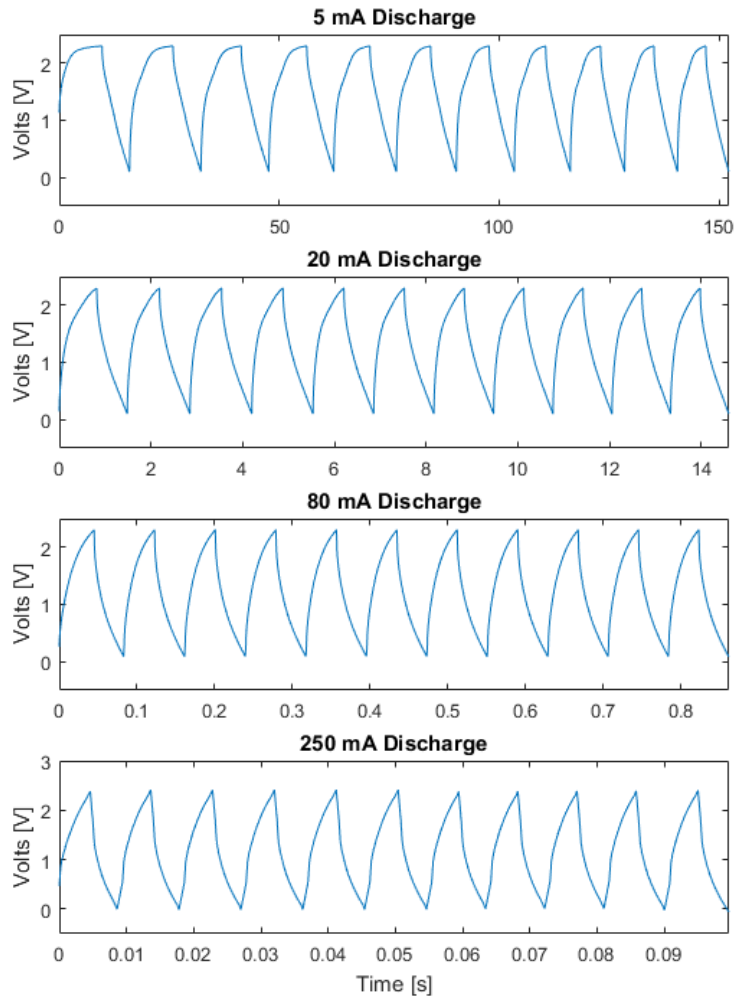


Figure 71. KOH 10% Concentration (Charge=Discharge)

Figure 72 shows the energy density characteristics for KOH at 10% concentration by weight when charge rate equals discharge rate. The longest discharge time was measured at 5 seconds, which corresponds to an energy density of 17 J/cm³. The longest discharge time corresponds to the highest dielectric constant of 8.44E7. The shortest discharge time was measured at 3.8E-3 seconds, which corresponds to an energy density of 0.5 J/cm³. The shortest discharge time corresponds to the lowest dielectric constant of 3.70E6. Per the power trendline, a discharge of 100 seconds would predict an energy density of 66 J/cm³.

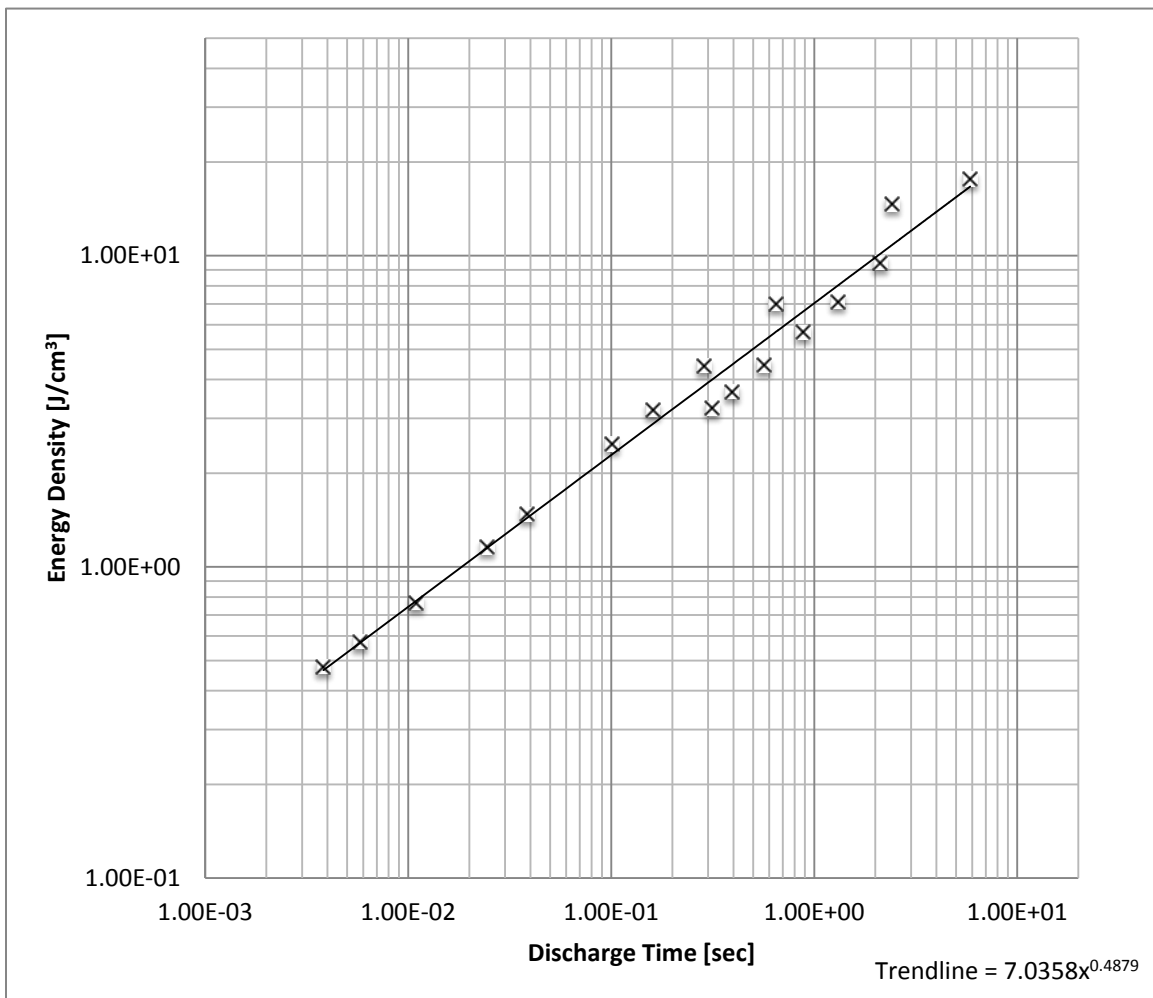


Figure 72. KOH 10% Energy Density vs. Discharge Time (Charge=Discharge)

2. KOH 20 wt% Charge Equals Discharge

KOH at 20% concentration, shown in Figure 73, holds the signature wave-like pattern through lower frequency testing. No significant change in the wave-like pattern is observed for all discharge rates. Frequency range was consistent and 2.3 volts was attainable for all discharge rates. Aliasing was observed at the 80 mA discharge rate.

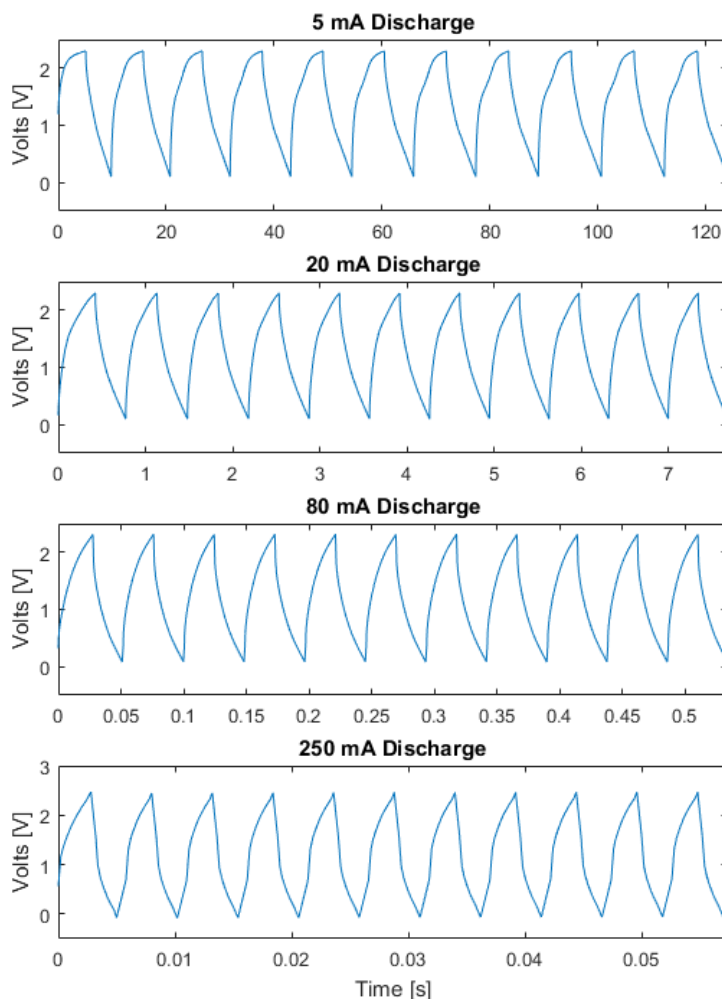


Figure 73. KOH 20% Concentration (Charge=Discharge)

Figure 74 shows the energy density characteristics for KOH at 20% concentration by weight when charge rate equals discharge rate. The longest discharge time was measured at 5 seconds, which corresponds to an energy density of 14 J/cm³. The longest discharge time corresponds to the highest dielectric constant of 8.63E7. The shortest discharge time was measured at 1.8E-3 seconds, which corresponds to an energy density of 2.6E-1 J/cm³. The shortest discharge time corresponds to the lowest dielectric constant of 1.94E6. Per the power trendline, a discharge of 100 seconds would predict an energy density of 69 J/cm³.

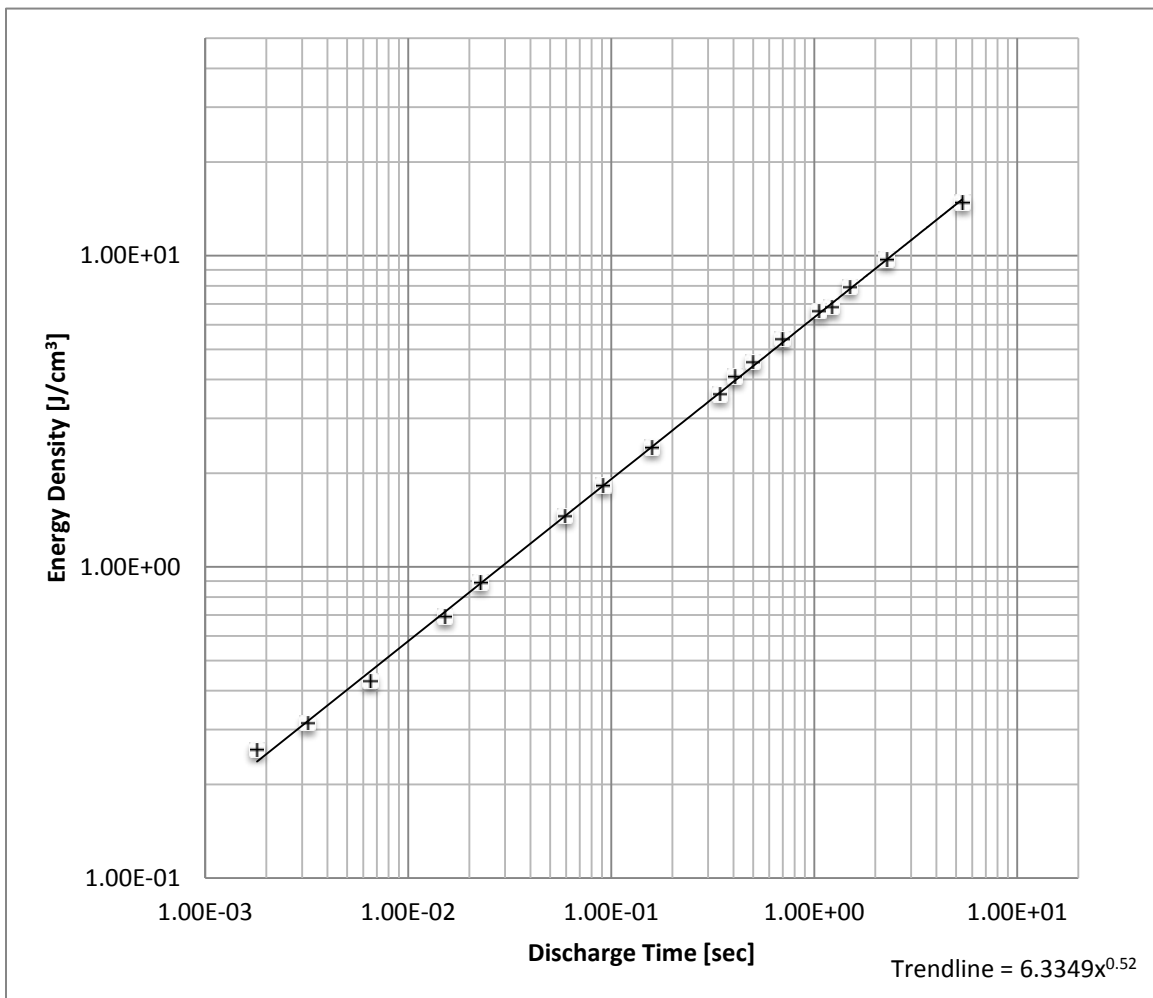


Figure 74. KOH 20% Energy Density vs. Discharge Time (Charge=Discharge)

3. KOH 30 wt% Charge Equals Discharge

KOH at 30% concentration, shown in Figure 75, holds the signature wave-like pattern through lower frequency testing. A significant change in the wave-like pattern is observed when the discharge rate is set to 250 mA. Frequency range was consistent and 2.3 volts was attainable for all discharge rates. Aliasing was observed at the 80 mA discharge rate.

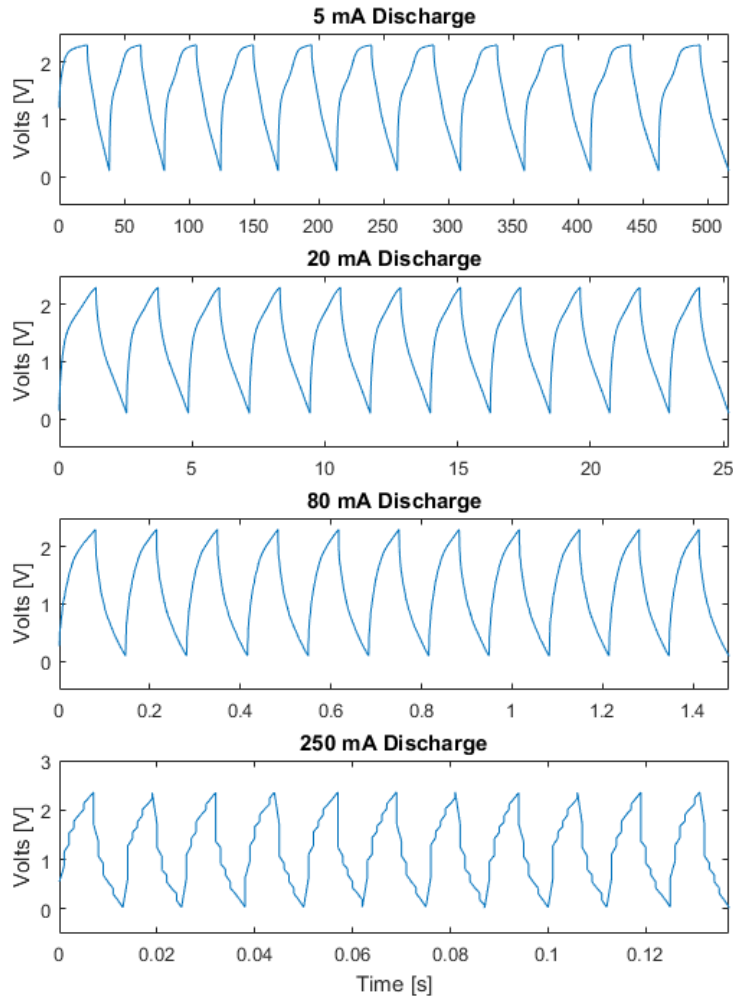


Figure 75. KOH 30% Concentration (Charge=Discharge)

Figure 76 shows the energy density characteristics for KOH at 30% concentration by weight when charge rate equals discharge rate. The longest discharge time was measured at 20 seconds, which corresponds to an energy density of 59 J/cm³. The longest discharge time corresponds to the highest dielectric constant of 2.99E8. The shortest discharge time was measured at 5.8E-3 seconds, which corresponds to an energy density of 0.6 J/cm³. The shortest discharge time corresponds to the lowest dielectric constant of 5.75E6. Per the power trendline, a discharge of 100 seconds would predict an energy density of 160 J/cm³.

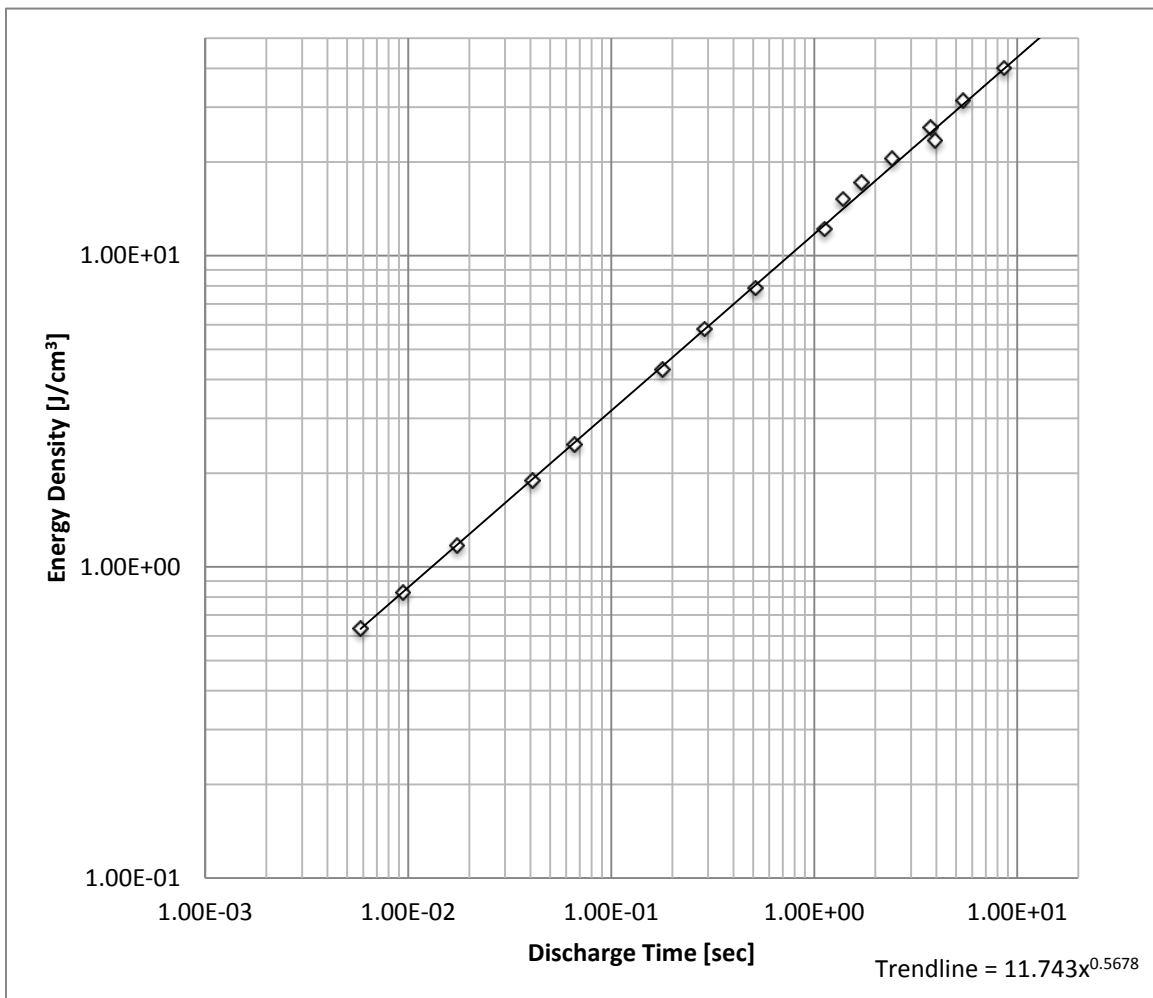


Figure 76. KOH 30% Energy Density vs. Discharge Time (Charge=Discharge)

4. KOH 10 wt% Charge Fixed

KOH at 10% concentration, shown in Figure 77, holds the signature wave-like pattern through lower frequency testing. A significant change in the wave-like pattern is observed when the discharge rate is set to 80 mA. Frequency range was consistent and 2.3 volts was attainable for all discharge rates. Aliasing was observed at the 80 mA discharge rate.

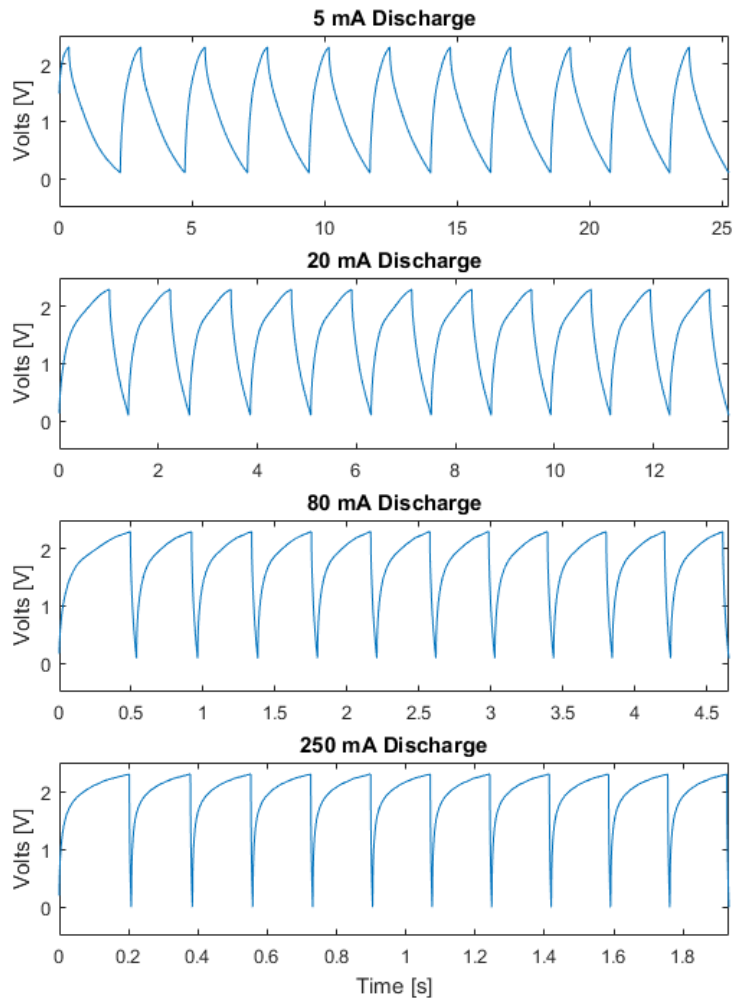


Figure 77. KOH 10% Concentration (Charge≠Discharge)

Figure 78 shows the energy density characteristics for KOH at 10% concentration by weight when charge rate is constant at 10 mA. The longest discharge time was measured at 1 seconds, which corresponds to an energy density of 5.5 J/cm³. The longest discharge time corresponds to a dielectric constant of 3.27E7. The shortest discharge time was measured at 5.4E-3 seconds, which corresponds to an energy density of 0.7 J/cm³. The shortest discharge time corresponds to a dielectric constant of 4.75E6. Per the power trendline, a discharge of 100 seconds would predict an energy density of 39.5 J/cm³.

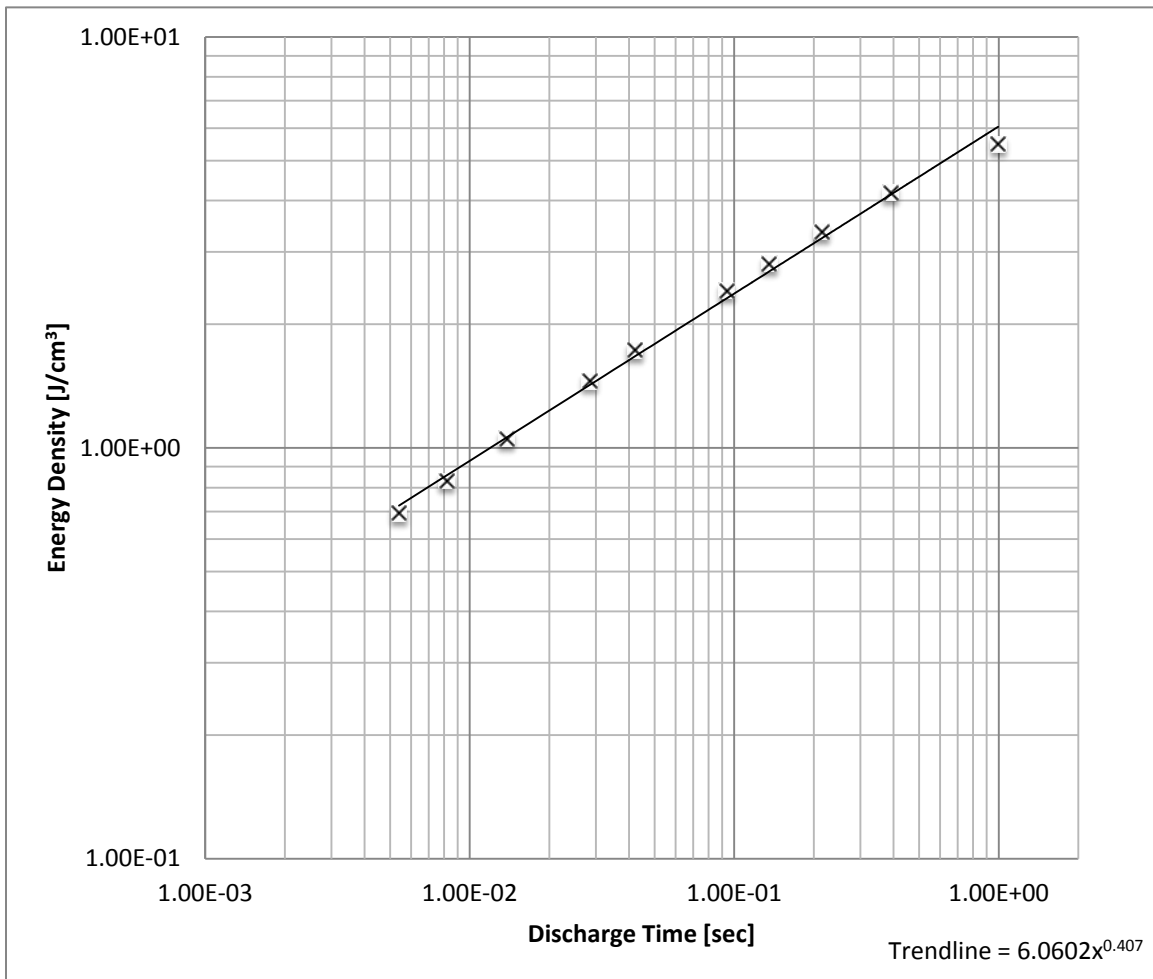


Figure 78. KOH 10% Energy Density vs. Discharge Time (Charge≠Discharge)

5. KOH 20 wt% Charge Fixed

KOH at 20% concentration, shown in Figure 79, holds the signature wave-like pattern through lower frequency testing. A significant change in the wave-like pattern is observed when the discharge rate is set to 50 mA. Frequency range was consistent and 2.3 volts was attainable for all discharge rates. Aliasing was observed at the 80 mA discharge rate.

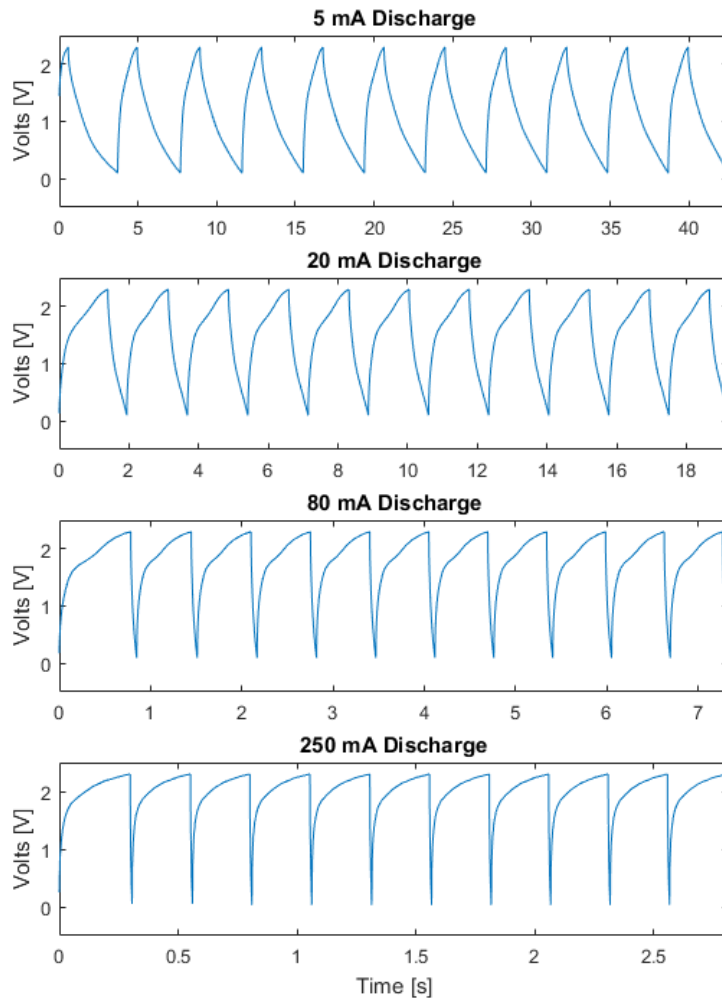


Figure 79. KOH 20% Concentration (Charge≠Discharge)

Figure 80 shows the energy density characteristics for KOH at 20% concentration by weight when charge rate is constant at 10 mA. The longest discharge time was measured at 1.4 seconds, which corresponds to an energy density of 7 J/cm³. The longest discharge time corresponds to a dielectric constant of 4.51E7. The shortest discharge time was measured at 8.0E-3 seconds, which corresponds to an energy density of 1 J/cm³. The shortest discharge time corresponds to a dielectric constant of 7.35E6. Per the power trendline, a discharge of 100 seconds would predict an energy density of 46 J/cm³.

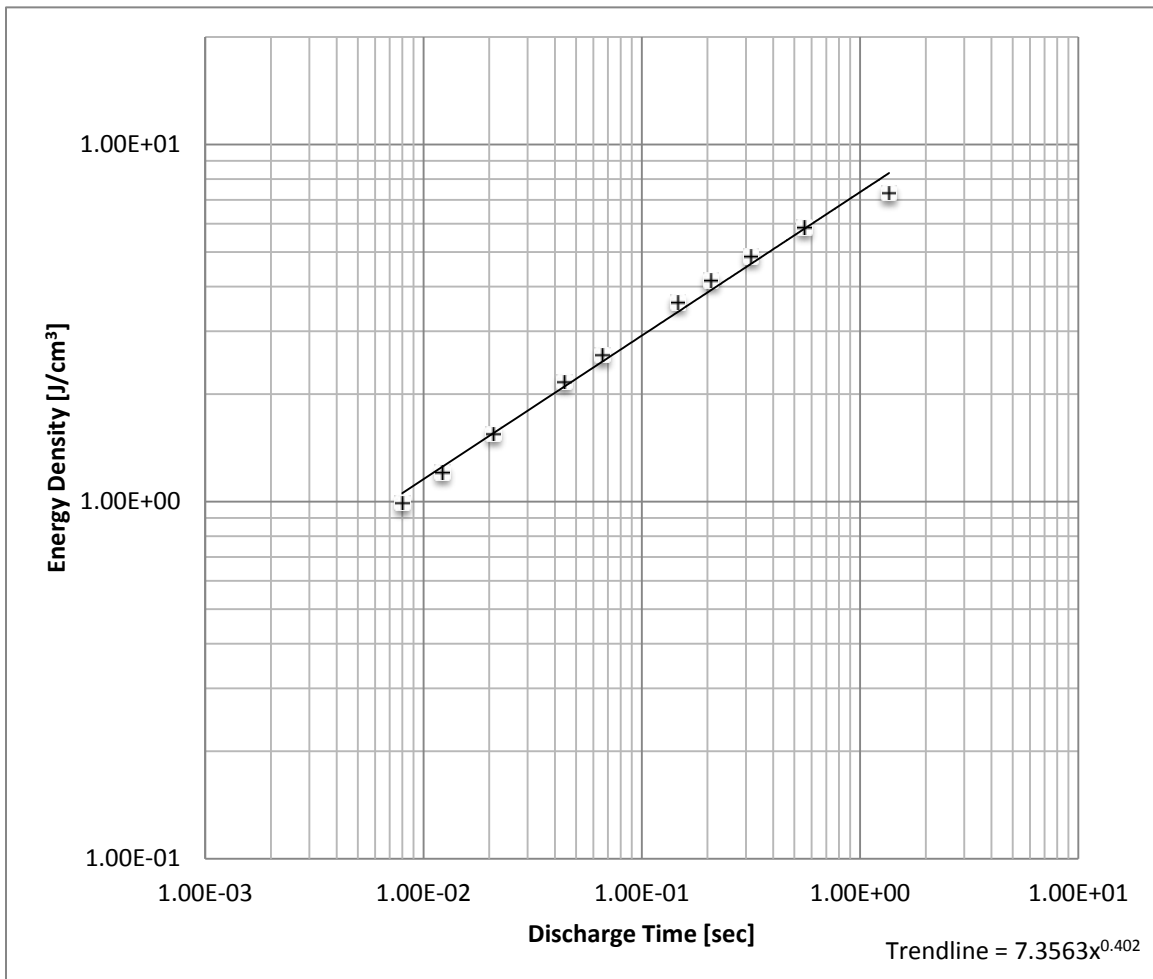


Figure 80. KOH 20% Energy Density vs. Discharge Time (Charge≠Discharge)

6. KOH 30 wt% Charge Fixed

KOH at 30% concentration, shown in Figure 81, holds the signature wave-like pattern through lower frequency testing. A significant change in the wave-like pattern is observed when the discharge rate is set to 80 mA. Frequency range was consistent and 2.3 volts was attainable for all discharge rates. Aliasing was observed at the 150 mA discharge rate.

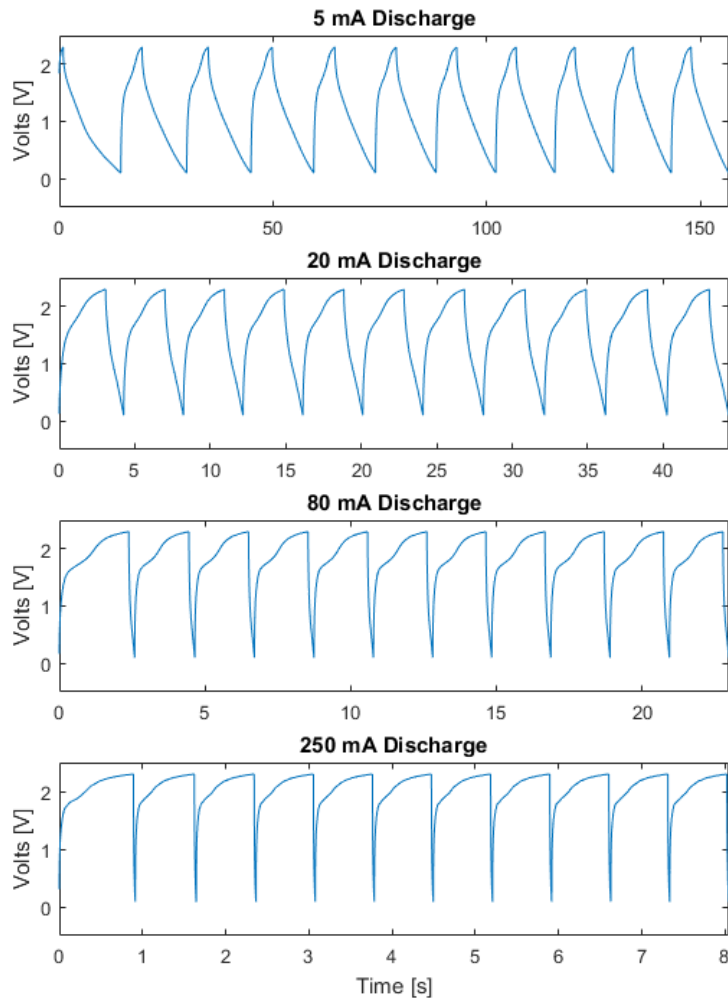


Figure 81. KOH 30% Concentration (Charge≠Discharge)

Figure 82 shows the energy density characteristics for KOH at 30% concentration by weight when charge rate is constant at 10 mA. The longest discharge time was measured at 2.7 seconds, which corresponds to an energy density of 16.5 J/cm³. The longest discharge time corresponds to a dielectric constant of 7.53E7. The shortest discharge time was measured at 2.23E-2 seconds, which corresponds to an energy density of 2 J/cm³. The shortest discharge time corresponds to a dielectric constant of 2.58E7. Per the power trendline, a discharge of 100 seconds would predict an energy density of 91 J/cm³.

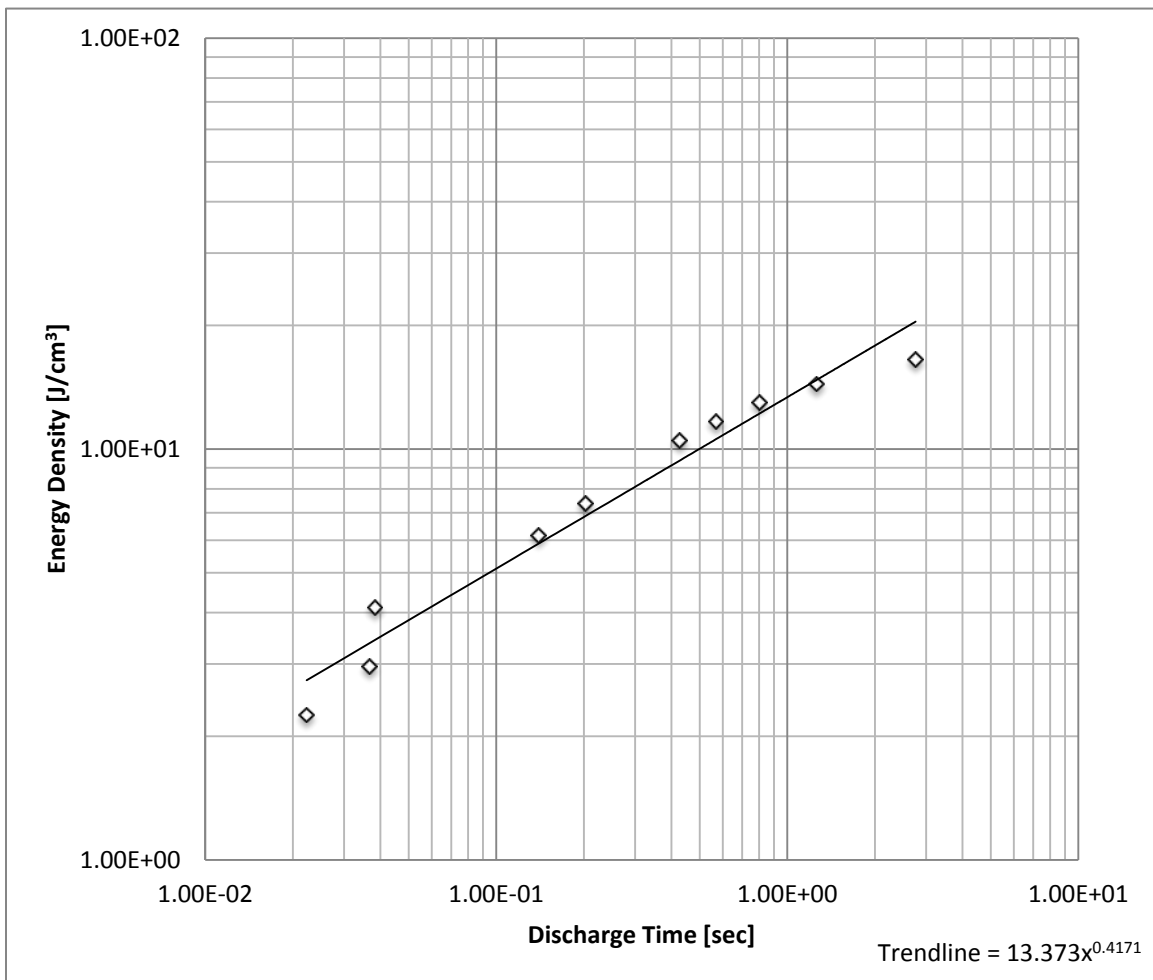


Figure 82. KOH 30% Energy Density vs. Discharge Time (Charge≠Discharge)

THIS PAGE INTENTIONALLY LEFT BLANK

IV. DISCUSSION

The experimental work was designed to determine the capacitance, dielectric constant, energy density, and power density of nine capacitors. Each capacitor was constructed of anodized titanium oxide nanotubes on individual titania substrates filled with aqueous solutions. As previously discussed, anodized films employed nearly identical nanotubes of $\sim 8 \mu\text{m}$ lengths and $\sim 90 \text{ nm}$ diameters. Three salts utilized to saturate the hollow titanium oxide nanotubes were: NH_4Cl , NaNO_3 , and KOH . Each aqueous salt solution was saturated in DI water at the following weight concentrations: 10, 20, and 30%. In sum, there were nine permutations: three salts and three concentrations.

The data for capacitance, dielectric constant, and energy density in every case was found to decrease in magnitude at a variety of fixed rates when discharge time was decreased. Utilizing simple power curve trendlines, the data for these parameters enabled acceptable data extrapolation over longer discharge times. The data provides the ability to determine any of these parameters over a discharge time spanning from $1.0\text{E}-3$ seconds to 100 seconds. The power density, defined as the energy released during discharge from 2.3 to 0.1 volts and divided by the discharge time for this period, was found to increase with decreasing discharge time. Simple power curves empirically appear to accurately model NH_4Cl and KOH but NaNO_3 capacitance, dielectric constant, and energy density are not as easily described by the same methods. Using these simple power curves, data plots can be used to determine with limited accuracy the discharge power density over many orders of magnitude of discharge time.

Finally, the data permitted empirical conclusions to be drawn regarding the impact of salt identity and salt concentration on key parameter values. The first conclusion is salt identity is more significant than salt concentration. It is clear capacitors prepared with NH_4Cl and KOH have higher capacitance, dielectric constant and energy density than capacitors prepared with NaNO_3 . The second conclusion is capacitors prepared with NaNO_3 have values approximately a factor of ten lower than those prepared with NH_4Cl and KOH for all calculated parameters. The third conclusion is salt

concentration provides similar values of capacitance, dielectric constant, and energy density for all concentrations of salt compared at similar discharge times. The impact of salt concentration had limited significance, if any change was observed, and less impact than salt identity. The final conclusion determined from this research was the similarity of the capacitance, dielectric, energy density roll-off as a function of discharge time. The power law relationships for all salts and salt concentrations appear to be similar.

A. AMMONIUM CHLORIDE RESULTS CHARGE EQUALS DISCHARGE

As discussed in the Introduction of this chapter and as seen in Figure 83, capacitance is approximately equal for any concentration of NH_4Cl . This is of concern as it challenges the original SDM theory. According to SDM theory [8], as the number of ions in solution increases, the capacitance should also increase.

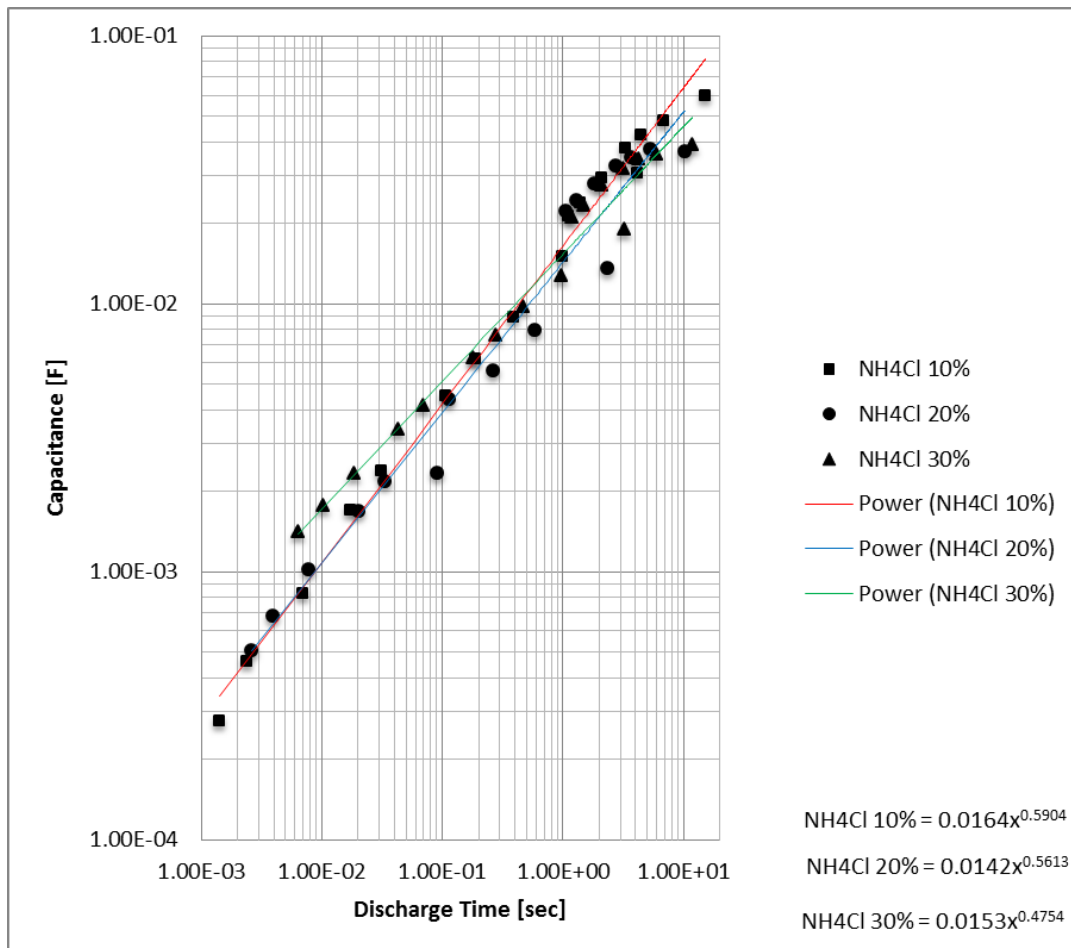


Figure 83. Capacitance vs. Discharge Time (NH_4Cl) (Charge=Discharge)

As discussed in the Introduction of this chapter and as seen in Figure 84, dielectric is approximately equal for any concentration of NH₄Cl. Further inspection of the trendlines shows that higher concentrations perform better at discharge times less than 1 second and conversely lower concentrations perform better at discharge times greater than 5 seconds.

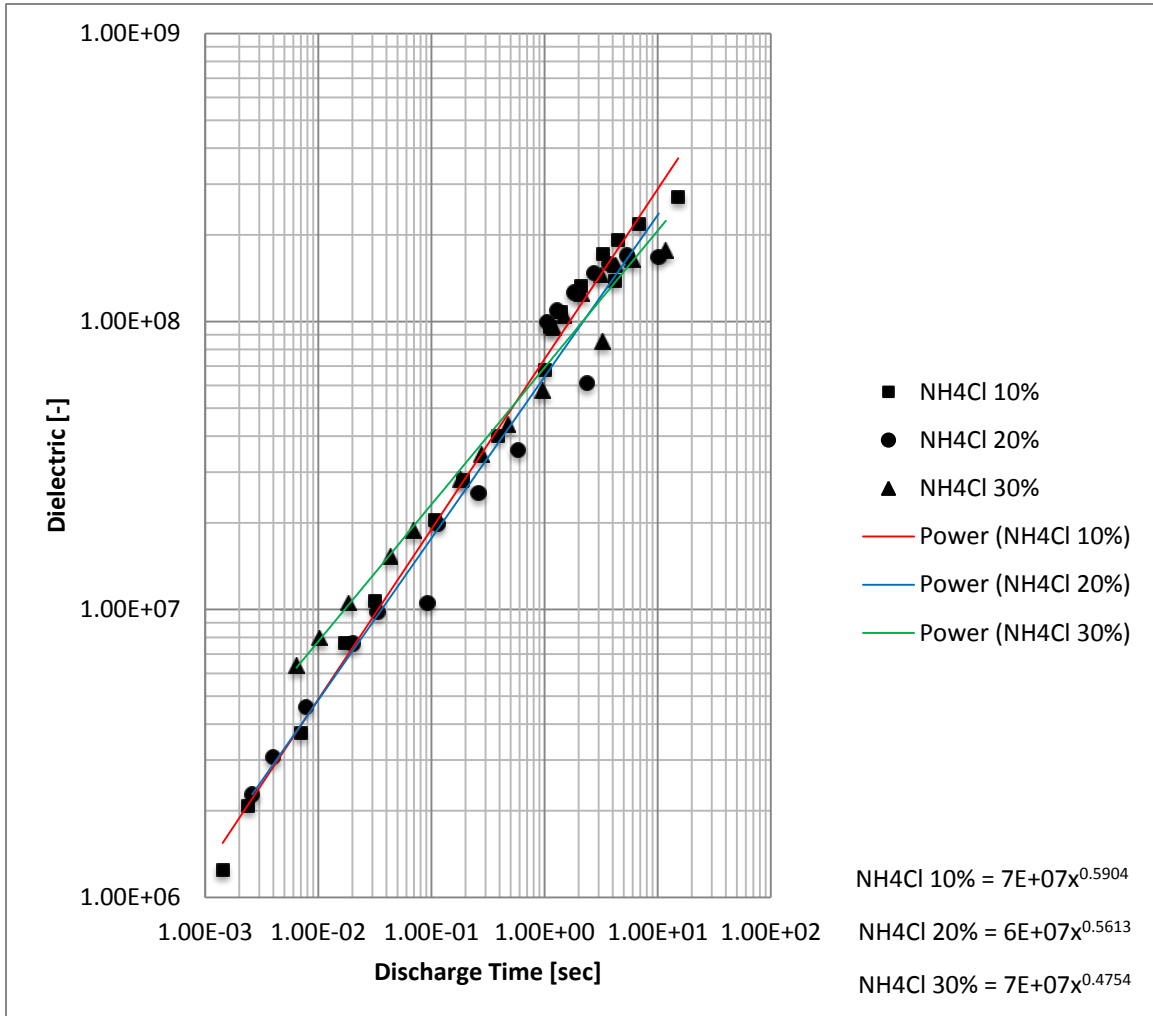


Figure 84. Dielectric vs. Discharge Time (NH₄Cl) (Charge=Discharge)

As discussed in the Introduction of this chapter and as seen in Figure 85, energy density is approximately equal for any concentration of NH_4Cl . Further inspection of the trendlines shows that higher concentrations perform better at discharge times less than 7 seconds and conversely lower concentrations perform better at discharge times greater than 7 seconds. As expected, data from the median concentration falls in between the high and low concentrations below 1 second before rolling off at higher discharge times in the same manner at the higher concentration.

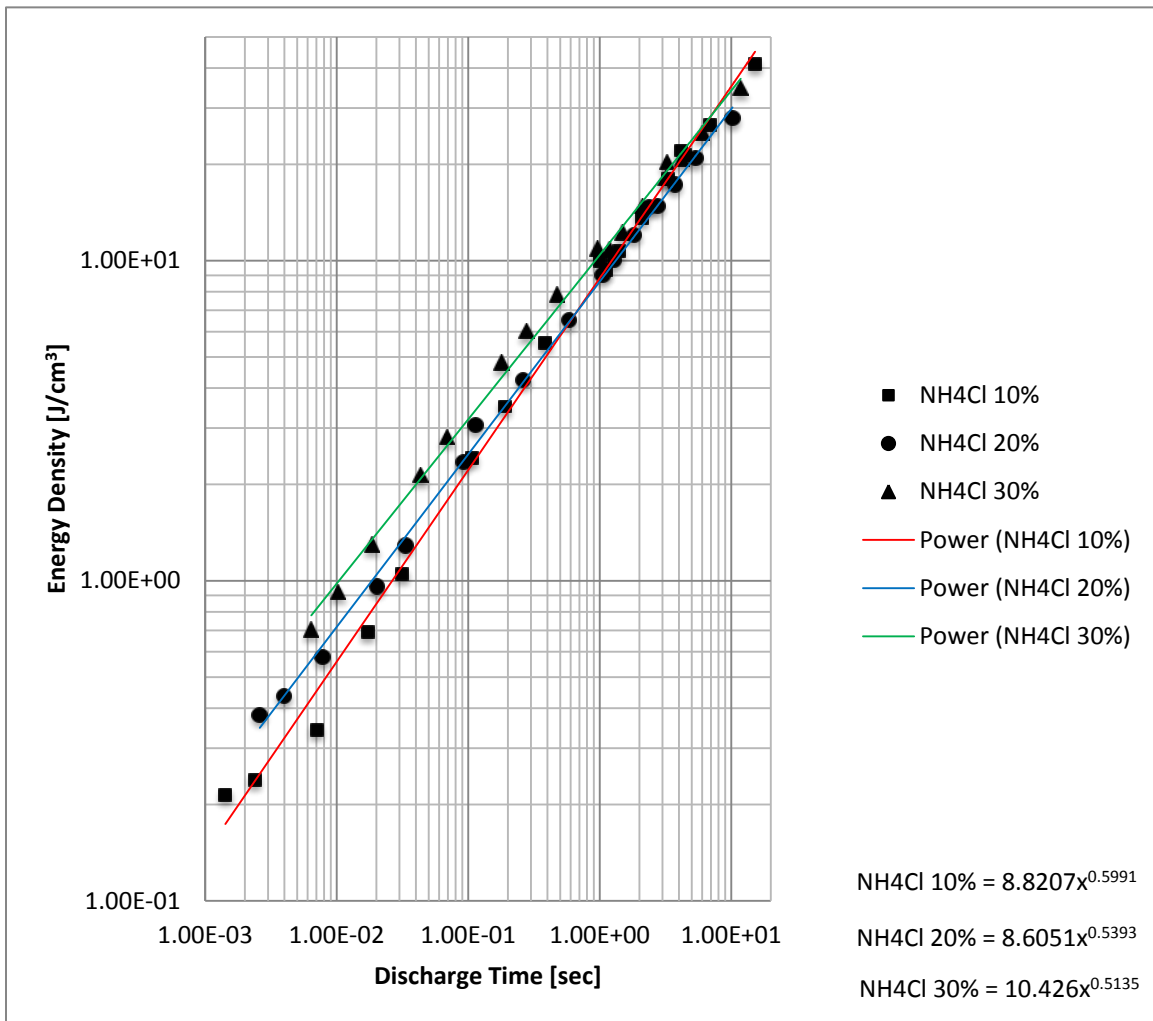


Figure 85. Energy Density vs. Discharge Time (NH_4Cl) (Charge=Discharge)

As discussed in the Introduction of this chapter and as seen in Figure 86, power density is approximately equal for any concentration of NH_4Cl . Further inspection of the trendlines shows that higher concentrations perform better at discharge times less than 7 second and conversely lower concentrations perform better at discharge times greater than 7 seconds. As expected, data from the median concentration falls in between the high and low concentrations below 0.6 second before rolling off at higher discharge times in the same manner at the higher concentration.

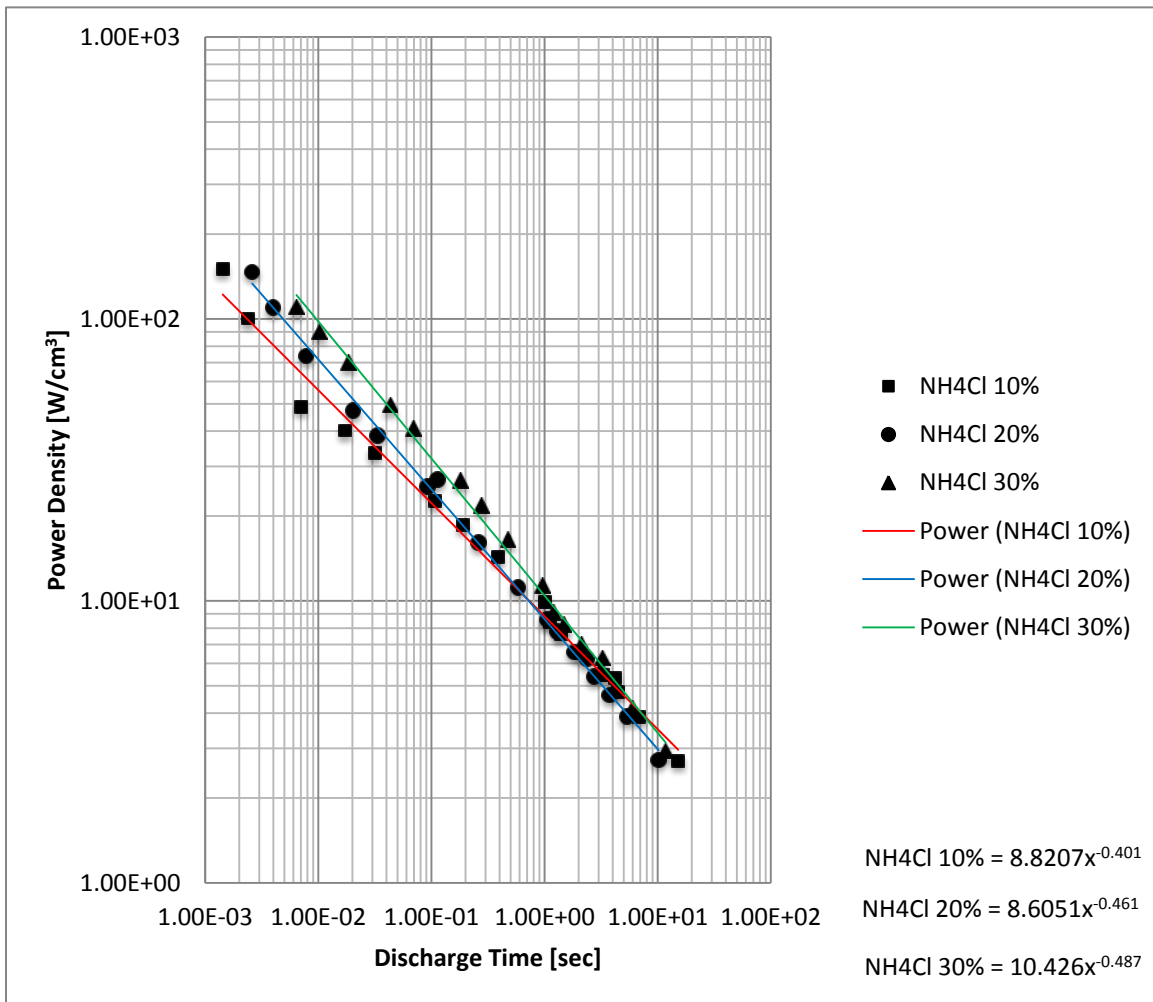


Figure 86. Power Density vs. Discharge Time (NH_4Cl) (Charge=Discharge)

B. SODIUM NITRATE RESULTS CHARGE EQUALS DISCHARGE

As seen in Figure 87, capacitance is approximately equal for higher concentrations of NaNO₃. As with NH₄Cl, NaNO₃ has an ideal concentration between 20 and 30 wt%. Based on the trendlines, this ideal concentration maintains optimum performance over the other concentrations regardless of discharge time.

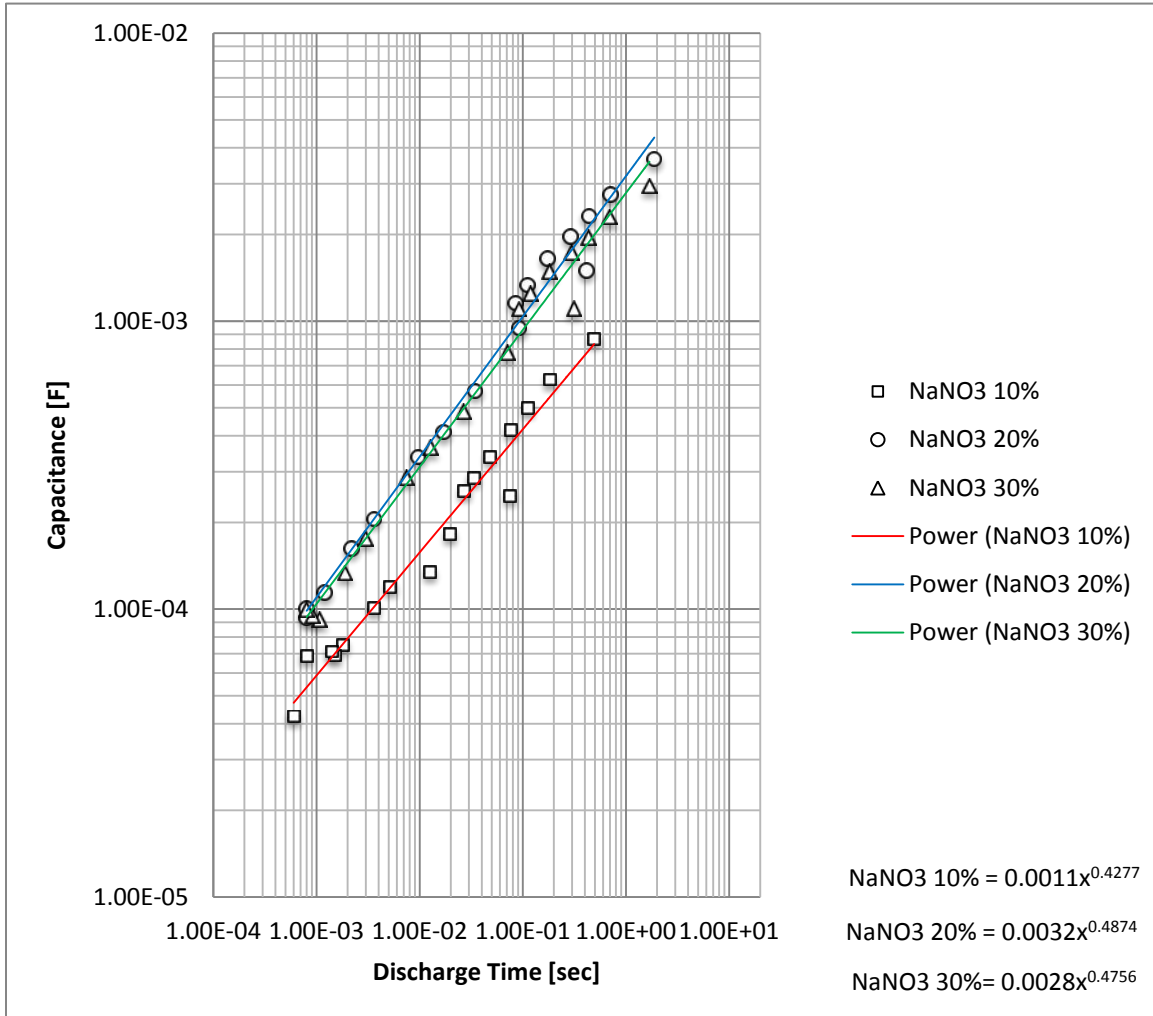


Figure 87. Capacitance vs. Discharge Time (NaNO₃) (Charge=Discharge)

As seen in Figure 88, dielectric is approximately equal for any concentration of NaNO₃. Further inspection of the trendlines shows that higher concentrations perform better for all discharge times. As with NaNO₃ capacitance, the dielectric of higher concentrations are approximately equal for discharge times below 3 seconds before the the 20% concentration begins to perform better than the 30% concentration.

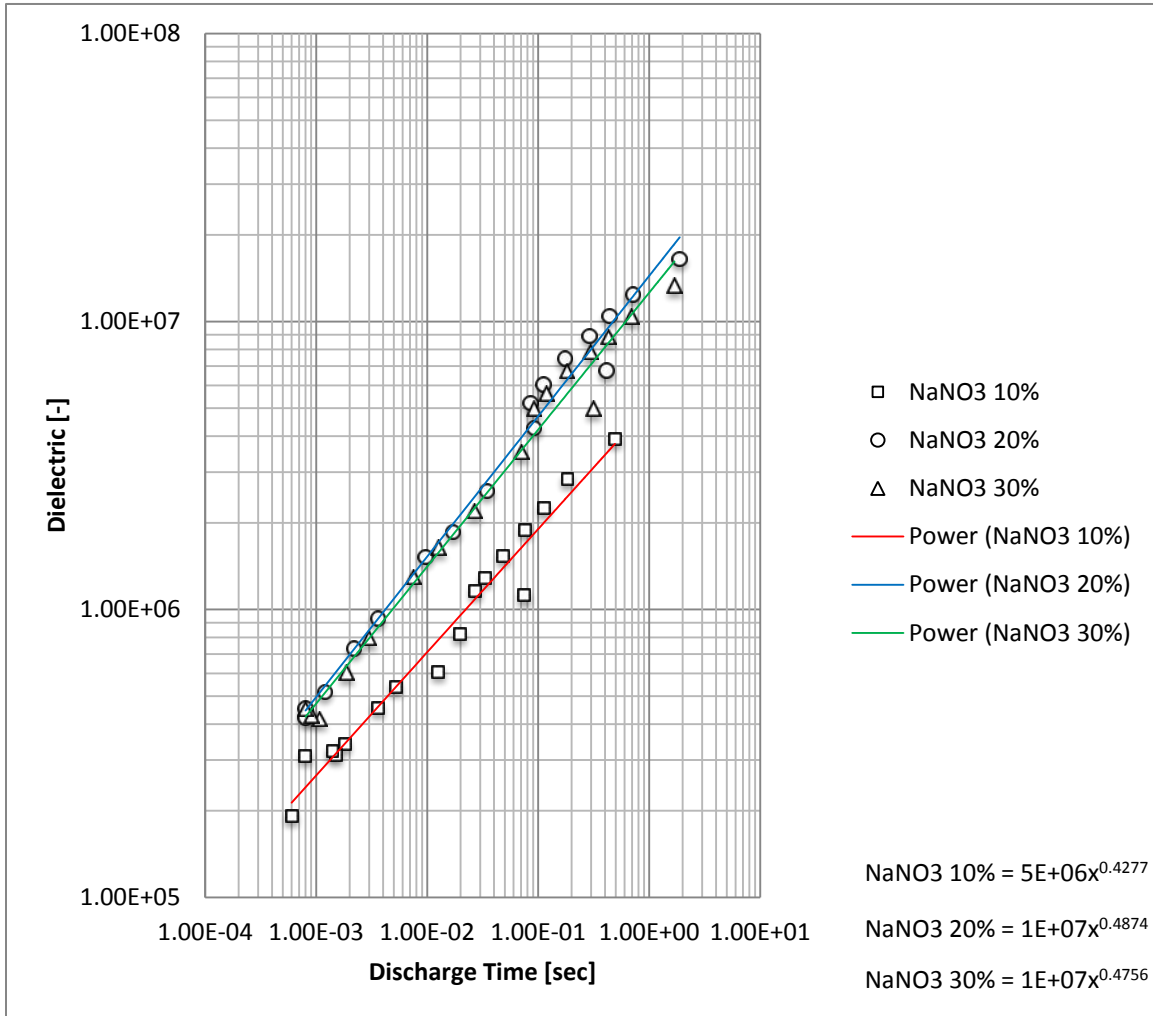


Figure 88. Dielectric vs. Discharge Time (NaNO₃) (Charge=Discharge)

As seen in Figure 89, energy density is approximately equal for higher concentrations of NaNO₃. Further inspection of the trendlines shows that higher concentrations perform better for all discharge times. Unlike NaNO₃ capacitance and dielectric, the higher concentration of 30% performs better than the 20% concentration for all discharge times.

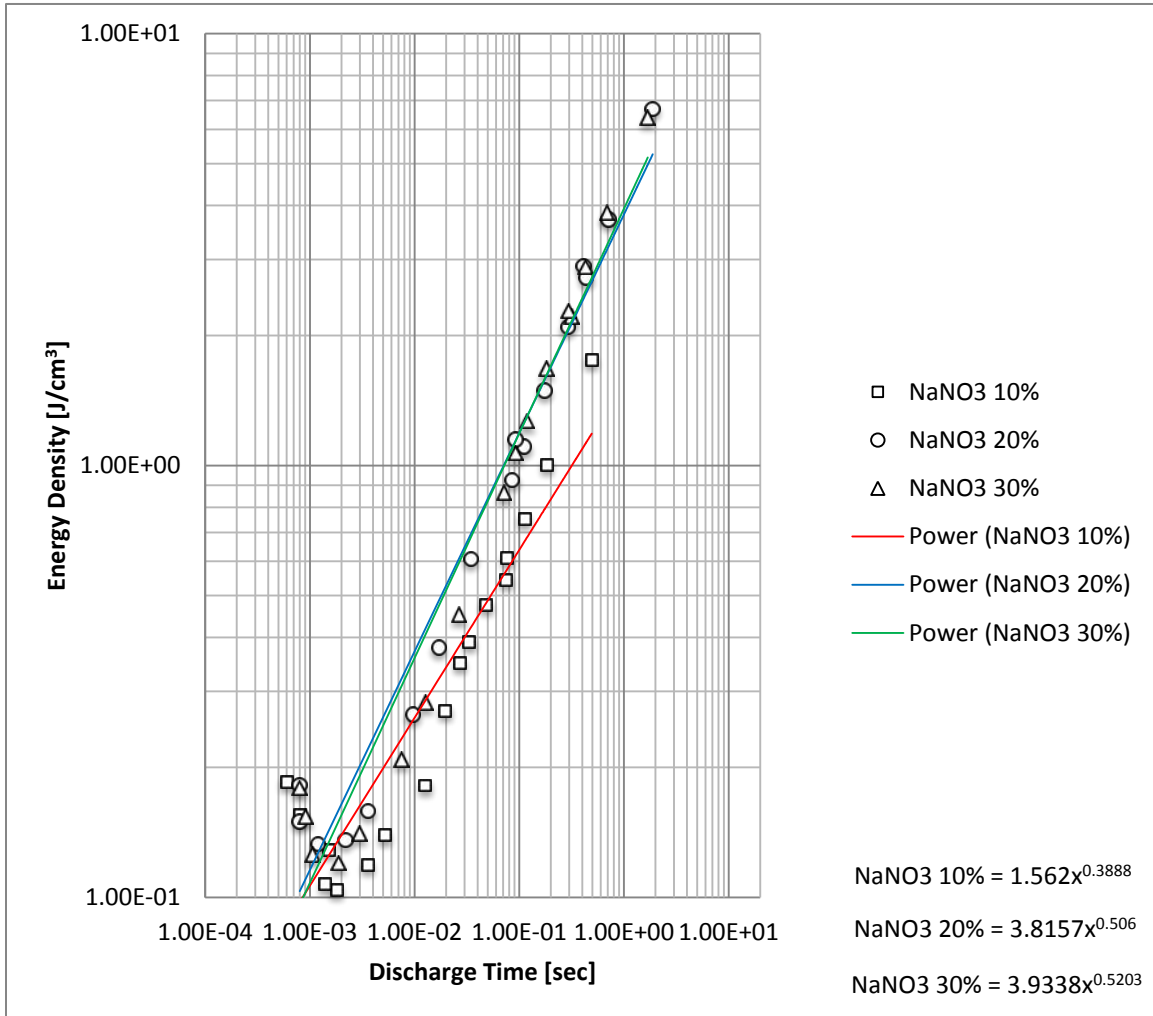


Figure 89. Energy Density vs. Discharge Time (NaNO₃) (Charge=Discharge)

As seen in Figure 90, power density is approximately equal for higher concentrations of NaNO₃. Further inspection of the trendlines shows that higher concentrations perform better at all discharge times. Similar to NaNO₃ energy density, the higher concentration of 30% performs better than the 20% concentration for all discharge times.

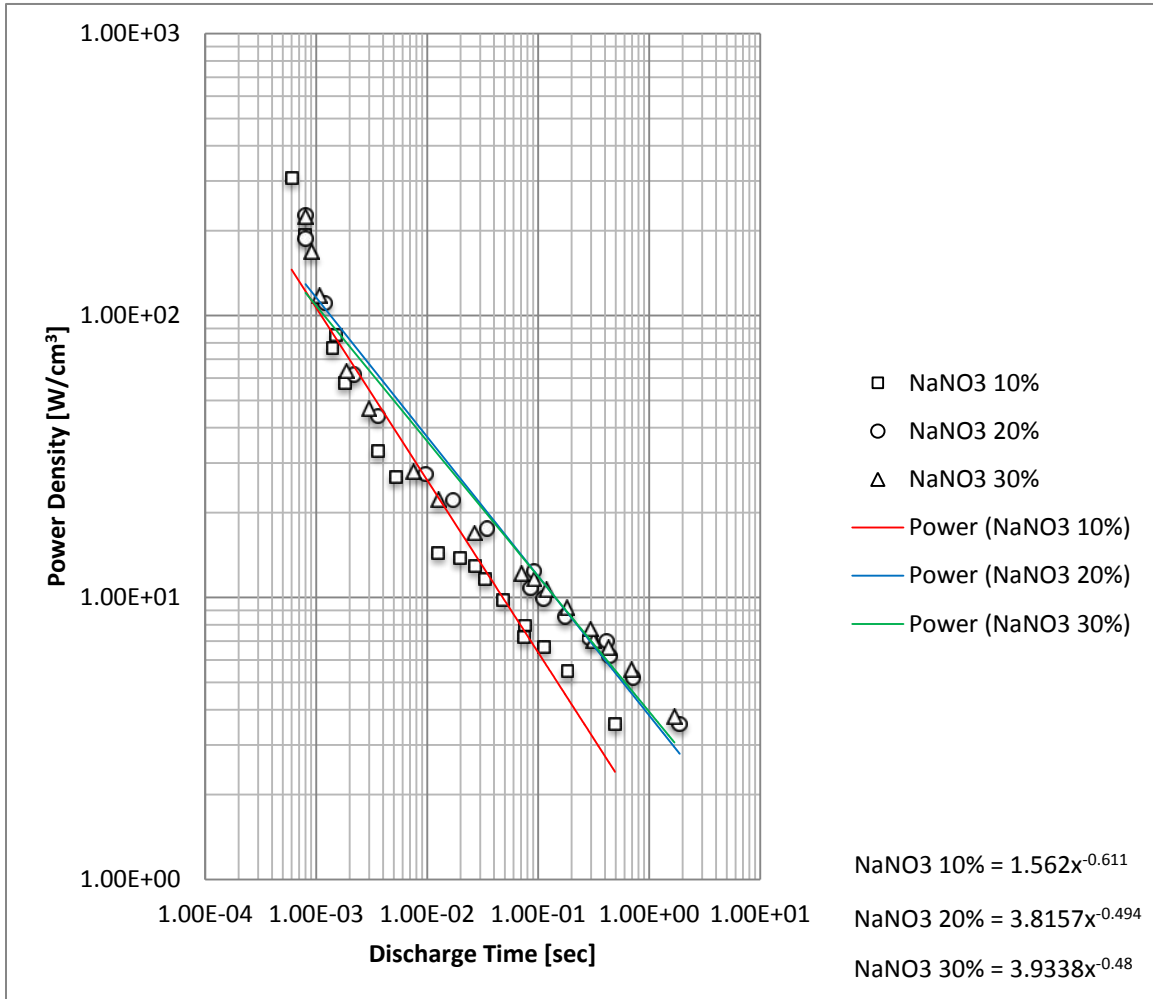


Figure 90. Power Density vs. Discharge Time (NaNO₃) (Charge=Discharge)

C. POTASSIUM HYDROXIDE RESULTS CHARGE EQUALS DISCHARGE

As seen in Figure 91, capacitance is significantly higher for the 30% concentration of KOH. For all discharge times, the 30% concentration out-performs the lower concentrations. Lower concentrations at all discharge times have similar performance. This supports the original hypothesis that more ions in solutions can improve the performance of the capacitor.

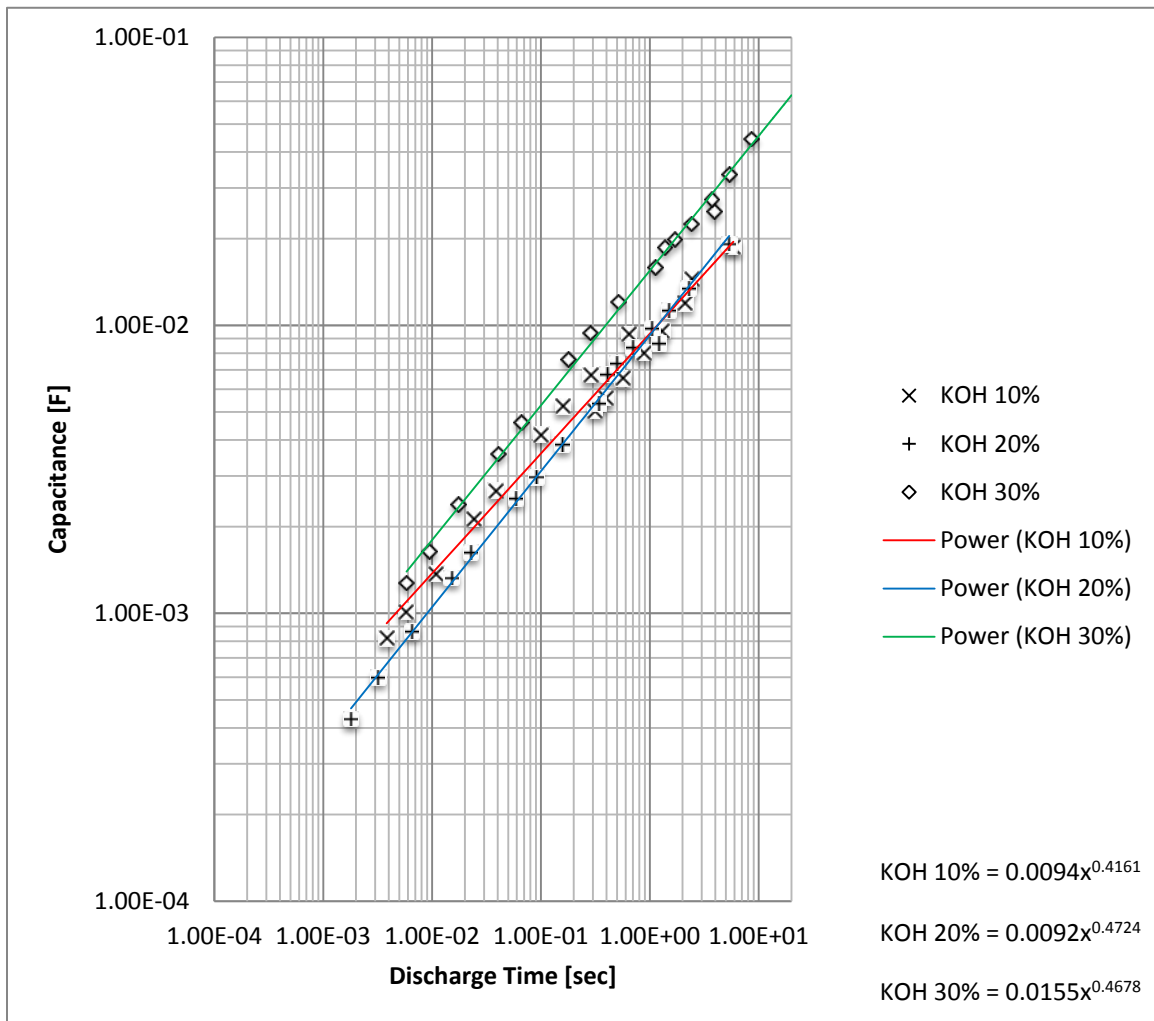


Figure 91. Capacitance vs. Discharge Time (KOH) (Charge=Discharge)

As seen in Figure 92, dielectric is significantly higher for the 30% concentration of KOH. For all discharge times, the 30% concentration out-performs the lower concentrations. Lower concentrations at all discharge times have similar performance. This supports the original hypothesis that more ions in solutions can improve the performance of the capacitor.

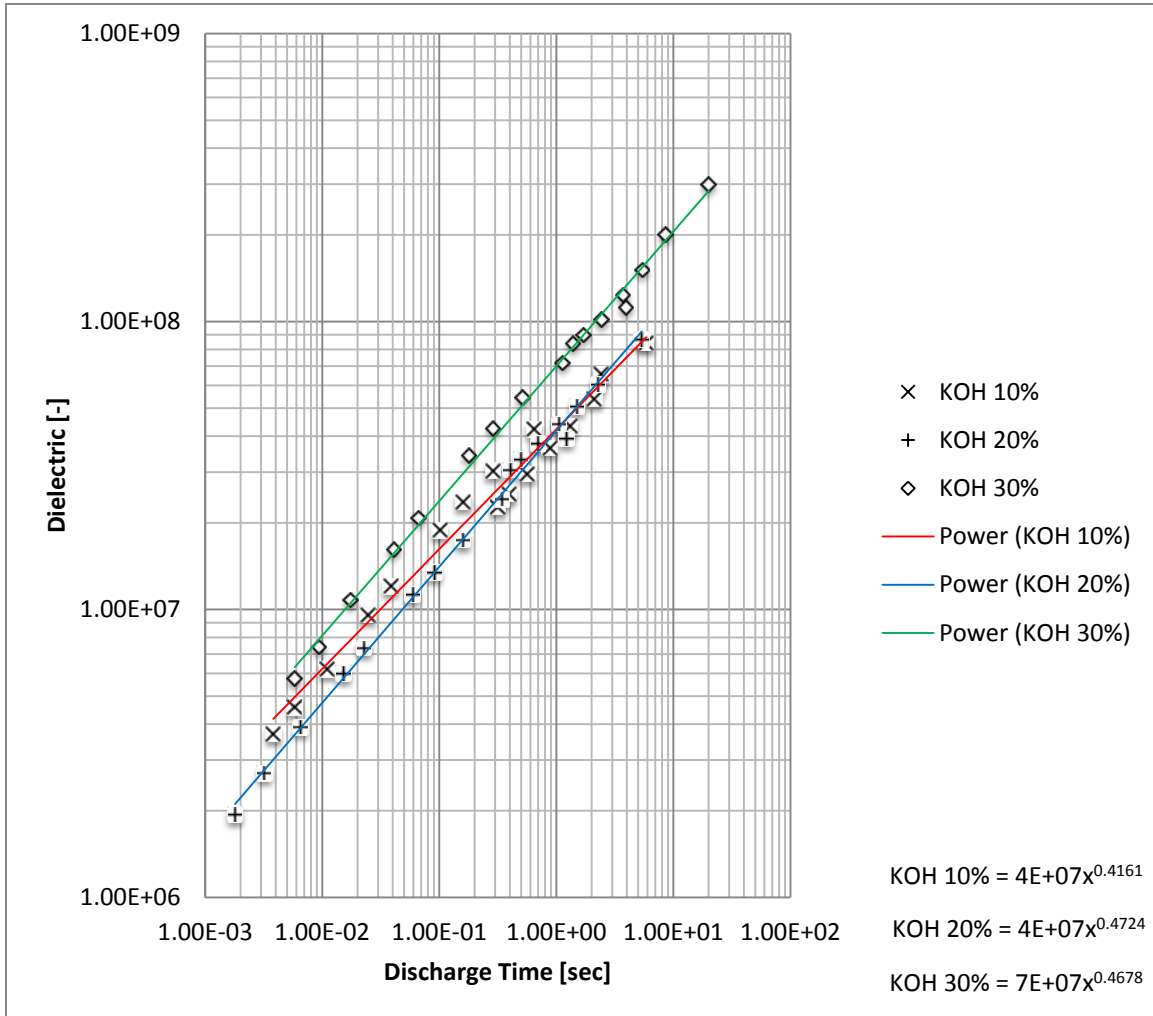


Figure 92. Dielectric vs. Discharge Time (KOH) (Charge=Discharge)

As seen in Figure 93, energy density is significantly higher for the 30% concentration of KOH. For all discharge times, the 30% concentration out-performs the lower concentrations. Lower concentrations at all discharge times have similar performance. This supports the original hypothesis that more ions in solutions can improve the performance of the capacitor.

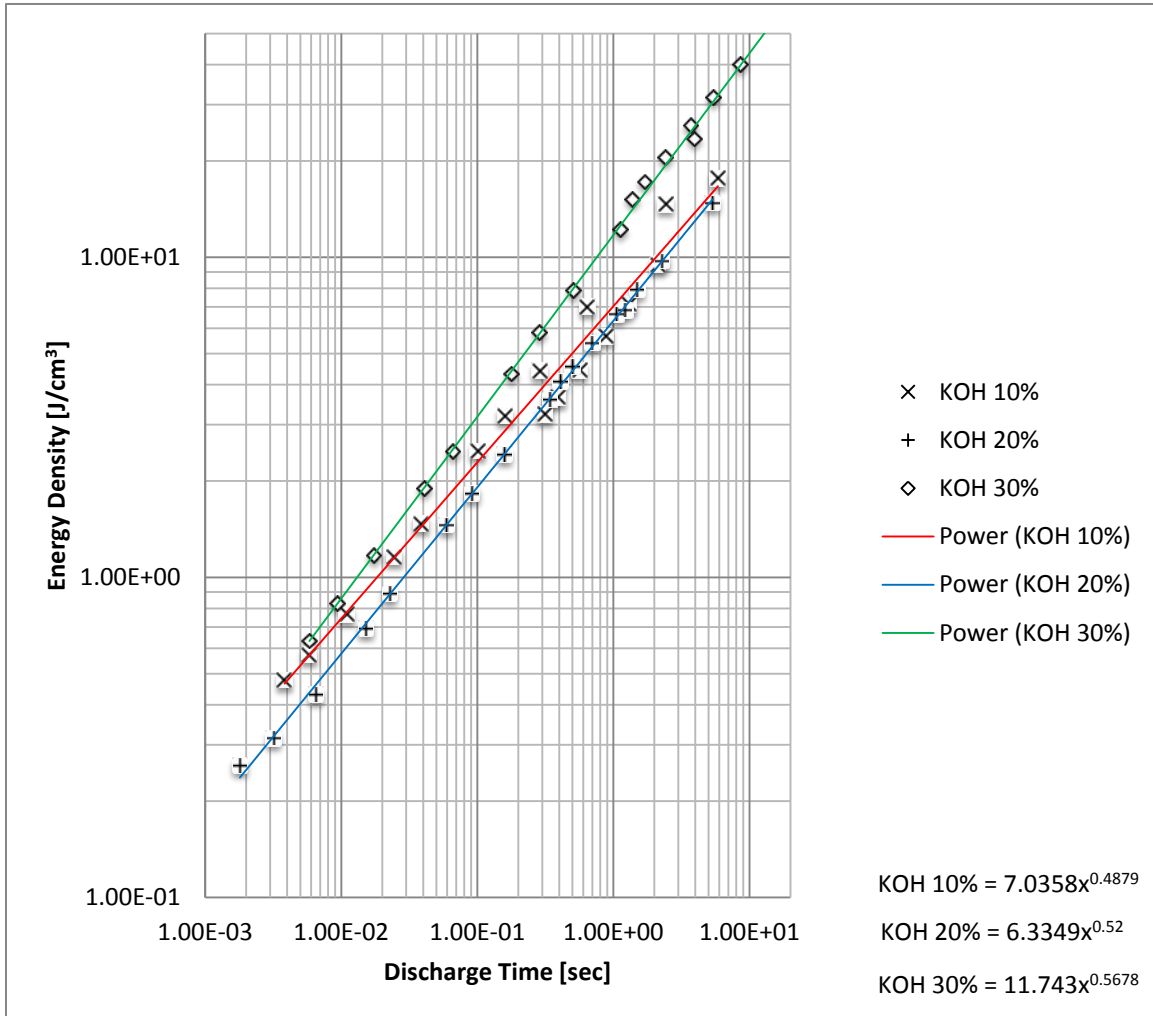


Figure 93. Energy Density vs. Discharge Time (KOH) (Charge=Discharge)

As seen in Figure 94, power density is significantly higher for the 30% concentration of KOH. For all discharge times, the 30% concentration out-performs the lower concentrations. Lower concentrations at all discharge times have similar performance. This supports the original hypothesis that more ions in solutions can improve the performance of the capacitor.

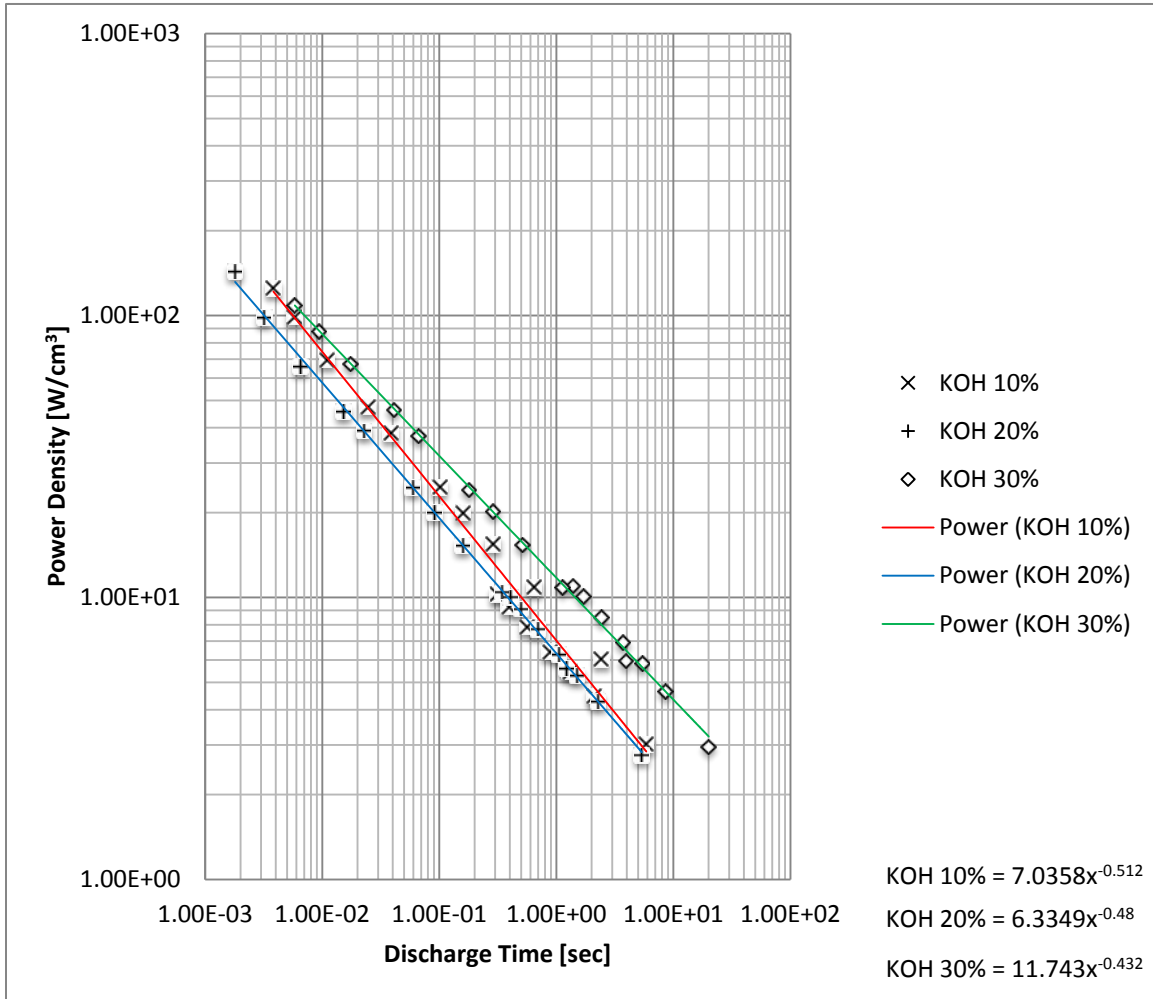


Figure 94. Power Density vs. Discharge Time (KOH) (Charge=Discharge)

D. COMBINED RESULTS CHARGE EQUALS DISCHARGE

As seen in Figure 95, capacitance values were significantly higher for NH_4Cl and KOH . NaNO_3 performed lower than the other salt solutions for all concentrations. Although difficult to differentiate on the graph, NH_4Cl demonstrated the highest overall capacitance values when discharge times are disregarded.

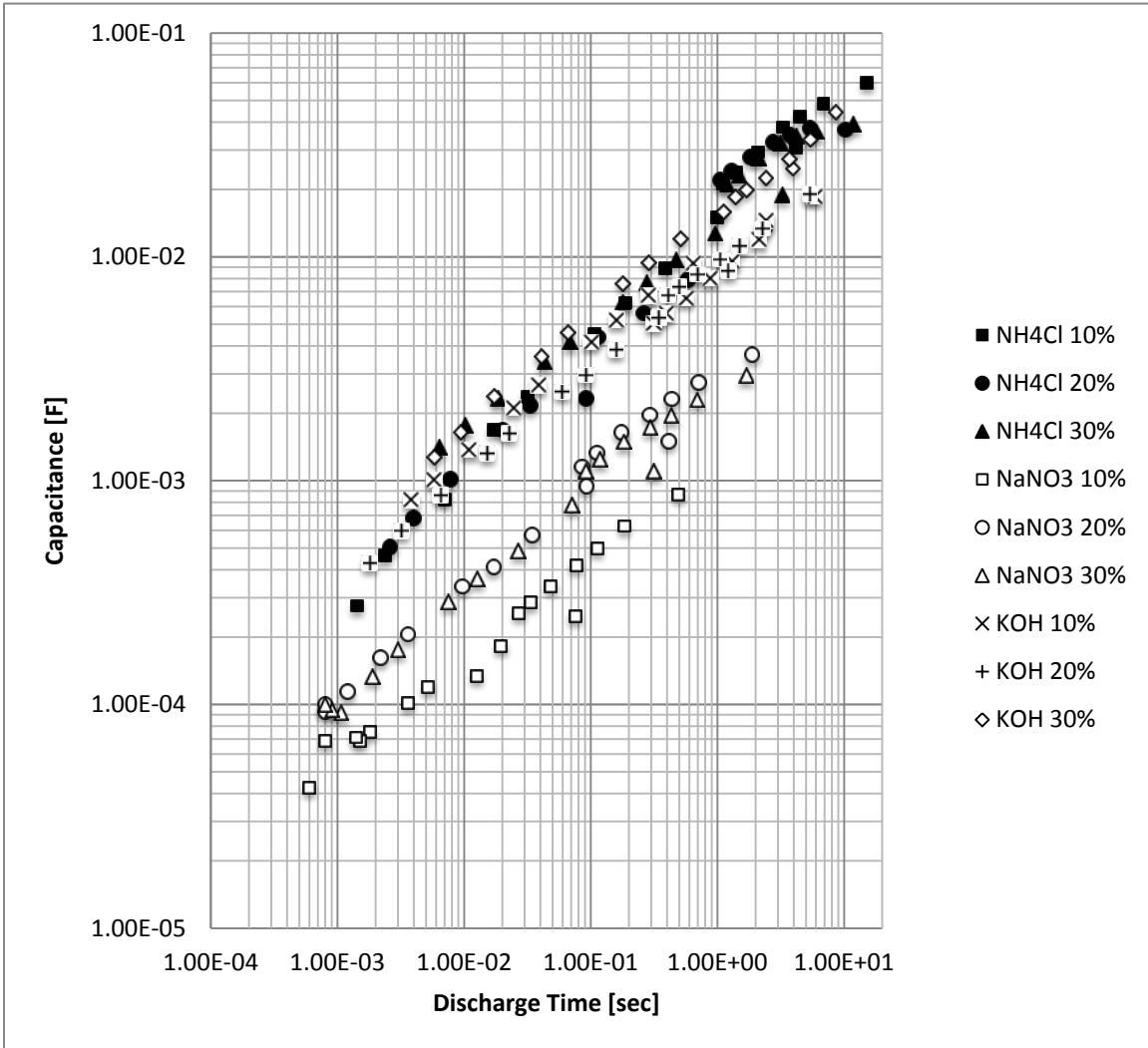


Figure 95. Capacitance vs. Discharge Time (All Salt Solutions)
(Charge=Discharge)

As seen in Figure 96, dielectrics were significantly higher for NH_4Cl and KOH . NaNO_3 performed lower than the other salt solutions for all concentrations. Although difficult to differentiate on the graph, KOH , at the highest salt concentration, demonstrated the highest overall dielectric values when discharge times are disregarded. NH_4Cl performed better than KOH at lower salt concentrations.

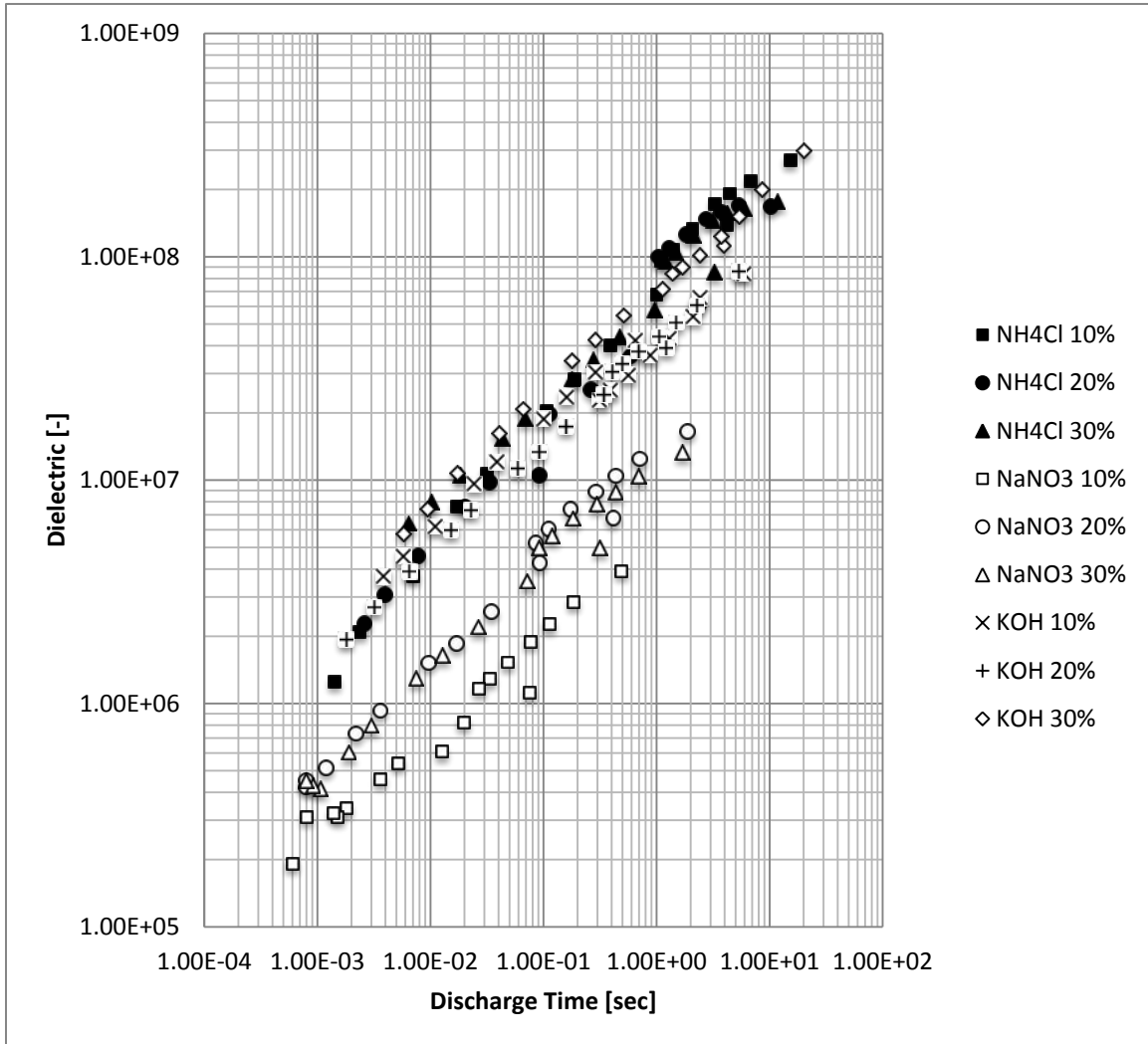


Figure 96. Dielectric vs. Discharge Time (All Salt Solutions)
(Charge=Discharge)

As seen in Figure 97, energy densities were significantly higher for NH_4Cl and KOH . NaNO_3 performed lower than the other salt solutions for all concentrations. Although difficult to differentiate on the graph, KOH demonstrated the highest overall energy density when discharge times are disregarded.

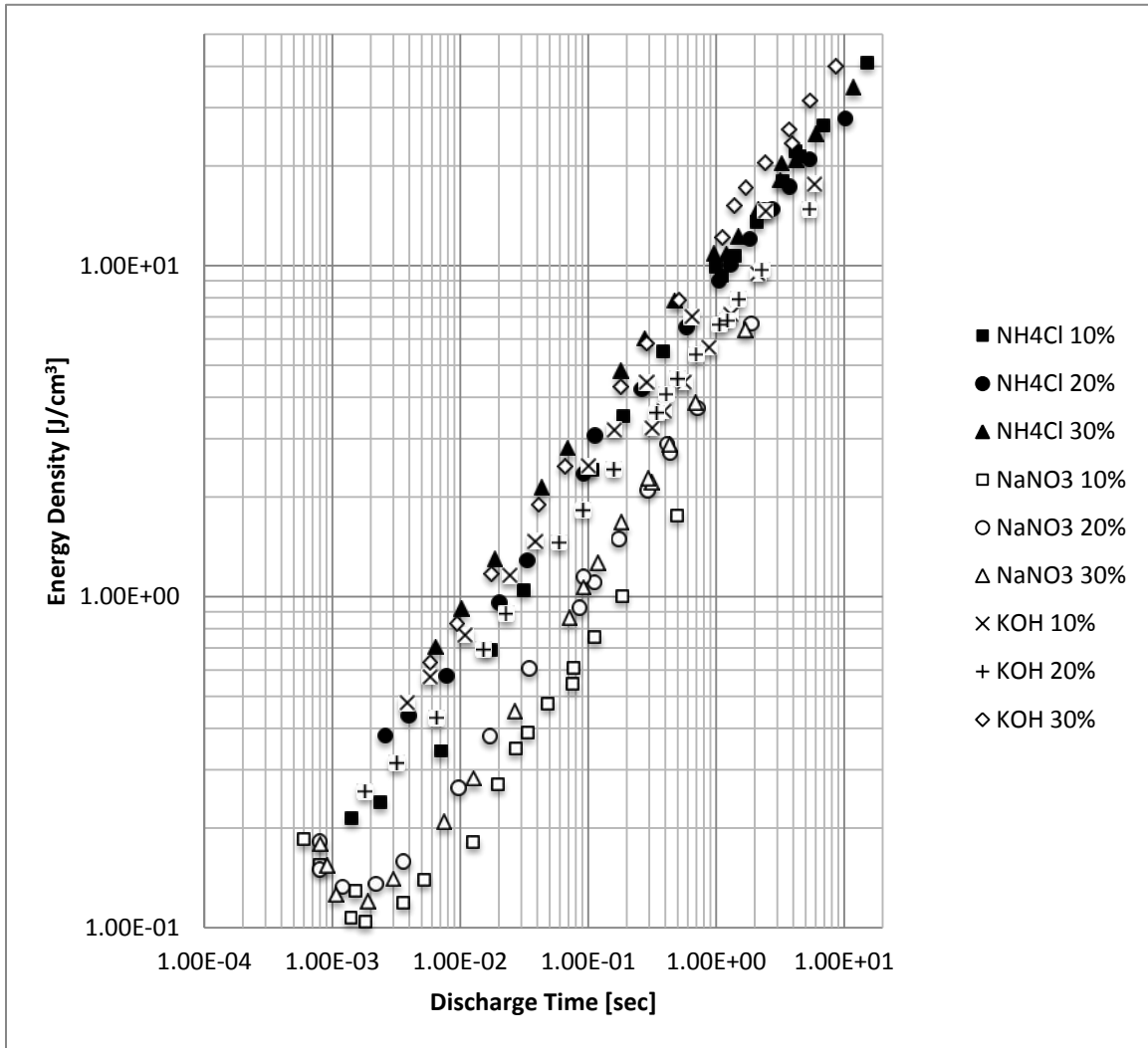


Figure 97. Energy Density vs. Discharge Time (All Salt Solutions)
(Charge=Discharge)

As seen in Figure 98, power density was significantly higher for NaNO₃. NH₄Cl and KOH performed lower than the other salt solution for all concentrations. Although difficult to differentiate on the graph, NaNO₃ demonstrated the highest overall power density values when discharge times are disregarded.

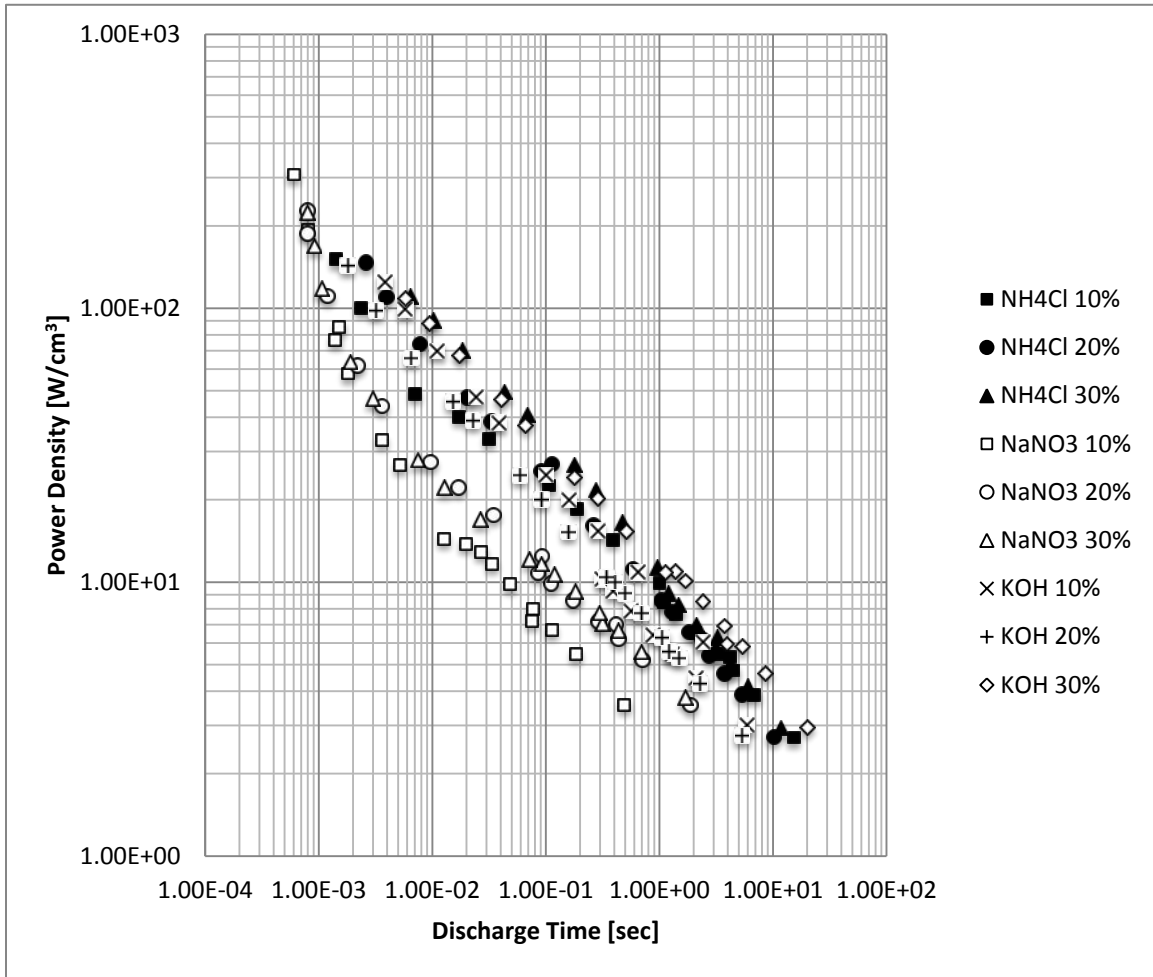


Figure 98. Power Density vs. Discharge Time (All Salt Solutions)
(Charge=Discharge)

E. AMMONIUM CHLORIDE RESULTS CHARGE FIXED

As seen in Figure 99, capacitance is consistent for all concentrations of NH_4Cl . The 10 and 20 wt% concentrations have a similar power log relationship. The 30 wt% sample demonstrates the expected power log relationship with minor roll-off at lower frequency rates. Additional tests should be conducted with the same parameters to increase the confidence interval of the power log relationship during asymmetric cycle tests in order accurately extrapolate data beyond the current data points. Lower discharge current tests were disregarded due to the error discussed in the Results section.

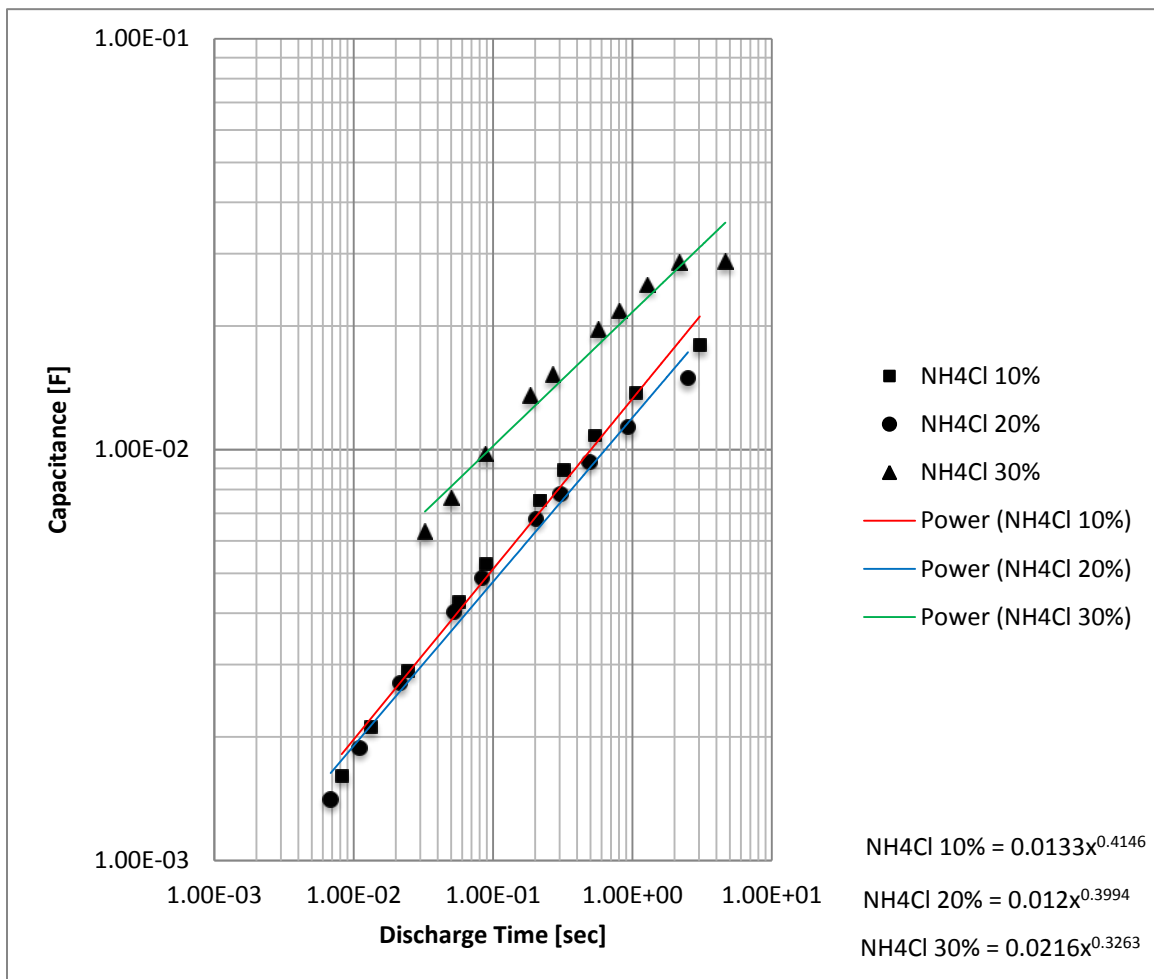


Figure 99. Capacitance vs. Discharge Time (NH_4Cl) (Charge \neq Discharge)

As seen in Figure 100, dielectrics are consistent for all concentrations of NH₄Cl. The 10 and 20 wt% concentrations have a similar power log relationship. The 30 wt% sample demonstrates the expected power log relationship with minor roll-off at lower frequency rates. A continuing phenomenon occurred with all salt identities when utilizing an asymmetric test cycle. Additional tests should be conducted with the same parameters to increase the confidence interval of the power log relationship when asymmetric test cycles are utilized. Lower discharge current tests were disregarded due to the error discussed in the Results section.

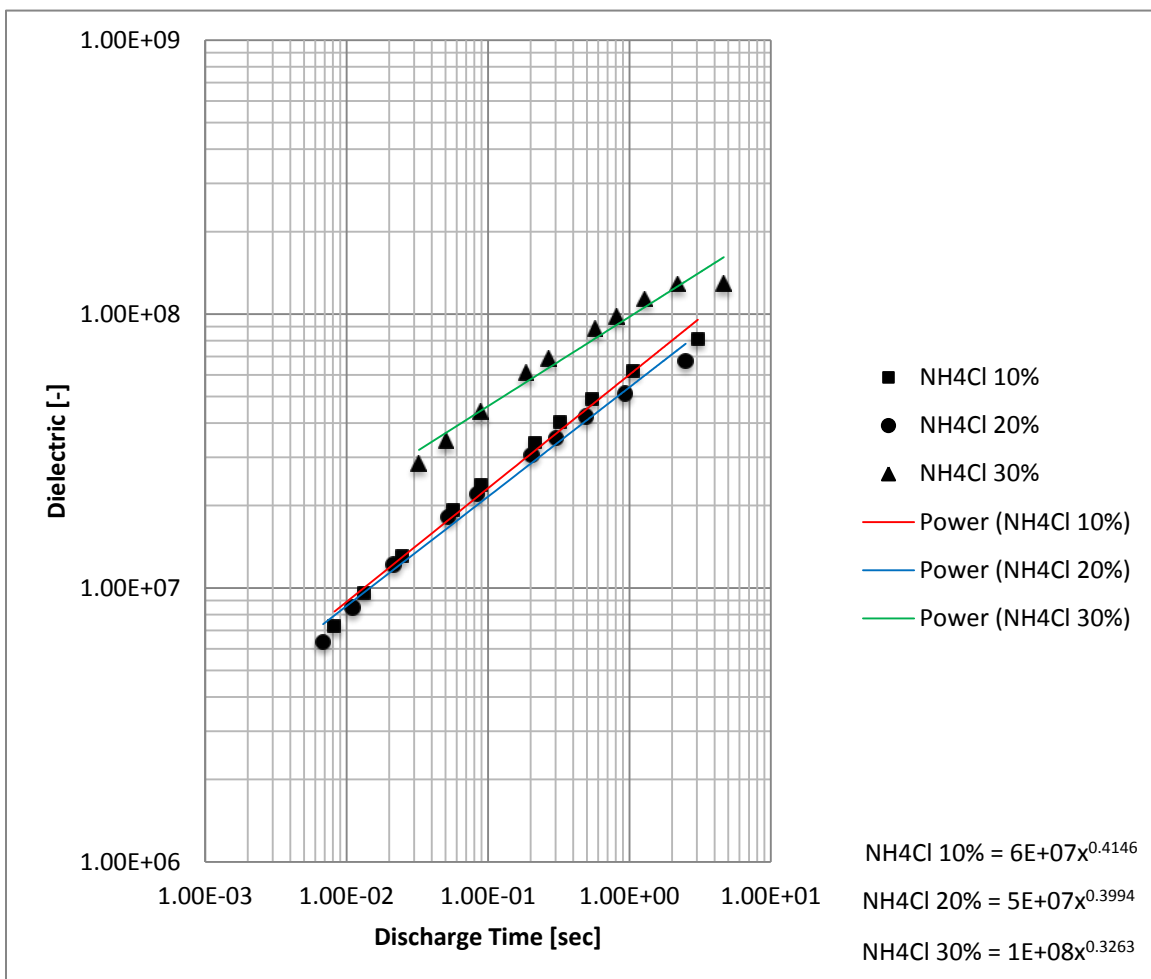


Figure 100. Dielectric vs. Discharge Time (NH₄Cl) (Charge≠Discharge)

As seen in Figure 101, energy densities are consistent for all concentrations of NH₄Cl. The 10 and 20 wt% concentrations have a similar power log relationship. The 30 wt% sample demonstrates demonstrates the expected power log relationship with minor roll-off at lower frequency rates. Additional tests should be conducted with the same parameters to increase the confidence interval of the power log relationship during asymmetric cycle tests. Lower discharge current tests were disregarded due to the error discussed in the Results section.

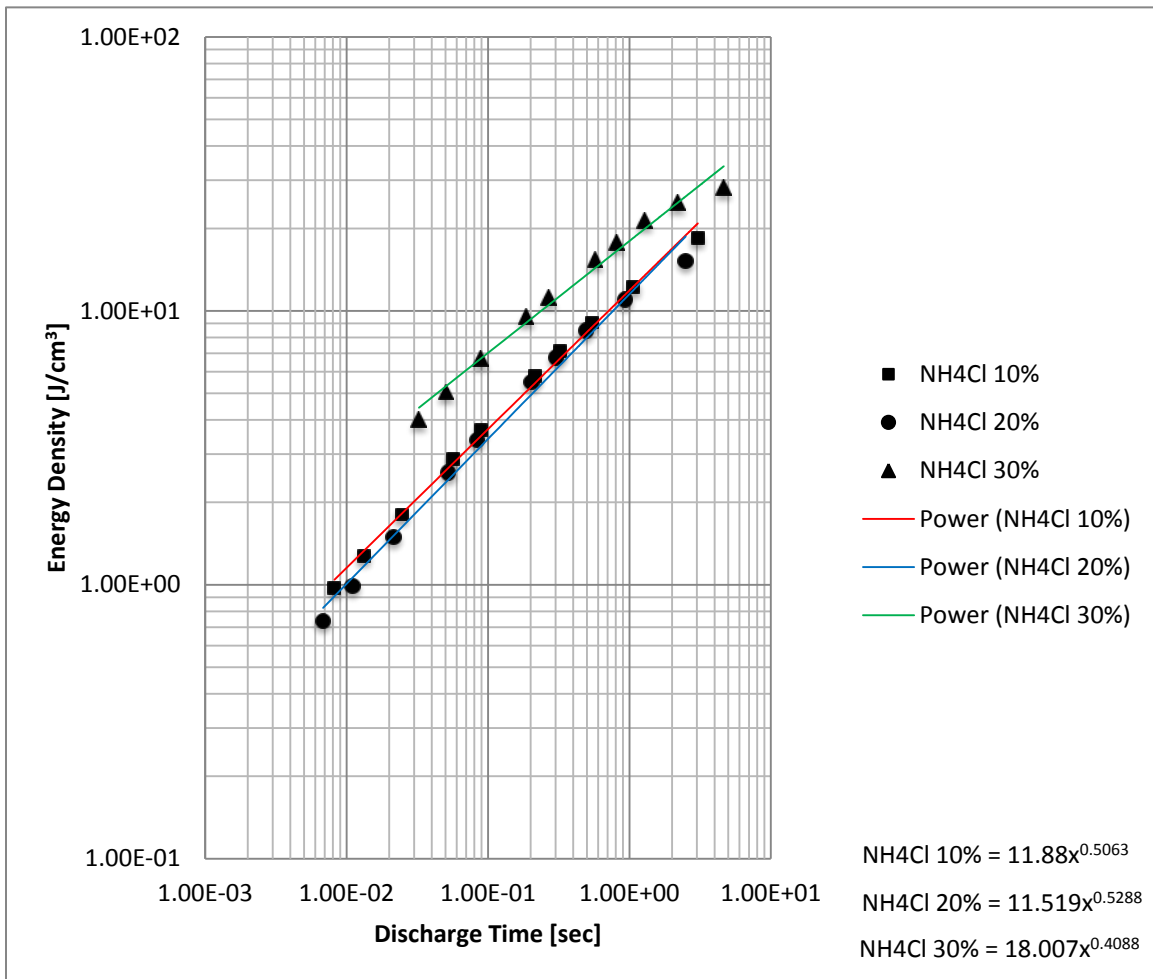


Figure 101. Energy Density vs. Discharge Time (NH₄Cl) (Charge≠Discharge)

As seen in Figure 102, power densities are consistent for all concentrations of NH_4Cl . The 10 and 20 wt% concentrations have a similar power log relationship. The 30 wt% sample demonstrates a significant departure from the power log relationship for lower frequency rates. Of interesting to note, as frequency increases and discharge times decrease the highest power densities correspond to the lowest energy densities. When comparing the rate of change of discharge to the rate of change of energy density, the rate of change of discharge is decreasing significantly faster than the rate of change of energy density and therefore a larger power density occurs at higher frequencies. Lower discharge current tests were disregarded due to the error discussed in the Results section.

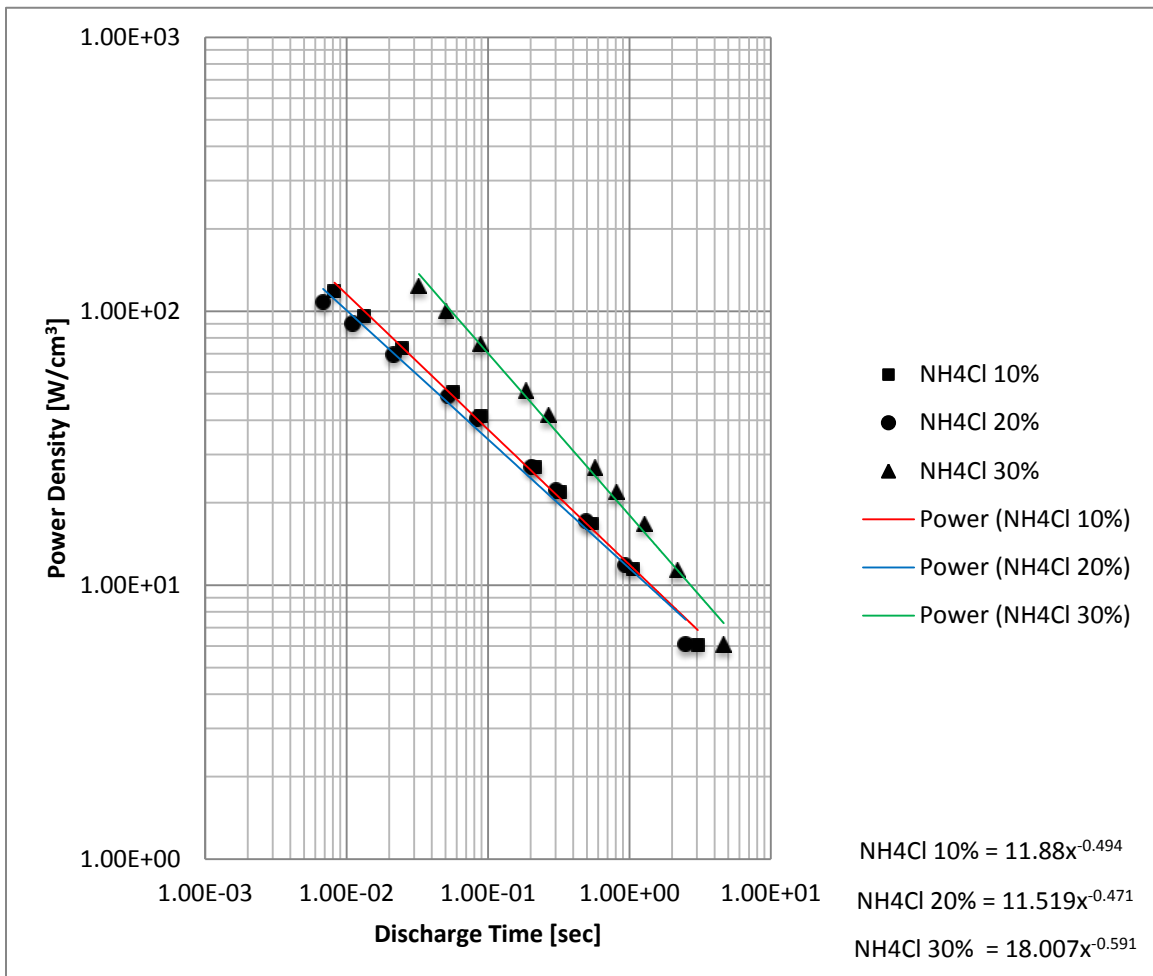


Figure 102. Power Density vs. Discharge Time (NH_4Cl) (Charge \neq Discharge)

F. SODIUM NITRATE RESULTS CHARGE FIXED

As seen in Figure 103, capacitance is inconsistent for the higher concentrations of NaNO_3 . The tested concentrations are poorly predicted by the power log relationship suggesting additional variables affect performance. Future studies are required to determine a power log correction factor. Despite a fixed constant charge rate, the discharge rates provided considerably higher frequencies than NH_4Cl and KOH . This higher frequencies resulted in considerable aliasing of data points and inaccuracies when measuring higher discharge rates above 20 mA. Low frequencies are required for NaNO_3 if an increase in confidence interval is required.

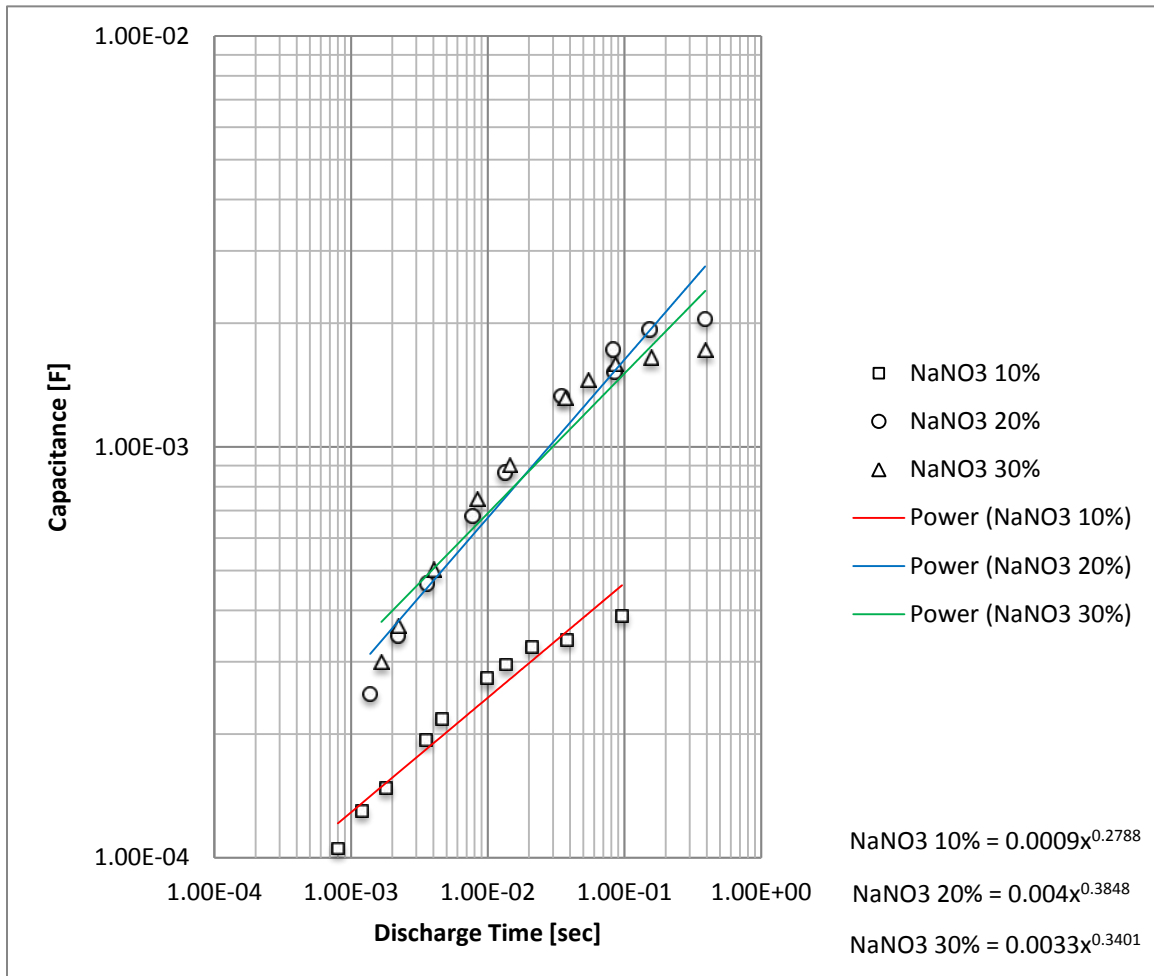


Figure 103. Capacitance vs. Discharge Time (NaNO_3) (Charge \neq Discharge)

As seen in Figure 104, dielectrics are inconsistent for the higher concentrations of NaNO₃. The tested concentrations are poorly predicted by the power log relationship suggesting additional variables affect performance. Future studies are required to determine a power log correction factor. In terms of SDM theory, as the salt concentration increases in solution, it becomes more difficult for ions to move in solution. This hypothesis supports why lower concentrations are more reactive to frequency phase direction as there is more volume for the individual ions to maneuver in solution. Lower discharge current tests were disregarded due to the error discussed in the Results section.

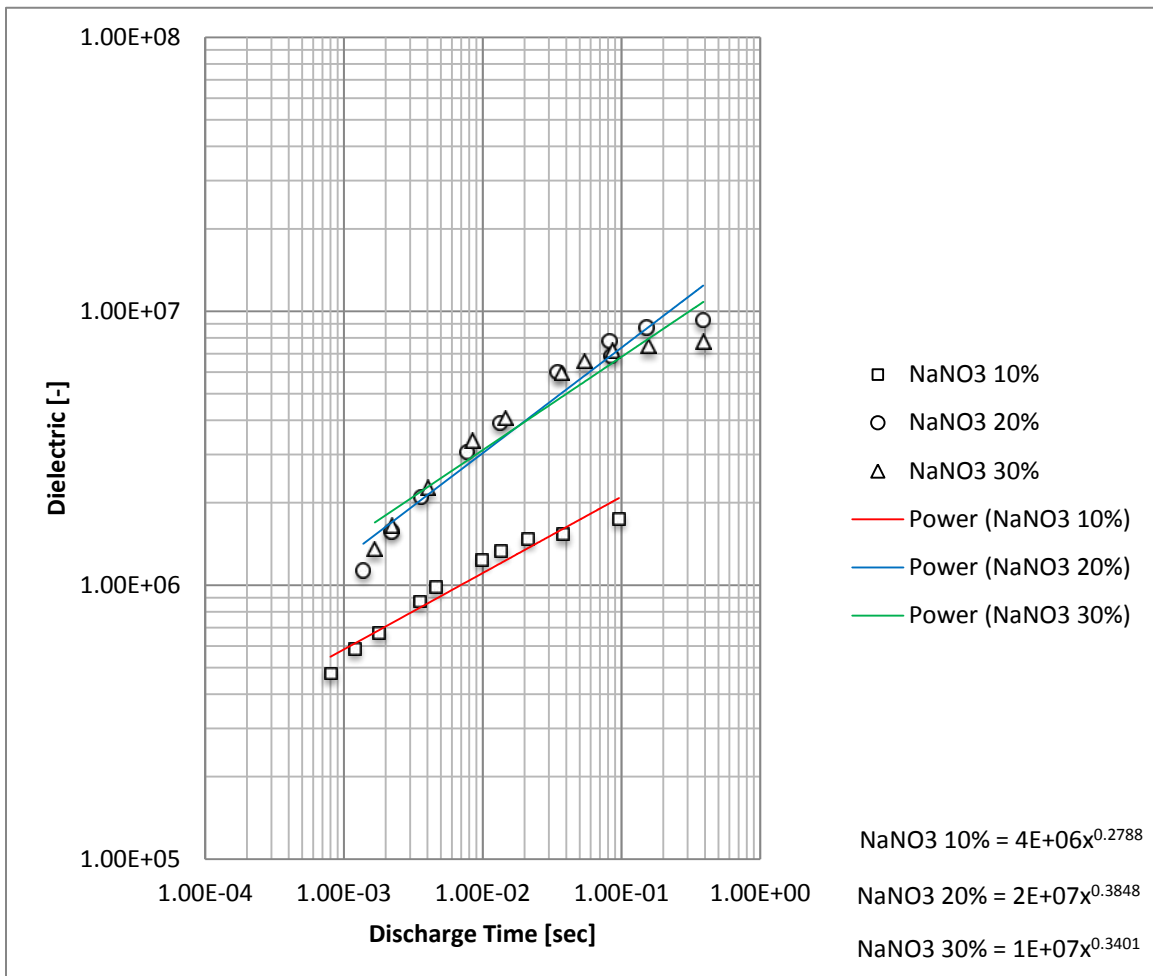


Figure 104. Dielectric vs. Discharge Time (NaNO₃) (Charge≠Discharge)

As seen in Figure 105, energy densities are relatively consistent for all concentrations of NaNO₃. All concentrations demonstrate a power log relationship for lower frequencies. Lower concentrations have higher than expected energy density. Lower discharge current tests were disregarded due to the error discussed in the Results section.

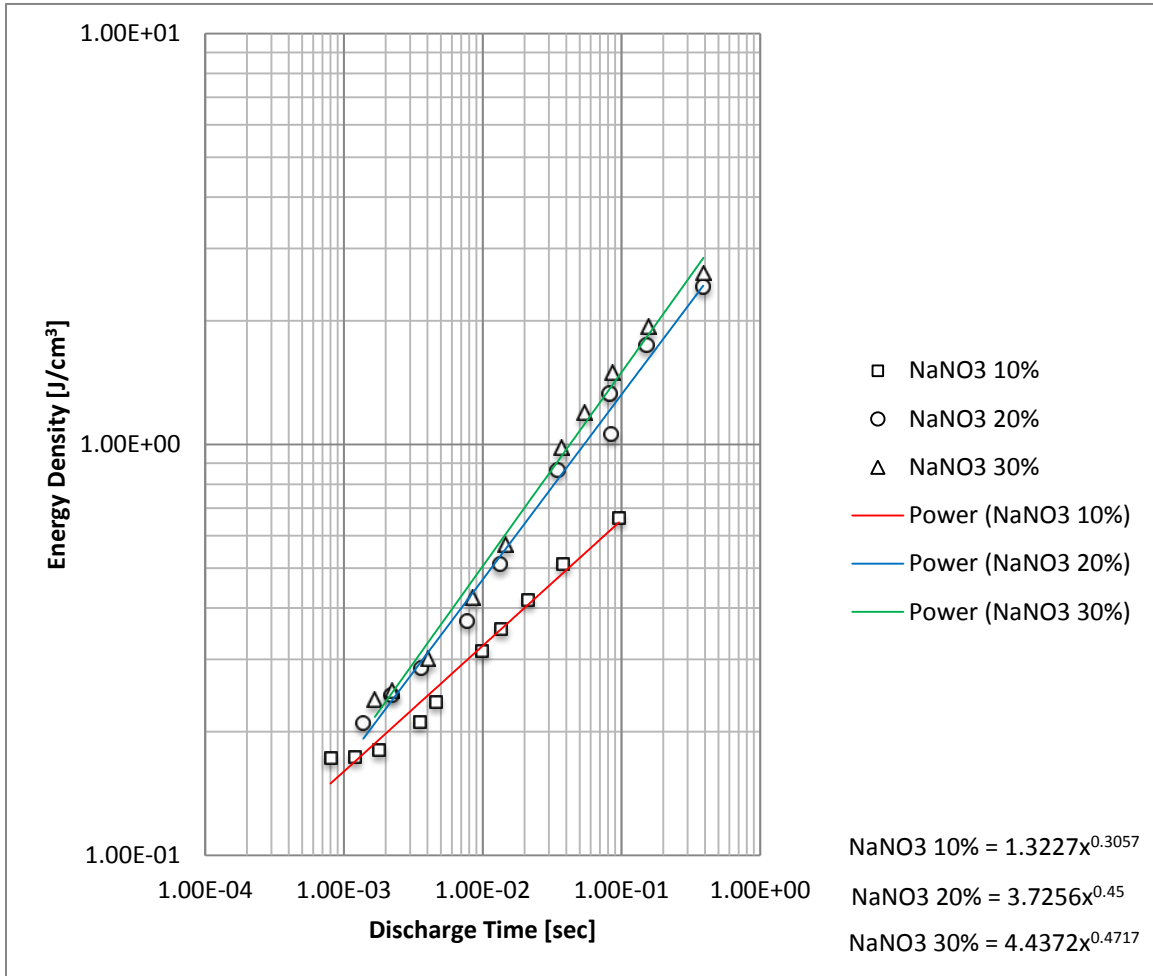


Figure 105. Energy Density vs. Discharge Time (NaNO₃) (Charge≠Discharge)

As seen in Figure 106, power densities are relatively consistent for all concentrations of NaNO₃. All concentrations demonstrate the expected power log relationship. Further analysis of the salt identity would require collecting more data through similar test frequencies. Lower discharge current tests were disregarded due to the error discussed in the Results section.

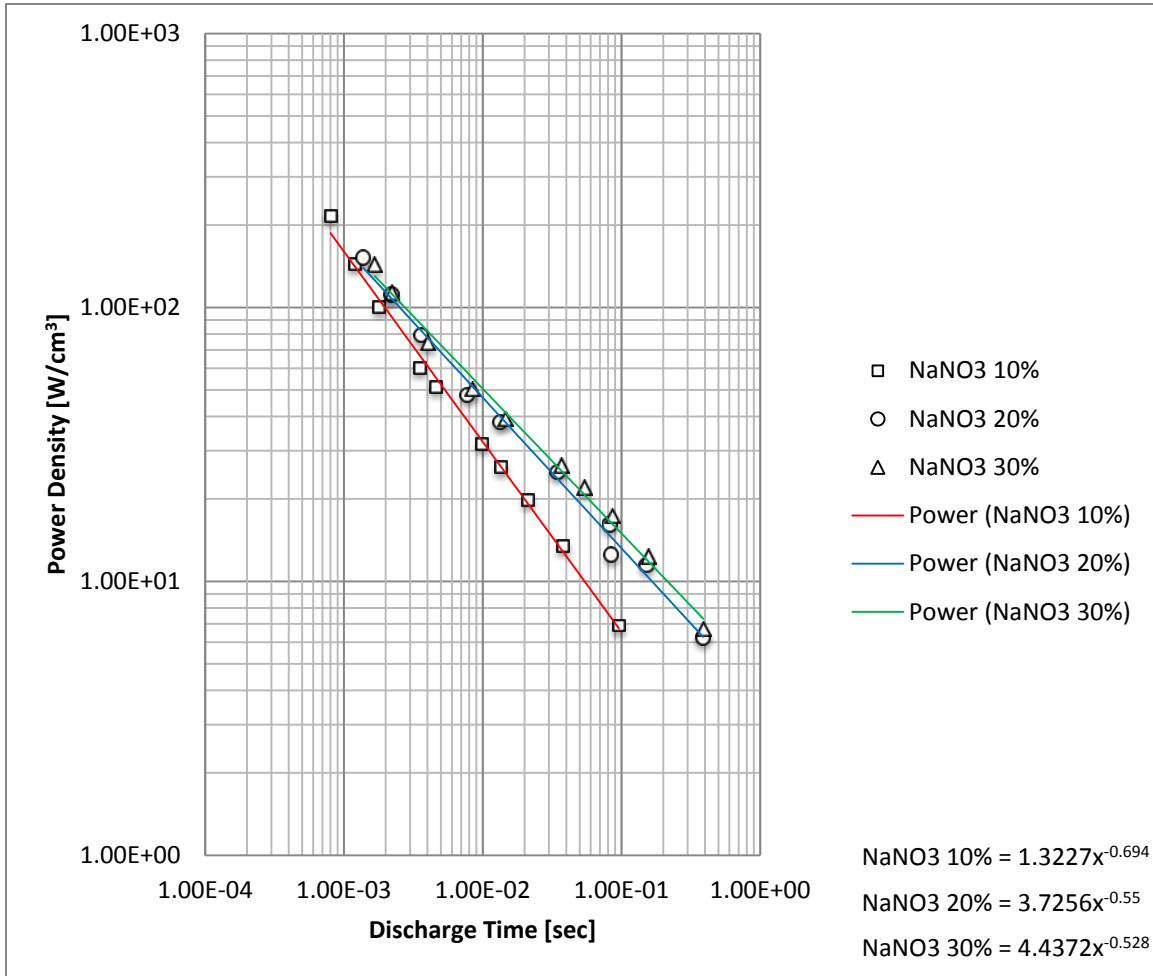


Figure 106. Power Density vs. Discharge Time (NaNO₃) (Charge≠Discharge)

G. POTASSIUM HYDROXIDE RESULTS CHARGE FIXED

As seen in Figure 107, capacitances are consistent for lower concentrations of KOH. Lower concentrations demonstrate the expected power log relationship with roll-off occurring at low frequencies or long discharge times. Higher concentrations poorly follow the expected power log relationship suggesting additional variables affect performance. Additional tests should be conducted with the same parameters to increase the confidence interval of the power log relationship during asymmetric cycle tests. Lower discharge current tests were disregarded due to the error discussed in the Results section.

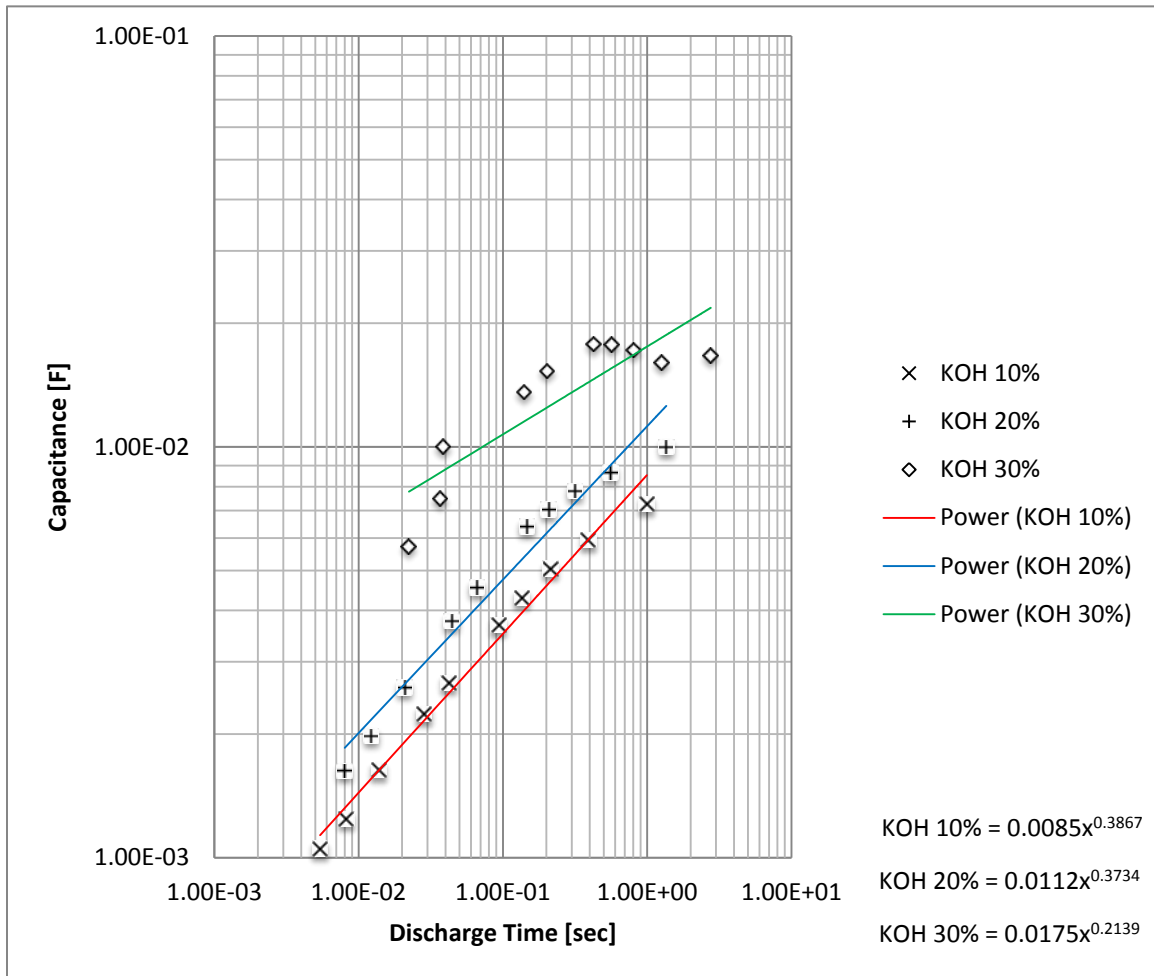


Figure 107. Capacitance vs. Discharge Time (KOH) (Charge≠Discharge)

As seen in Figure 108, dielectrics are consistent for lower concentrations of KOH. Lower concentrations demonstrate the expected power log relationship with roll-off occurring at low frequencies or long discharge times. Higher concentrations poorly follow the expected power log relationship suggesting additional variables affect performance. Additional tests should be conducted with the same parameters to increase the confidence interval of the power log relationship during asymmetric cycle tests. Lower discharge current tests were disregarded due to the error discussed in the Results section.

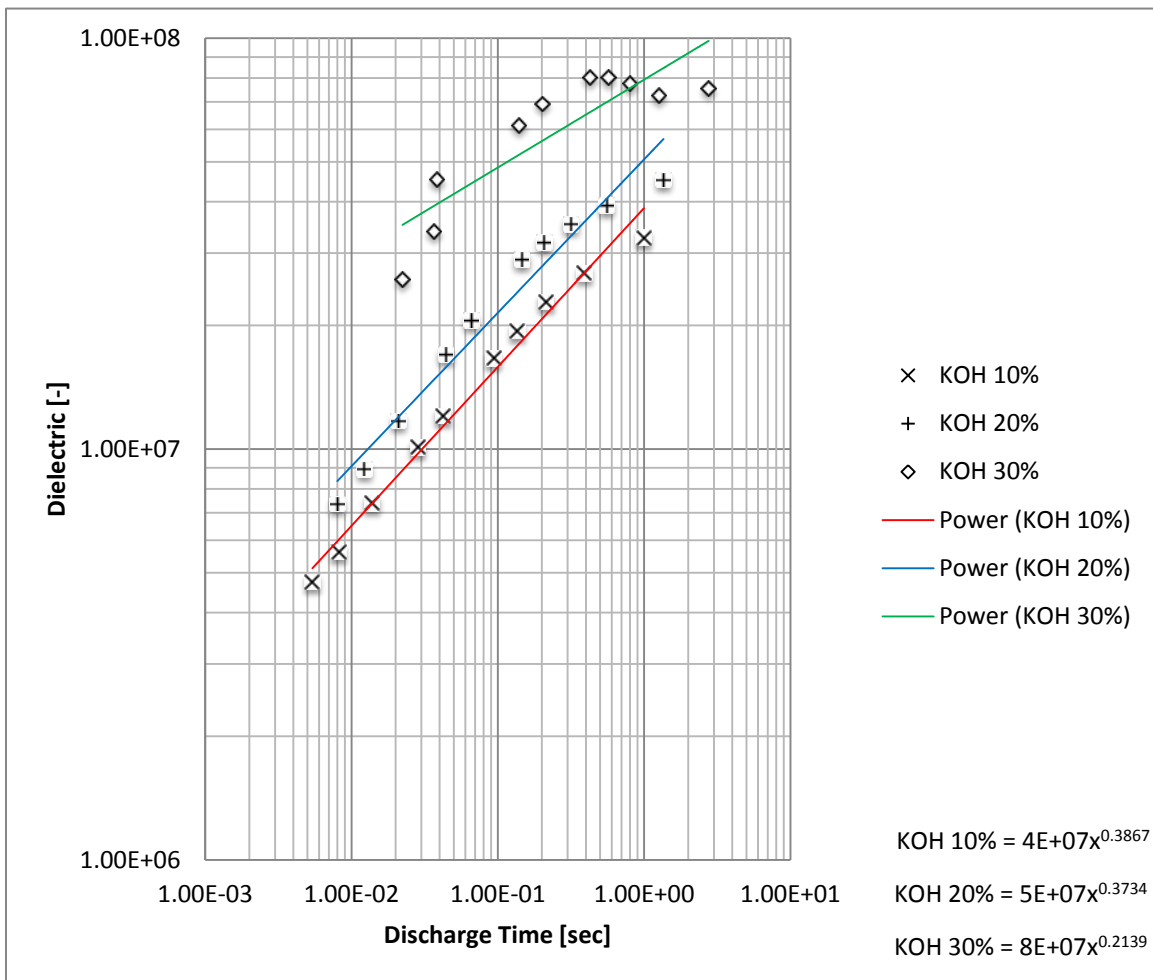


Figure 108. Dielectric vs. Discharge Time (KOH) (Charge≠Discharge)

As seen in Figure 109, energy densities are consistent for all concentrations of KOH. All concentrations demonstrated the expected power log relationship with roll-off occurring at low frequencies or long discharge times. Again, titanium oxide delamination and DI water evaporation are suspected to cause the error. Additional tests should be conducted with the same parameters to increase the confidence interval of the power log relationship during asymmetric cycle tests. Lower discharge current tests were disregarded due to the error discussed in the Results section.

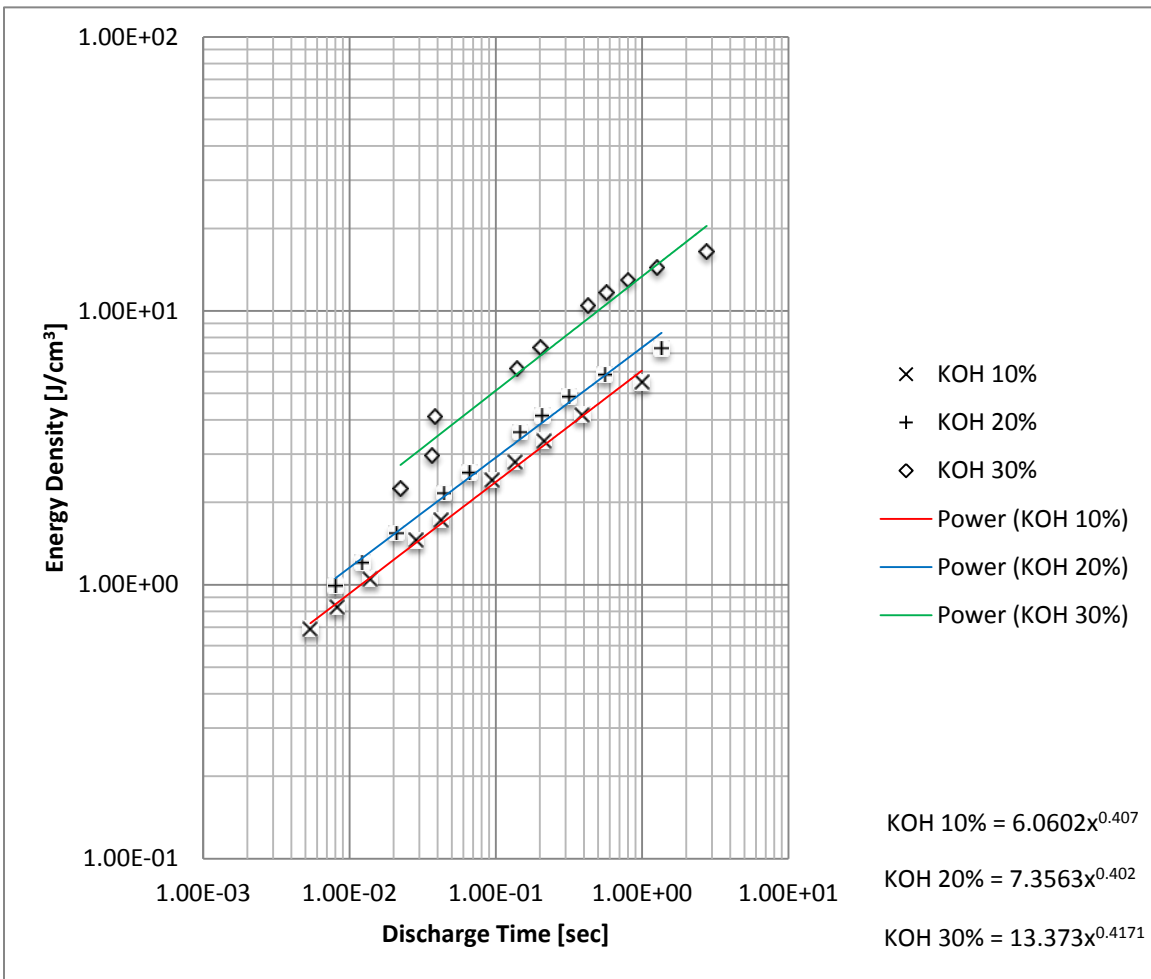


Figure 109. Energy Density vs. Discharge Time (KOH) (Charge \neq Discharge)

As seen in Figure 110, power densities are consistent for all concentrations of KOH. All concentrations demonstrated the expected power log relationship with roll-off occurring at low frequencies or long discharge times. Again, titanium oxide delamination and DI water evaporation are suspected to cause the error. Additional tests should be conducted with the same parameters to increase the confidence interval of the power log relationship during asymmetric cycle tests. Lower discharge current tests were disregarded due to the error discussed in the Results section.

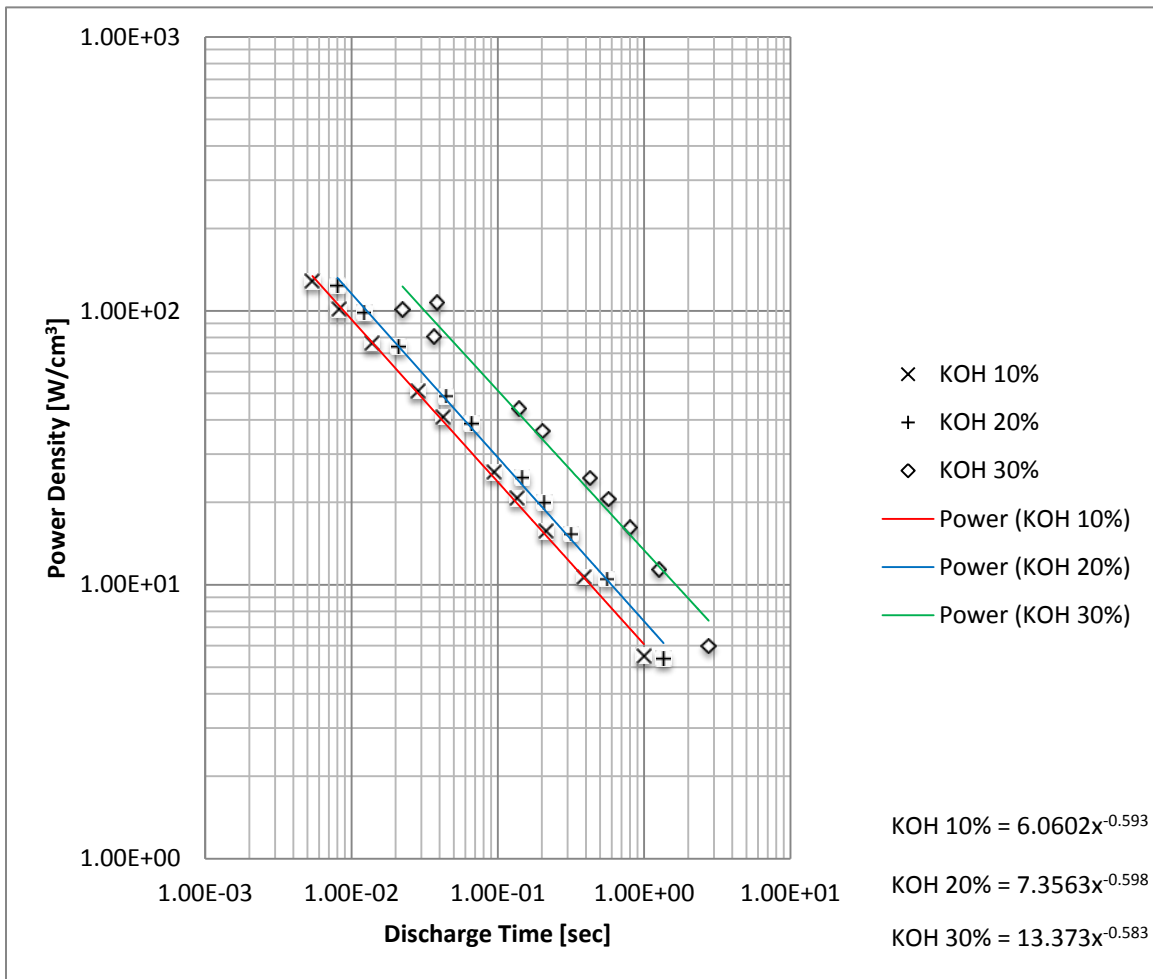


Figure 110. Power Density vs. Discharge Time (KOH) (Charge≠Discharge)

H. COMBINED RESULTS CHARGE FIXED

As seen in Figure 111, capacitance values were significantly higher for NH_4Cl and KOH . NaNO_3 performed lower than the other salt solutions for all concentrations during asymmetric cycle tests. Although difficult to differentiate on the graph, NH_4Cl demonstrated the highest overall capacitance values when discharge times are disregarded.

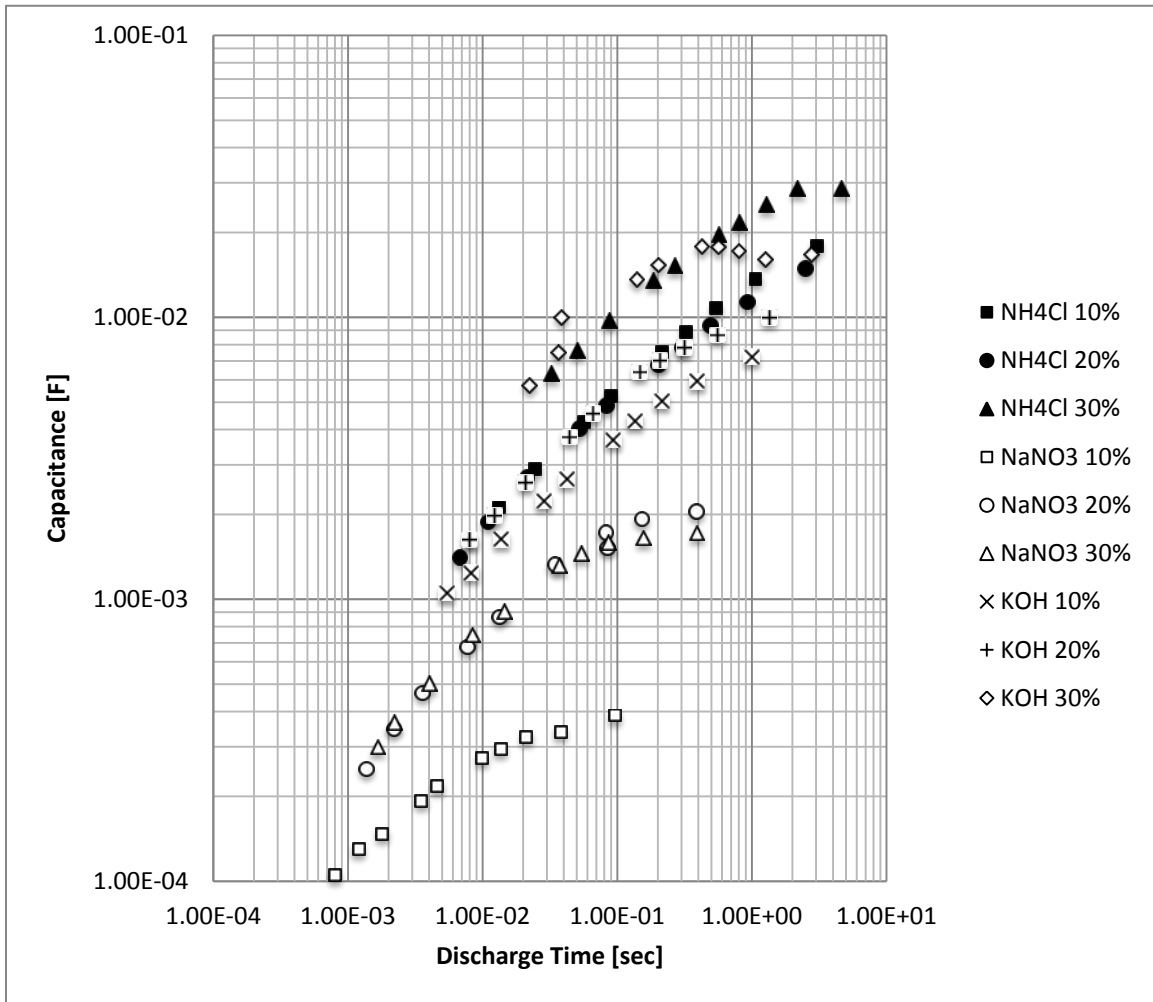


Figure 111. Capacitance vs. Discharge Time (All Salt Solutions)
(Charge≠Discharge)

As seen in Figure 112, dielectrics were significantly higher for NH₄Cl and KOH. NaNO₃ performed lower than the other salt solutions for all concentrations. Although difficult to differentiate on the graph, NH₄Cl, at the lowest salt concentration, demonstrated the highest overall dielectric values when discharge times are disregarded. KOH performed better than NH₄Cl at higher equivalent salt concentrations.

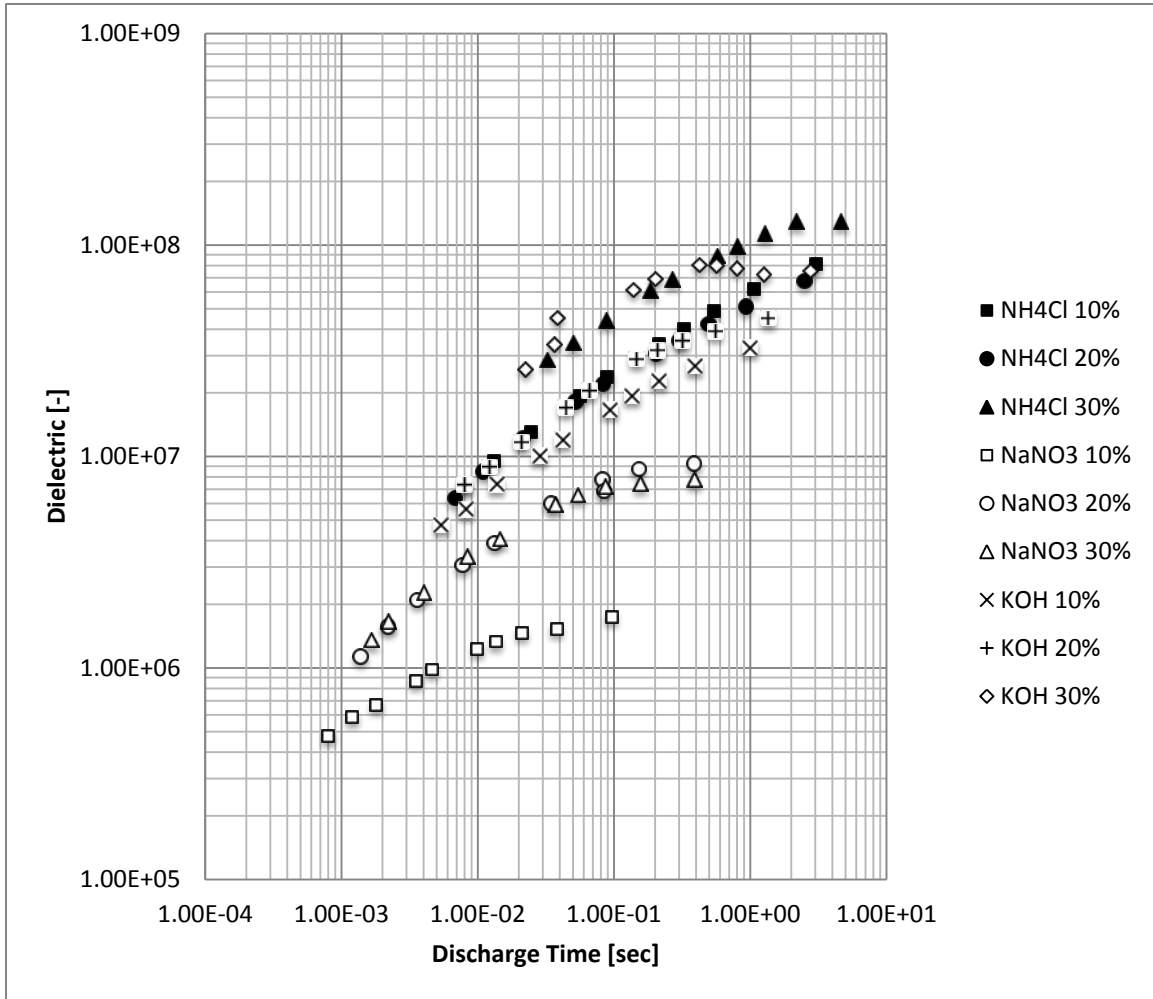


Figure 112. Dielectric vs. Discharge Time (All Salt Solutions)
(Charge≠Discharge)

As seen in Figure 113, energy densities were significantly higher for NH_4Cl and KOH . NaNO_3 performed lower than the other salt solutions for all concentrations. Although difficult to differentiate on the graph, NH_4Cl demonstrated the highest overall energy density when discharge times are disregarded.

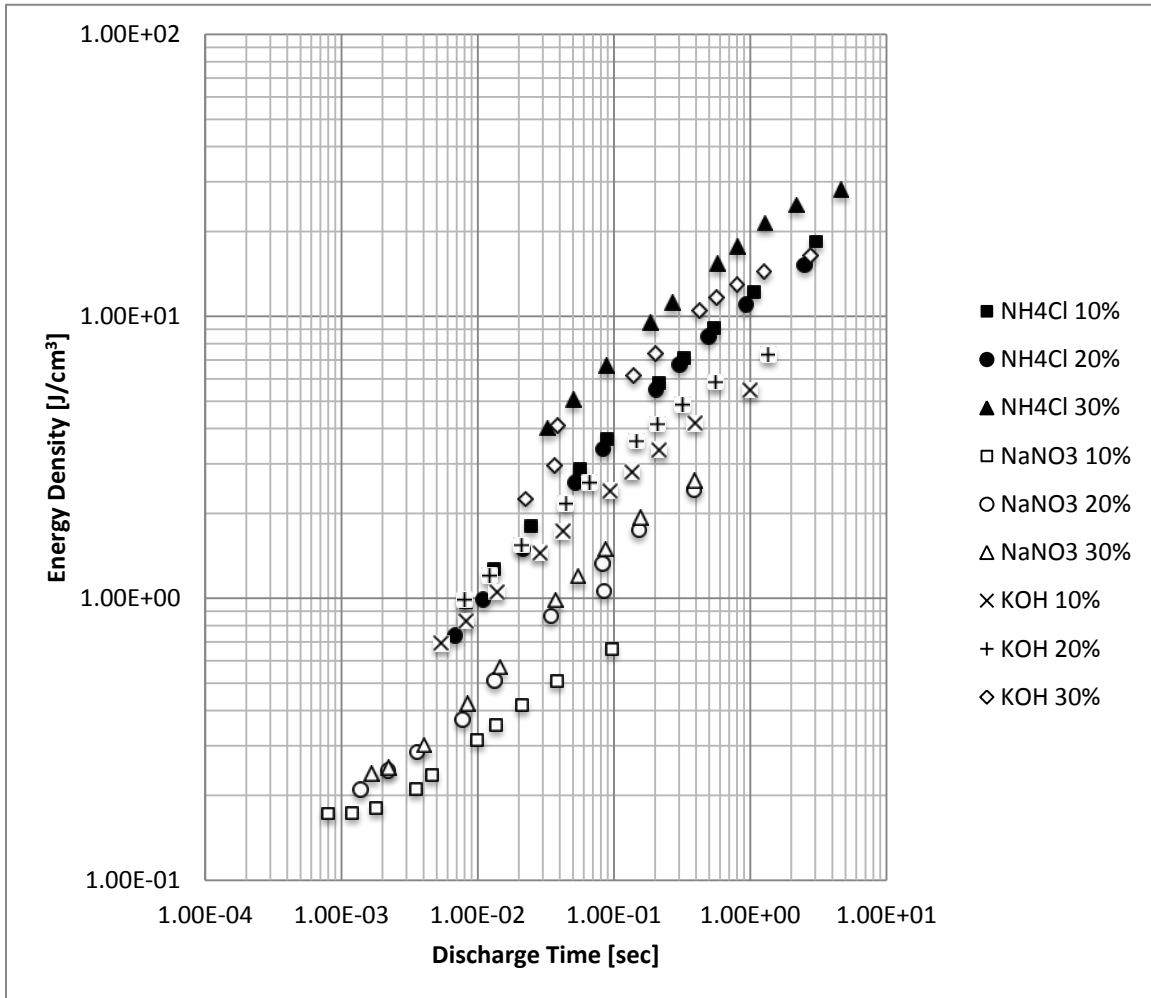


Figure 113. Energy Density vs. Discharge Time (All Salt Solutions)
(Charge \neq Discharge)

As seen in Figure 114, power density was significantly higher for NaNO₃. NH₄Cl and KOH performed lower than the other salt solution for all concentrations. Although difficult to differentiate on the graph, NaNO₃ demonstrated the highest overall power density values when discharge times are disregarded.

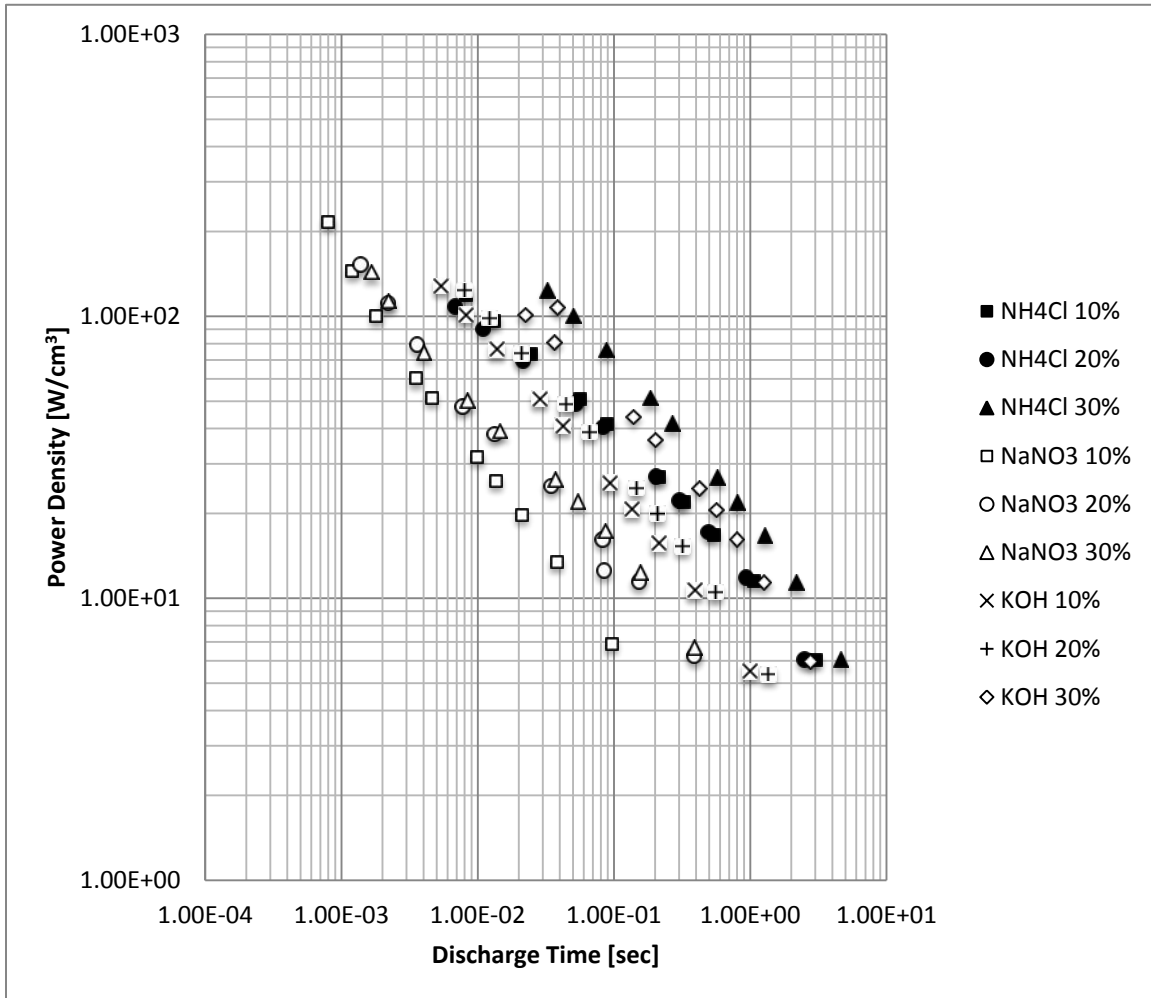


Figure 114. Power vs. Discharge Time (All Salt Solutions) (Charge≠Discharge)

THIS PAGE INTENTIONALLY LEFT BLANK

V. CONCLUSION AND FUTURE WORK

For salt identity conclusions, NH_4Cl was the least affected by salt concentration. As shown in Table 4, dielectric constants extrapolated at a 10 second discharge are approximately the same value for all NH_4Cl concentrations. For dielectric constants extrapolated at a 100 second discharge, NH_4Cl is two orders of magnitude higher than the DI water control sample and one order of magnitude higher than the NaNO_3 samples. Only when KOH concentration is increased to 30 wt% concentration are the dielectric values comparable to NH_4Cl .

As shown in Table 5, for asymmetric test cycles, dielectric constants extrapolated at a 10 second discharge are approximately the same value for the 10 and 20 wt% NH_4Cl concentrations. For dielectric constants extrapolated at a 100 second discharge, low concentrations of NH_4Cl and high concentrations of KOH are approximately equal. These two salt identities are approximately two orders of magnitude higher than the DI water control sample and one order of magnitude higher than the NaNO_3 samples. Figure 115 provides a comparison of currently available power storage systems to NTSDM nanotubes during this research.

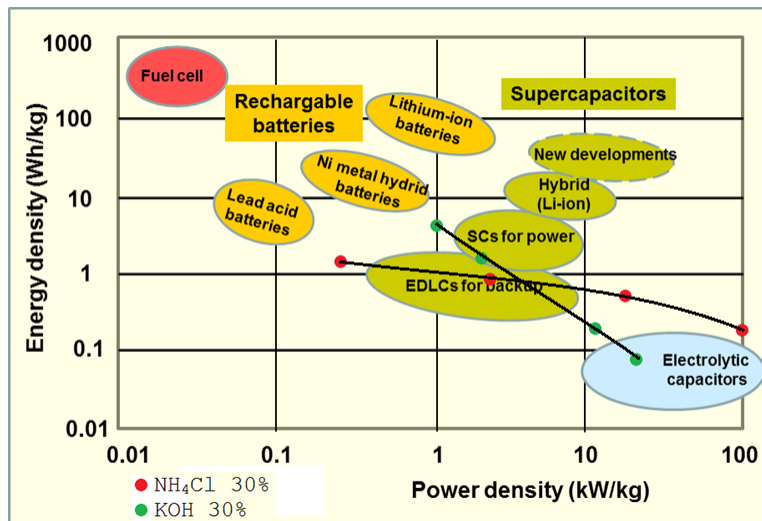


Figure 115. Ragone Plot of Supercapacitors vs. Batteries with NH_4Cl 30 wt% and KOH 30 wt%. Adapted from [18].

In terms of energy density, NH_4Cl and KOH outperformed the NaNO_3 for all concentrations. NH_4Cl outperformed KOH for the 10 and 20 wt% concentrations. Only when KOH concentration is increased to 30 wt% does it outperform NH_4Cl . Additional studies are recommended with KOH to determine whether higher concentrations will continue to improve energy density values.

In terms of power density, NH_4Cl and KOH outperformed the NaNO_3 for all concentrations. NH_4Cl outperformed KOH for the 10 and 20 wt% concentrations. Only when KOH concentration is increased to 30 wt% does it outperform NH_4Cl . Additional studies are recommended with KOH to determine whether higher concentrations will continue to improve power density values. It is important to note that utilizing lower frequencies, especially for NaNO_3 , will increase the accuracy for all measured values and will increase the confidence interval of calculated values.

Additional observations show that a power log relationship accurately describes roll-off phenomena for all salts identities when constant charging rates equal constant discharge rates. The theory loses shape when the constant charging rate is fixed at 10 mA. Fixed rate tests were typically conducted following the equal rate tests. As the capacitors undergo cyclical loading, the titanium oxide would start to delaminate from the substrate. Additional testing with multiple samples at the same conditions will improve the confidence interval of the calculated values.

Table 4. Data Extrapolated to 10 and 100 Seconds for Charge Equals Discharge Rate Tests

| Charge=Discharge | Dielectric [-] 10 s | Dielectric [-] 100s | Energy Density [J/cm ³] 10 s | Energy Density [J/cm ³] 100 s | Power Density [W/cm ³] 10 s | Power Density [W/cm ³] 100 s |
|------------------------|------------------------|------------------------|--|---|--|---|
| DI Water | 1.04E+06 | 2.02E+06 | 0.00 | 0.00 | 0.00 | 0.00 |
| NH ₄ Cl 10% | 2.73E+08 | 1.06E+09 | 35.04 | 139.22 | 3.50 | 1.39 |
| NH ₄ Cl 20% | 2.18E+08 | 7.96E+08 | 29.79 | 103.12 | 2.98 | 1.03 |
| NH ₄ Cl 30% | 2.09E+08 | 6.25E+08 | 34.01 | 110.95 | 3.40 | 1.11 |
| NaNO ₃ 10% | 1.34E+07 | 3.58E+07 | 3.82 | 9.36 | 0.38 | 0.09 |
| NaNO ₃ 20% | 3.07E+07 | 9.44E+07 | 12.23 | 39.23 | 1.22 | 0.39 |
| NaNO ₃ 30% | 2.99E+07 | 8.94E+07 | 13.04 | 43.19 | 1.30 | 0.43 |
| KOH 10% | 1.04E+08 | 2.72E+08 | 21.64 | 66.54 | 2.16 | 0.67 |
| KOH 20% | 1.19E+08 | 3.52E+08 | 20.98 | 69.46 | 2.10 | 0.69 |
| KOH 30% | 2.06E+08 | 6.04E+08 | 43.41 | 160.46 | 4.34 | 1.61 |

Table 5. Data Extrapolated to 10 and 100 Seconds for Fixed Charge Rate Tests

| Charge Fixed 10 [mA] | Dielectric [-] 10 s | Dielectric [-] 100s | Energy Density [J/cm ³] 10 s | Energy Density [J/cm ³] 100 s | Power Density [W/cm ³] 10 s | Power Density [W/cm ³] 100 s |
|-------------------------|------------------------|------------------------|--|---|--|---|
| DI Water | 1.17E+06 | 2.35E+06 | 0.01 | 0.00 | 0.0 | 0.00 |
| NH ₄ Cl 10% | 1.56E+08 | 4.05E+08 | 38.12 | 122.30 | 3.8 | 1.2 |
| NH ₄ Cl 20% | 1.25E+08 | 3.15E+08 | 38.92 | 131.35 | 3.9 | 1.3 |
| NH ₄ Cl 30% | 2.12E+08 | 4.49E+08 | 46.16 | 118.32 | 4.6 | 1.2 |
| NaNO ₃ 10% | 7.60E+06 | 1.44E+07 | 2.67 | 5.41 | 0.3 | 0.1 |
| NaNO ₃ 20% | 4.85E+07 | 1.18E+08 | 10.50 | 29.59 | 1.1 | 0.3 |
| NaNO ₃ 30% | 2.19E+07 | 4.79E+07 | 13.15 | 38.95 | 1.3 | 0.4 |
| KOH 10% | 9.74E+07 | 2.37E+08 | 15.47 | 39.49 | 1.5 | 0.4 |
| KOH 20% | 1.18E+08 | 2.79E+08 | 18.56 | 46.84 | 1.9 | 0.5 |
| KOH 30% | 1.31E+08 | 2.14E+08 | 34.94 | 91.29 | 3.5 | 0.9 |

For frequency conclusions, as the frequency increases, the dielectric values for all tested salt identities decreased. As shown in Figure 2 in the Background section, when the power source to the circuit is disconnected and the electric field is no longer present, the ions are free to release their energy and move to a relaxed state. As the frequency increases, the ions are unable to establish a stretched dipole to take advantage of the entire length of the nanotube. Additionally, as the density of salt dissolved in solution increases, similar to rush-hour traffic, ions become jammed and locked in place unable to discharge their full energy capacity at the desired rate. Only when the optimal number of ions dissolved solution, sufficient charge carriers to counteract the applied but not cause ion-lock, are energy densities at their maximum.

For the salt identities and concentrations tested, similar roll-off of dielectric values could be observed. This was especially apparent during the even periodic frequency testing. As discussed, asymmetric testing requires additional data points to increase the confidence interval and reduce error caused by titanium oxide delamination, DI water dehydration, and data aliasing.

As the first step in understanding frequency response of NTSDM Supercapacitors, a large amount of data was collected across a wide variety of frequencies. The significance of these frequencies, and corresponding discharge times, is that they fall directly in line with current design efforts to shape pulse patterns at the 0.01 second discharge time. Unlike commercial capacitors, the data provided in this thesis directly encompasses the discharge times of future USN applications without the need to extrapolate beyond the tested frequency boundaries. Whether the discharge times are 0.01 seconds or 10 seconds, the data is now currently available without a questionable upper or lower prediction boundary.

Despite the sheer volume of tests conducted, continued research is required. Additional iterations of each solution are required on multiple samples instead of one sample per solution conducted. Post-processing is labor intensive. An effort was made to write a self-automated MATLAB script to analyze the data. The data provided by the EC-Lab fails to be compatible with MATLAB without considerable file manipulation. The initial MATLAB scripts lacked robustness to handle false peaks in the data and

ultimately failed. A script that is streamlined to accept data directly from the EC-Lab software and the ability to differentiate maximum peak from local peaks would greatly enhance the ability of the NPS material science team to conduct experiments with near instant recognition of salt identity success.

For this thesis, three salt identities and three concentrations were tested in one solution. Future work needs to be expanded to include additional salts and solutions such as Polypropylene Carbonate (PPC), Dimethyl Sulfoxide (DMSO), and N-Methyl 2 Pyrrolidone (NMP). In addition to salt identities, concentrations, and solutions, further analysis should include additional substrates for the nanotube array base.

APPENDIX A. RAILGUN EQUATIONS

The projectile is estimated to travel at Mach 7 (2,401 m/s) and with a contact time with the rails of 0.008 seconds [9]. This requires an acceleration of $3.0 * 10^5 \text{ m/s}^2$.

$$a = \frac{dv}{dt} = \frac{(2,401 \left[\frac{m}{s} \right]) - (0 \left[\frac{m}{s} \right])}{(0.008 \left[s \right])} = 300,125 \left[\frac{m}{s^2} \right] \quad (7)$$

Using this acceleration calculation and a projectile weight of 3.125 kg [9], the required force to attain the desired velocity is $9.38 * 10^5 \text{ N}$.

$$F = ma = (3.125 \left[kg \right]) \left(300,125 \left[\frac{m}{s^2} \right] \right) = 937,890.625 \left[N \right] = 9.38 * 10^5 \left[N \right] \quad (8)$$

Using this force calculation and a designed rail length of 10 meters, the required work to attain the desired force is $9.38 \text{E}6 \text{ J}$. 9.38 MJ is an ideal value to launch a projectile and does not account for losses due to friction and ancillary equipment required to operate the system.

$$Work = Fd = (937,890.625 \left[N \right]) (10 \left[m \right]) = 9,378,906.25 \left[J \right] = 9.38 * 10^6 \left[J \right] \quad (9)$$

Using this work calculation and the previous contact time of 0.008 seconds, the required power to attain the desired work is $1.17 \text{E}8 \text{ W}$.

$$Power = \frac{Work}{t} = \frac{9,378,906.25 \left[J \right]}{(0.008 \left[s \right])} = 117,236,328.125 \left[W \right] = 1.17 * 10^8 \left[W \right] \quad (10)$$

Using the work calculation and the empirical data from previous capacitor research, the required volume to attain the desired power is 0.313 m^3 .

$$Volume = \frac{W}{\rho} = \frac{(9.38 * 10^6 \left[J \right])}{(30 \left[\frac{J}{cm^3} \right])} = 3.13 * 10^5 \left[cm^3 \right] = 0.313 \left[m^3 \right] \quad (11)$$

When viewing a simple capacitor circuit, as seen in Figure 116, the capacitor reaches approximately 66% of maximum charge within one time constant.

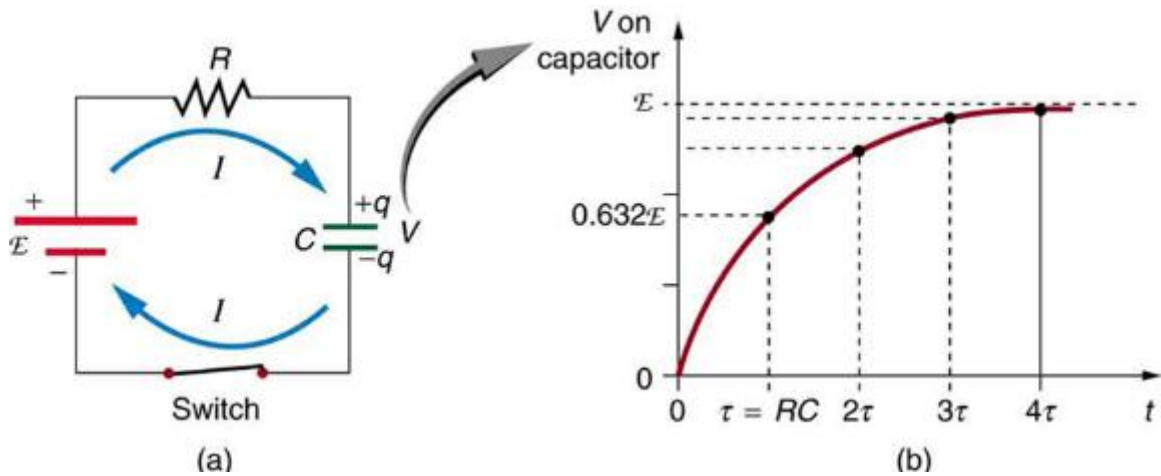


Figure 116. Basic Circuit Diagram of a Capacitor (Left) and the Associated Voltage vs. Time Charge Cycle (Right). Source: [19].

Likewise, when viewing the discharge cycle of the capacitor in Figure 117, the discharge current quickly drops to 33% of the maximum current within one time constant. This is significant if the current is too low before the projectile and armature exit the railgun at the designed muzzle velocity. The NPS supercapacitor group has determined approximately 1% of the initial discharge power stored in the capacitor meets the design objective. In addition to the 110.7 MW of power required to launch the projectile, this does not account for the ancillary equipment to operate the launch system.

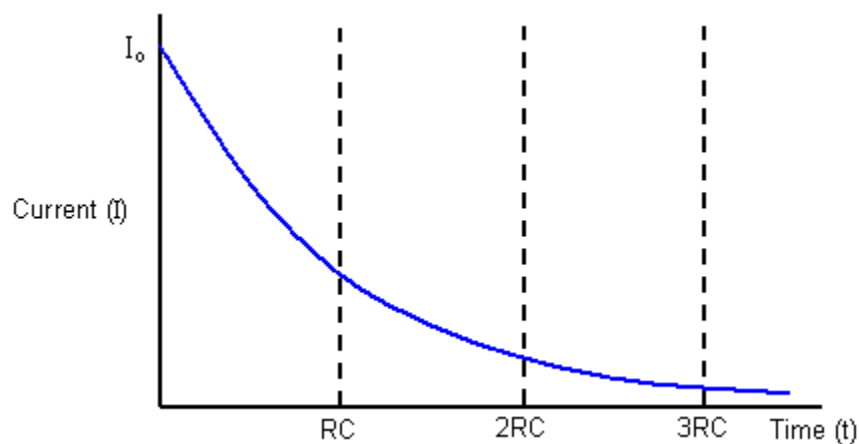


Figure 117. Current vs. Time Discharge Cycle of a Generic Capacitor. Adapted from [20].

Due to this inefficiency in capacitor discharge, the volume is adjusted by a factor of 100 to ensure sufficient current throughout the projectile discharge. A volume of 31.3 m³ would require a large portion to be dedicated strictly to capacitors leaving little space for power generation, fuel, berthing, and other shipboard operations.

$$Volume_{Corrected} = 0.313 [m^3] * 100 = 31.3 [m^3] \quad (12)$$

$$Volume_{Ideal} = \frac{W}{\rho} = \frac{(9.38 * 10^6 [J])}{(1000 [J/cm^3])} = 9.38 * 10^3 [cm^3] = 9.38 * 10^{-3} [m^3] \quad (13)$$

$$Volume_{Ideal-Corrected} = 9.38 * 10^{-3} [m^3] * 100 = 0.938 [m^3] \quad (14)$$

$$Work = Power * t = (1 * 10^5 [W]) (15 [s]) = 1.5 * 10^6 [J] \quad (15)$$

Using this power calculation and the empirical data from previous capacitor research, the required volume to attain the desired power is 0.313 m³.

$$Volume = \frac{W}{\rho} = \frac{(1.5 * 10^6 [J])}{(30 [J/cm^3])} = 5.0 * 10^4 [cm^3] = 0.5 * 10^{-3} [m^3] \quad (16)$$

Correcting for volume inefficiency provides an actual volume of 0.05 m³.

$$Volume_{Corrected} = 0.5 * 10^{-3} [m^3] * 100 = 0.05 [m^3] \quad (17)$$

Ideal energy density adjusts the required volume to 1.5E-3 m³ and corrected for inefficiency to 0.15 m³.

$$Volume_{Ideal} = \frac{W}{\rho} = \frac{(1.5 * 10^6 [J])}{(1000 [J/cm^3])} = 1.5 * 10^3 [cm^3] = 1.5 * 10^{-3} [m^3] \quad (18)$$

$$Volume_{Ideal-Corrected} = 1.5 * 10^{-3} [m^3] * 100 = 0.15 [m^3] \quad (19)$$

THIS PAGE INTENTIONALLY LEFT BLANK

APPENDIX B. EMALS EQUATIONS

$$a = \frac{dv}{dt} = \frac{(100 \left[\frac{m}{s} \right]) - (0 \left[\frac{m}{s} \right])}{(2 \left[s \right])} = 50 \left[\frac{m}{s^2} \right]$$

$$F = ma = (45,000 \left[kg \right]) \left(50 \left[\frac{m}{s^2} \right] \right) = 2,250,000 \left[N \right] = 2.25 * 10^6 \left[N \right]$$

Using this force calculation and a launch length of 100 meters, the required work to attain the desired force is 2.25E8 J.

$$Work = Fd = (2.25 * 10^6 \left[N \right]) (100 \left[m \right]) = 225,000,000 \left[J \right] = 2.25 * 10^8 \left[J \right]$$

Using this work calculation and the previous contact time with the ship deck of 2 seconds, the required power to attain the desired work is 1.13E6 W.

$$Power = \frac{Work}{t} = \frac{(2.25 * 10^8 \left[J \right])}{(2 \left[s \right])} = 1,125,000 \left[W \right] = 1.13 * 10^6 \left[W \right]$$

Using the work calculation and the empirical data from previous capacitor research, the required volume to attain the desired power is 7.5 m³.

$$Volume = \frac{W}{\rho} = \frac{(2.25 * 10^8 \left[J \right])}{(30 \left[\frac{J}{cm^3} \right])} = 7.5 * 10^6 \left[cm^3 \right] = 7.5 \left[m^3 \right]$$

As computed in the railgun section, the volume is corrected to show the inefficient discharge of the capacitor. 750 m³ of the aircraft carrier would be dedicated strictly to capacitors.

$$Volume_{Corrected} = 7.5 \left[m^3 \right] * 100 = 750 \left[m^3 \right]$$

As computed in the railgun section, an ideal capacitor with 1000 J/cm³ energy density would reduce the capacitor bank input to 22.5 m³.

$$Volume_{Ideal} = \frac{W}{\rho} = \frac{(2.25 * 10^8 \left[J \right])}{(1000 \left[\frac{J}{cm^3} \right])} = 2.25 * 10^5 \left[cm^3 \right] = 0.225 \left[m^3 \right]$$

$$Volume_{Ideal-Corrected} = 0.225 \left[m^3 \right] * 100 = 22.5 \left[m^3 \right]$$

THIS PAGE INTENTIONALLY LEFT BLANK

APPENDIX C. COMMERCIAL CAPACITOR FIGURES

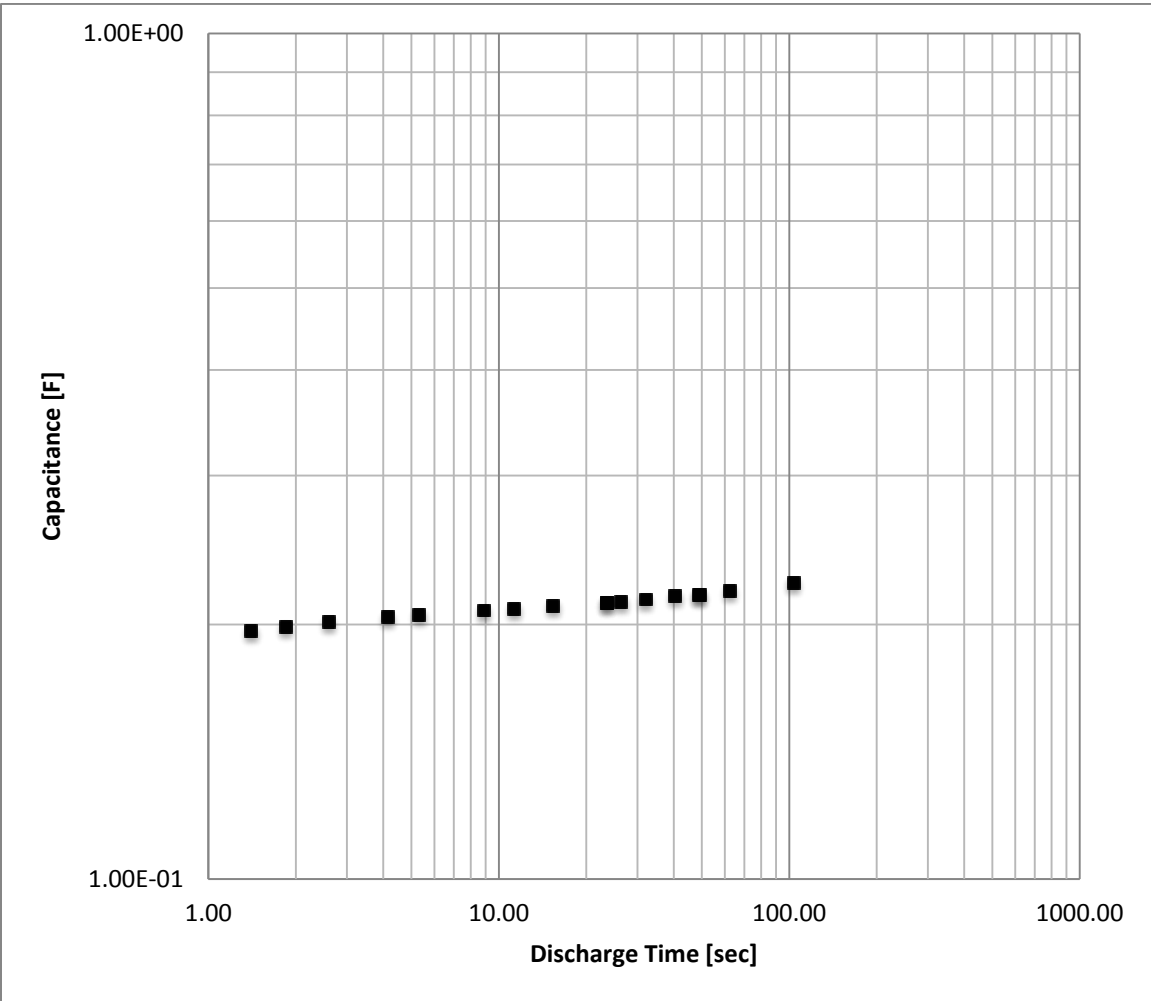


Figure 118. Capacitance vs. Discharge Time (220 mF) (Charge=Discharge)

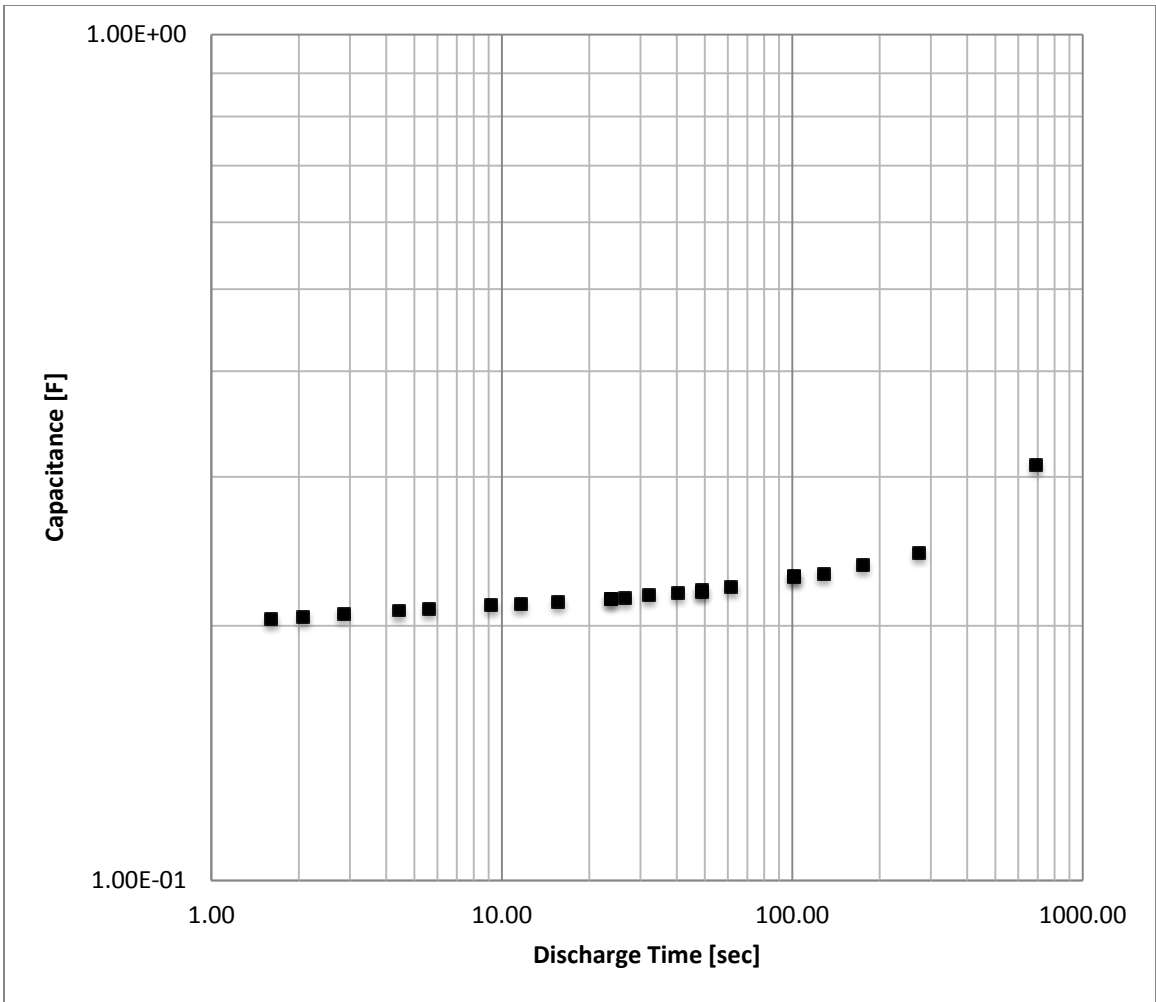


Figure 119. Capacitance vs. Discharge Time (220 mF) (Charge≠Discharge)

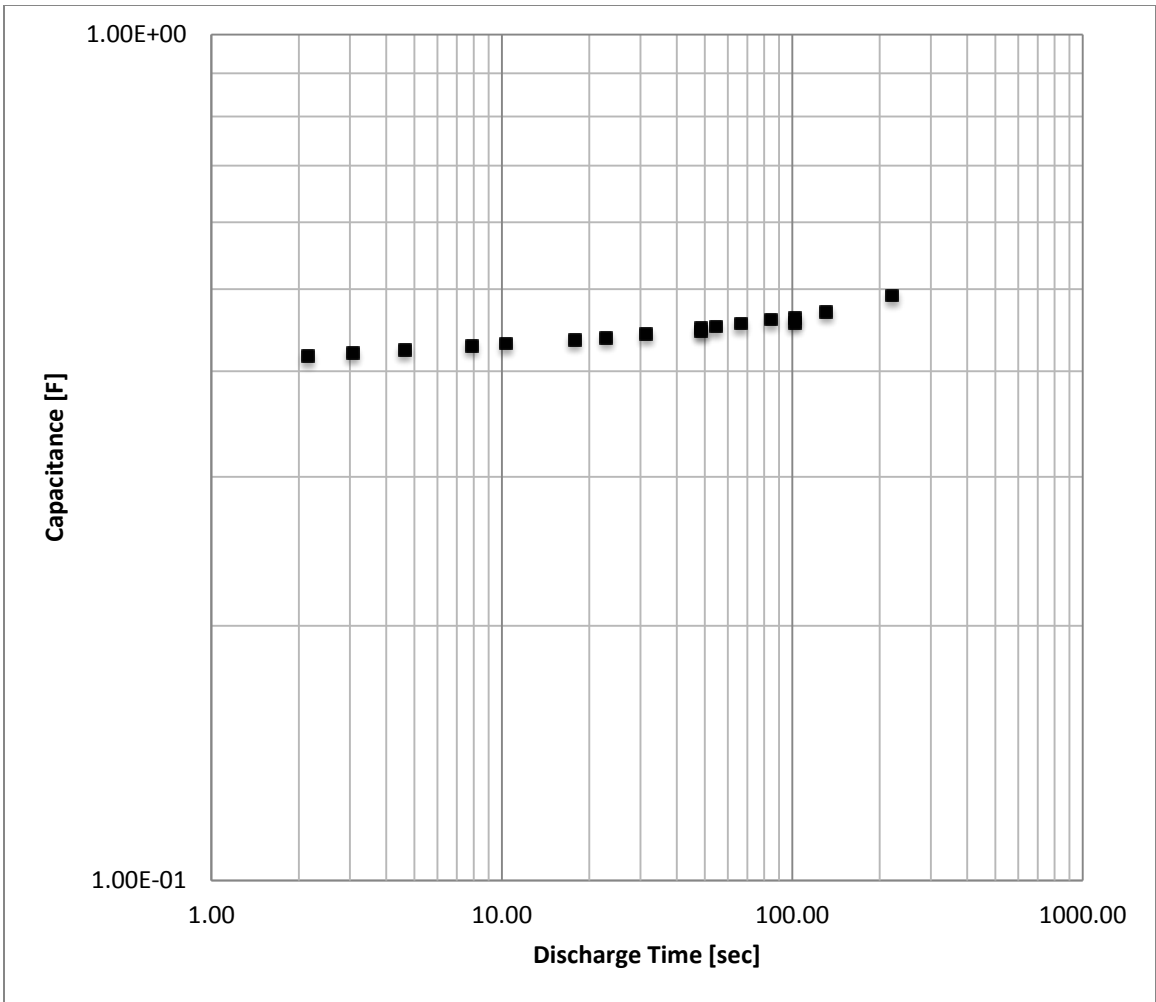


Figure 120. Capacitance vs. Discharge Time (470 mF) (Charge=Discharge)

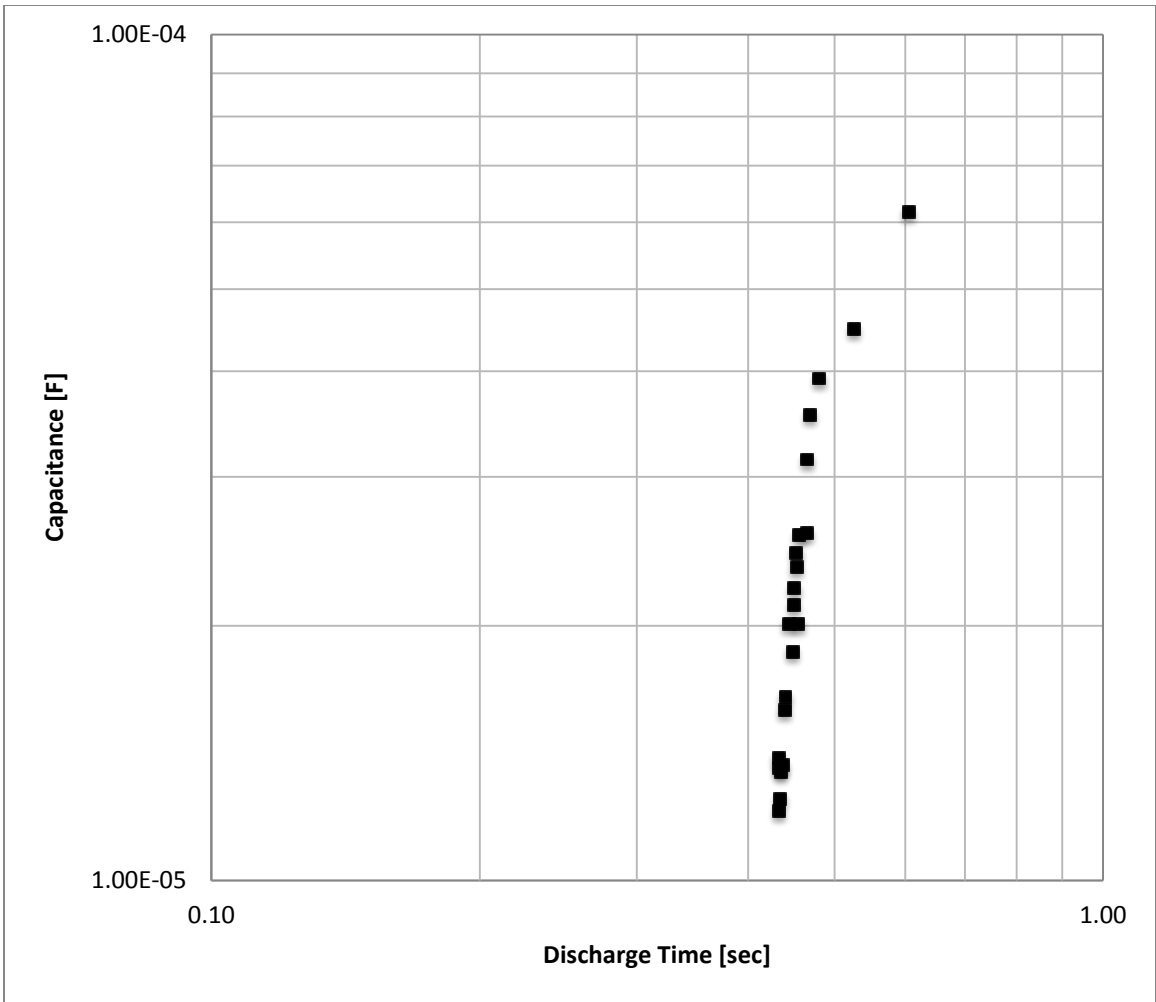


Figure 121. Capacitance vs. Discharge Time (470 mF) (Charge≠Discharge)

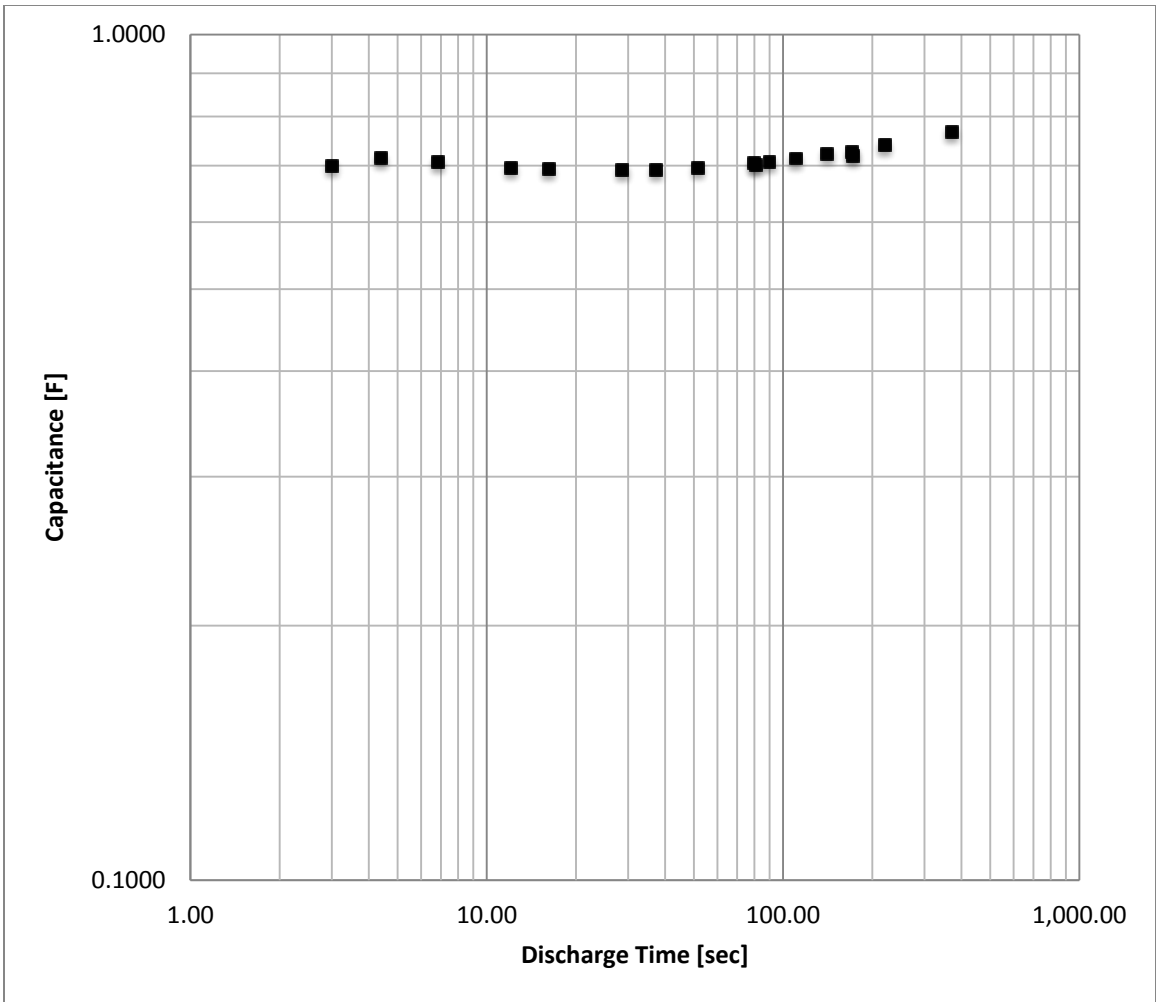


Figure 122. Capacitance vs. Discharge Time (1 F) (Charge=Discharge)

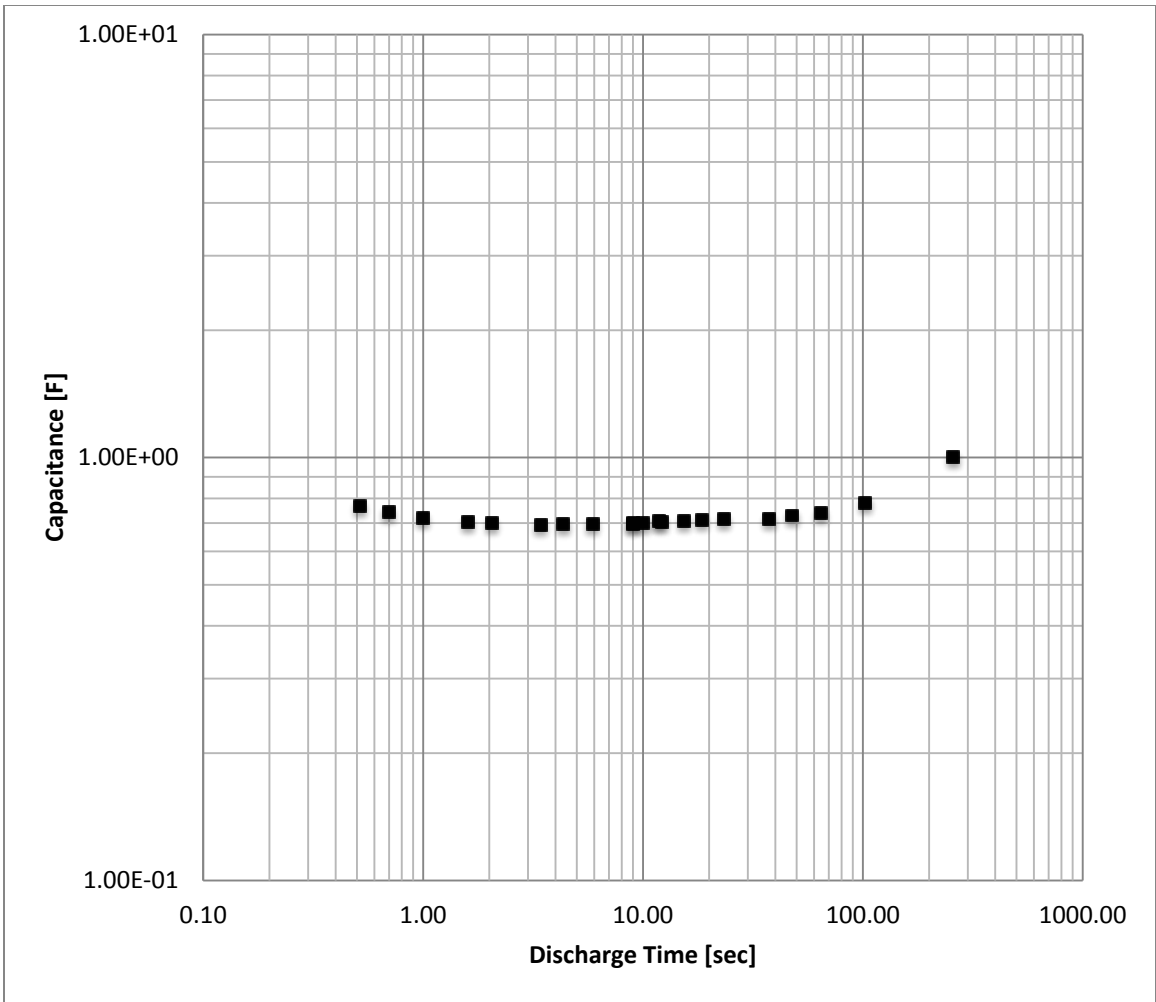


Figure 123. Capacitance vs. Discharge Time (1 F) (Charge≠Discharge)

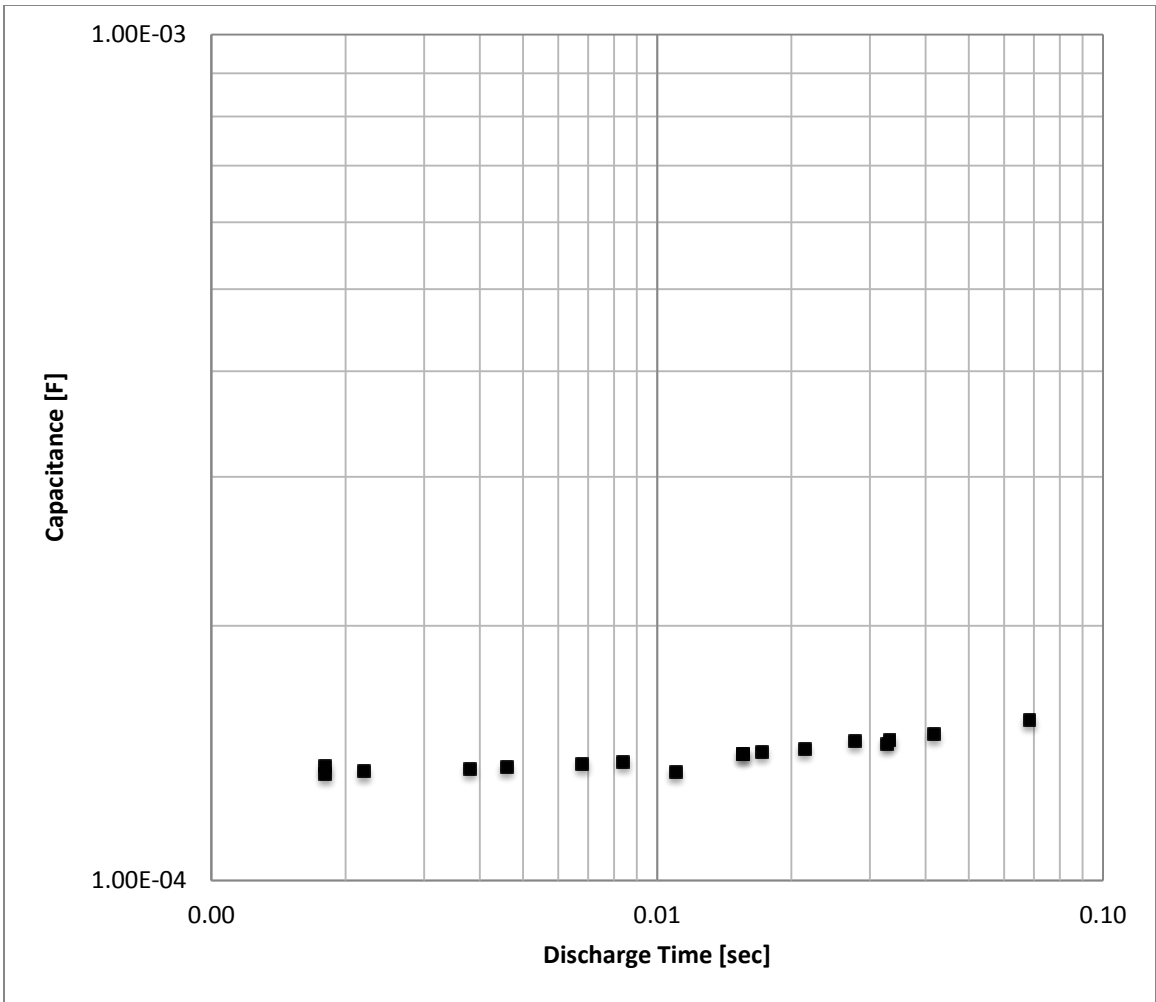


Figure 124. Capacitance vs. Discharge Time (2.2 F) (Charge=Discharge)

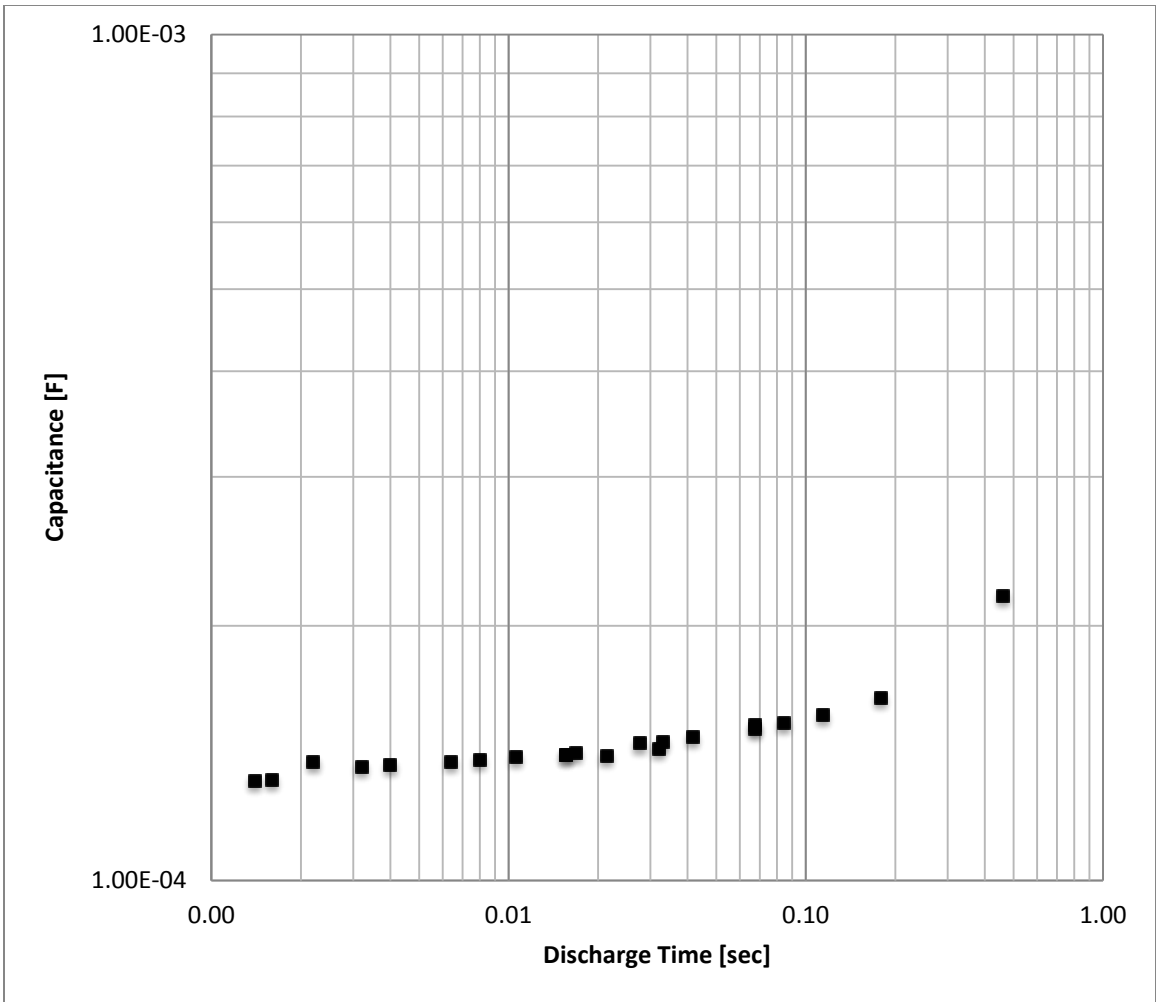


Figure 125. Capacitance vs. Discharge Time (2.2 F) (Charge≠Discharge)

LIST OF REFERENCES

- [1] N. L. Jenkins, "Optimal super dielectric material," M.S. thesis, Dept. Mech. Eng., Naval Postgraduate School, Monterey, CA, 2015.
- [2] J. W. Gandy, "Characterization of micron-scale nanotubular super dielectric materials," M.S. thesis, Dept. Mech. Eng., Naval Postgraduate School, Monterey, CA, 2015.
- [3] "Roadmap to an electric naval force," class notes for Electrical Power Engineering, Dept. of Mech. and Aerosp. Eng., Naval Postgraduate School, Monterey, CA, fall 2015.
- [4] J. Bennett. (2016, Jun. 6). The future of the Navy's electromagnetic railgun could be a big step backwards. [Online]. Available: <http://www.popularmechanics.com/military/weapons/a21174/navy-electromagnetic-railgun/>
- [5] Zumwalt-class destroyer. (n.d.). *Wikipedia*. [Online]. Available: https://en.wikipedia.org/wiki/Zumwalt-class_destroyer. Accessed Jan. 5, 2017.
- [6] M. C. Stewart, "Comparison of two railgun power supply architectures to quantify the energy dissipated after the projectile leaves the railgun," M.S. thesis, Dept. Elect. & Comp. Eng., Naval Postgraduate School, Monterey, CA, 2016.
- [7] S. J. Roundy, "Energy scavenging for wireless sensor nodes with a focus on vibration to electricity conversion," Ph. D. dissertation, Dept. Mech. Eng., Univ. of California, Berkeley, CA, 2003.
- [8] S. Fromille and J. Phillips, "Super dielectric materials," *Materials*, vol. 7, 8197–8212, 2014. doi: 10.3390/ma7128197
- [9] "Electric ship weapon system: directed energy weapons," class notes for Electrical Power Engineering, Dept. of Mech. and Aerosp. Eng., Naval Postgraduate School, Monterey, CA, fall 2015.
- [10] R. O'Rourke, *Navy Shipboard Lasers for Surface, Air, and Missile Defense: Background and Issues for Congress*, Washington, DC, Library of Congress Congressional Research Service, Aug. 2012, pp. 6–8.
- [11] A. M. Still, "Electromagnetic launchers for use in aircraft launch at sea," M.S. thesis, Cockrell School of Eng., University of Texas, Austin, TX, 1998.
- [12] Electromagnetic Aircraft Launch System. (n.d.). *Wikipedia*. [Online]. Available: https://en.wikipedia.org/wiki/Electromagnetic_Aircraft_Launch_System. Accessed Feb. 8, 2017.

- [13] Supercapacitor. (n.d.). *Wikipedia*. [Online]. Available: <https://en.wikipedia.org/wiki/Supercapacitor>. Accessed Feb. 7, 2017.
- [14] G. Feng, R. Qiao, J. Huang, B. Sumpter, and V. Meunier, “Computational modeling of carbon nanostructures for energy storage applications,” presented at 10th IEEE International Conference on Nanotechnology Joint Symposium with Nano Korea, Seoul, Republic of Korea, 2010.
- [15] F. J. Q. Cortes and J. Phillips, “Tube-super dielectric materials: electrostatic capacitors with energy density greater than 200 J·cm⁻³,” *Materials*, vol. 8, 6208–6227, 2015. doi: 10.3390/ma8095301
- [16] “Lecture 6 - some capacitor computations,” class notes for Advanced Energy Materials, Dept. of Mech. Eng., Naval Postgraduate School, Monterey, CA, summer 2016.
- [17] J. Phillips, “Novel super dielectric materials: aqueous salt solution saturated fabric,” *Materials*, vol. 9, 1–12, 2016. doi: 10.3390/ma9110918
- [18] Supercapacitors vs. Batteries Chart. (n.d.) *Wikimedia*. [Online]. Available: <https://commons.wikimedia.org/wiki/File:Supercapacitors-vs-batteries-chart.png>. Accessed Jan. 5, 2017.
- [19] DC circuits containing resistors and capacitors. (n.d.). OpenStax CNX. [Online]. Available: <http://cnx.org/contents/y3HdLx8N@3/DC-Circuits-Containing-Resisto>. Accessed Jan. 5, 2017.
- [20] K. Gibbs. (2013) Mathematical treatment of charging and discharging a capacitor. [Online]. Available: http://www.schoolphysics.co.uk/age16-19/Electricity%20and%20magnetism/Electrostatics/text/Capacitor_charge_and_discharge_mathematics/index.html

INITIAL DISTRIBUTION LIST

1. Defense Technical Information Center
Ft. Belvoir, Virginia
2. Dudley Knox Library
Naval Postgraduate School
Monterey, California